Modulation of Chemical Reactions by Glass Packing

By

Yue Qiu

A dissertation submitted in partial fulfillment

of the requirement for the degree of

Doctor of Philosophy

(Chemistry)

at the

UNIVERSITY OF WISCONSIN-MADISON

2018

Date of final oral examination: August 1st, 2018

The dissertation is approved by the following members of the Final Oral Committee:

Mark D. Ediger, Professor, Chemistry
Lian Yu, Professor, Pharmacy
John Wright, Professor, Chemistry
Robert McMahon, Professor, Chemistry

Acknowledgments

First of all, I would like to thank Prof. Mark Ediger for years of advising and support. Mark is a thoughtful advisor, a scientist who thinks critically, and a helpful friend. It has been my pleasure and privilege to work with him, in a group that he so successfully established and maintained over the years.

I would like to thank all the members of the Ediger group. I have learned new things from every one of you and gotten encouraged by your spirit of devotion and enthusiasm for research. Shakeel Dalal, Diane Walters, Ankit Gujral, and Jaritza Gomez, thank you for mentoring me when I first joined the group. You have established great role models for the group and I believe the impact will last even after you leave. Josh Ricci, thank you for teaching me English and sharing funny stories with me. Maddy Beasley, thank you for organizing the group activities. Kushal Bagchi, Camille Bishop, Trevor Bennin, Marie Fiori, Ben Kasting, and Enran Xing, you are thoughtful scientists with great talents, and I believe you will succeed in graduate school and achieve your goals. Mike Bieser, I feel really lucky to have worked with you. You are a talented and self-motived young chemist. I hope you will continue to create surprises for the Ediger group. Kelly Hebert, Mike Tylinski, Travis Powell, Audrey Laventure, Jing Jiang, Yeong Zen Chua, Jaroslav Bartak, and Niko Van, thank you all for being such great colleagues.

I also want to thank the chemistry department staffs, who have always been friendly and supportive. Thank Kristi Heming and Sue Martin, our path coordinators, who have helped to organize seminars and go to conferences. Thank Arrietta Clauss for organizing career fairs and helping me get opportunities for many outreach activities. Thank Chad Skemp and Mike Bradley for helping with purchasing and shipping. Thank Steve Meyers in the machine shop, Bill Goebel in the electronic shop, and Tracy Drier in the glass shop for helping me to design, develop, and fix experimental instruments. Many of my experiments cannot proceed without helps from you.

My undergraduate advisor at Nanjing University, Prof. Jianhua Zhu, gave me comprehensive training during my early career as a chemist. He taught me to be persistant in research and encouraged me to keep working during my Ph.D. study abroad. I really appreciate his efforts in teaching a undergraduate and giving advices that help me grow up.

I feel lucky to meet friends who share the same interest in playing volleyball in Madison and I have many great memories on the volleyball court with my teammates. Playing volleyball gives me happiness and confidence, which helps me to succeed in the graduate career. It is an honor for me to be the team captain, and I hope everyone in the team can keep enjoying the game.

At last, I would like to thank my wife, Shuyu Fang, who always stands by my side and gives me support. Five years ago, I started my graduate career at UW-Madison, and she is one of the most important reasons for me to come here, in addition to the fascinating science happening in the department. We have been together since the first year in college- thank you for accompanying me these years. I also want to thank my parents, who are currently living in China. I could never pay back the care and love you have given me since my childhood, and you will be my biggest motivation to face life's many challenges and strive for success.

Table of Contents

Abstract

Chemically stable solids are in demand for many applications, including pharmaceuticals and organic electronics. Previous efforts in crystals have established the importance of molecular packing in influencing chemical stability by comparing reaction kinetics in different polymorphs. However, efforts to improve chemical stability by modulating molecular packing in amorphous materials have seen much smaller effects. Recently, physical vapor deposition (PVD), a common method to prepare thin films for organic electronics, is reported to create organic glasses with exceptional properties that cannot be accessed by any other method. By vapor-depositing molecules onto a substrate maintained at the temperature below the glass transition temperature (T_g), PVD glasses can demonstrate significantly enhanced thermal stability and increased density relative to traditional liquid-cooled glasses; the optimum substrate temperature usually occurs near 0.85 T_g. The discovery of high-density and high-thermal-stability glasses by vapor-deposition provides an opportunity to address questions of how chemical stability can be improved in glasses. The body of this work deals with the characterization of a variety of chemical reactions in organic glasses and establishes the connection between enhanced chemical stability and the distinctive glass packing achieved by vapor-deposition.

Films of azobenzenes, photochromic molecules that can undergo *trans* to *cis* photoisomerization, were prepared by vapor-deposition at a wide range of substrate temperature. Photostability of vapor-deposited Disperse Orange 37, a push-pull azobenzene with fast *cis-trans* thermal isomerization, is found to increase by as much as a factor of 50 relative to the liquid-cooled glass. Photostability was determined by measuring density and molecular orientation changes by ellipsometry during irradiation to induce photoisomerization. We further show that the enhanced photostability in vapor-deposited glasses is a general phenomenon by using a non-push-pull azobenzene, 4,4’-diphenyl azobenzene (DPA). By

mixing DPA into the glass host of celecoxib, we directly measure populations of *trans* and *cis* DPA via UV-Vis spectroscopy and show that the rate of photoisomerization varies as a function of the substrate temperature. Photostability correlates with the density of packing, where the optimum glass is about one order of magnitude more photostable than the liquid-cooled glass. These results show substantially increased photostability of azobenzenes in both neat films and mixtures and provide a molecular explanation for enhanced photostability in glasses.

We further investigate the influence of dense glass packing on photodegradation, an important reaction type responsible for degradation in pharmaceuticals and failure in organic electronics. Indomethacin, a pharmaceutical molecule that can undergo photodecarboxylation reaction when irradiated by UV light, was studied as a model system. Photodegradation of indomethacin was assessed through the light-induced mass decrease in glassy thin films caused by the loss of CO_2, as characterized by a quartz crystal microbalance (QCM). For the most stable glass, vapor-deposited at 0.85 T_g, the photodegradation rate is about 50% slower than for the liquid-cooled glass when irradiated by a 312 nm UV light. The enhanced stability against degradation correlates with glass density. We speculate that high-density glasses limit the local molecular reconfiguration required for photodecarboxylation.

Additionally, to broaden the impact of vapor-deposition on chemical stability, we performed the solid-gas reaction of indomethacin with ammonia. Indomethacin has a carboxylic acid group that can react with ammonia to yield ammonium salt. In this case, chemical reactivity is assessed through the increase in mass induced by the addition of ammonia to glassy thin films, as characterized by a QCM. Vapor-deposited indomethacin with increased density shows slower reaction rates with ammonia relative to the liquid-cooled glass, and the maximum difference in reaction rates is over one order of magnitude. We suggest that the diminished solubility of ammonia in vapor-deposited glasses contributes to their remarkable chemical stability.

Chapter 1

Organic glasses and chemical reactions: An introduction

Yue Qiu

Introduction

Glasses are amorphous materials that have no long-range order. Unlike crystals, which have a repeating unit cell and a well-defined structure, glassy materials are more disordered and inherit the structural assembly from cooling a liquid. When we talk about glasses, the first impression that crosses our mind is typically window glass and glassware, which are based on inorganic silicon dioxide. In fact, glasses have other important applications in modern technology and everyday life. For example, optical fibers play an important role in modern communication technology, and the main component is made of amorphous silica.[1] All polymers are glasses (or at least partially glasses), and they are widely used as plastic products and fabrics such as polyesters.[2] Metallic glasses are important engineering materials due to the extraordinary properties of high strength (twice that of stainless steel), corrosion resistance, polymer-like formability, and excellent magnetic properties.[3]

The small-molecule organic glass is another important group of glassy materials and has important applications in pharmaceuticals[4, 5] and organic electronics.[6] In many cases, organic glasses are preferred over their crystalline counterparts. For example, there is a substantial interest in formulating pharmaceuticals into amorphous forms because of their enhanced solubility, dissolution rate, and better bioavailability.[7] In organic electronics, organic glasses have been used for the manufacture of cellphone displays that utilize organic light emitting diode (OLED) technology, such as the Samsung Galaxy and iPhone X. Those glassy materials usually function as active light emission layers in devices and have several advantages over crystals: (1) glassy thin films can be fabricated with a large area, while the difficulty of controlling crystal growth will increase rapidly as the area becomes large; (2) surfaces of glasses are smoother than crystals, which provides convenience for preparation of devices with multiple

stacked layers; (3) glasses have better flexibility in tuning compositions in a multi-component structure.

Although organic glasses have so many great advantages, there are still limitations that impose restrictions on the further development for applications. Typically, glasses exhibit lower density, higher enthalpy/entropy, and are chemically less stable relative to crystals. For pharmaceuticals, it has been reported that organic molecules with the least crystallinity are the most unstable, which suggests a faster rate of degradation that can shorten the shelf-life in the amorphous form.[8] In the OLED industry, chemical degradation can cause the failure of organic electronic devices, and this is sometimes a more limiting factor than the device efficiency.[9-11]

In this thesis, I investigate how molecular packing and preparation methods can influence the chemical properties of organic glasses. In particular, I will use physical vapor deposition (PVD) to prepare glasses, run chemical reaction tests, and compare chemical stability to liquid-cooled glasses. Photoisomerization, photodegradation, and solid-gas reactions are investigated in vapor-deposited glasses in neat films and mixtures. The experimental results demonstrate, for the first time, that chemical reactions can be significantly suppressed in glasses vapor-deposited at selected conditions. For photochemical reactions, enhanced stability is attributed to the increased constraint applied to the molecular rearrangement by the higher glass density. For the solid-gas reaction, enhanced chemical stability is explained by the decreased solubility of gases in high-density glasses.

This chapter will provide the background and introductory information for the thesis. Section 1.1 introduces the basic concepts and fundamental properties of supercooled liquids and glasses. Section 1.2 explains glass preparation methods and some extraordinary properties of glasses prepared by PVD. Section 1.3 discusses the control of chemical reactivity in organic materials (crystals and glasses) with emphasis on the influence of molecular packing on reaction kinetics.

Section 1.4 discusses several chemical reactions that will be investigated in this thesis, while section 1.5 explains the experimental methods employed in those investigations. Finally, section 1.6 summarizes how this thesis contributes to our understanding of chemistry in vapor-deposition glasses and provides suggestions for future directions.

1.1 Supercooled liquids and glasses

Glasses can be made by cooling a liquid. Figure 1 shows the enthalpy changes as a material is cooled from the liquid state,[5] and similar graphs may be found for volume and entropy changes. Upon cooling, a liquid may crystallize at the melting point (T_m) with a sharp decrease in enthalpy. This is a first-order transition, and the resulting material is in the equilibrium crystalline state. In some conditions, for example, cooling with fast rates, materials may manage to avoid crystallization and stay in the liquid state even below T_m. We call the liquid below T_m a supercooled liquid. Upon further cooling, the viscosity of the supercooled liquid will increase sharply and molecules move slower and slower. Eventually, molecules move too slowly to maintain equilibrium and form a glass at the point called glass transition temperature (T_g). In this case, T_g is defined by the kinetics of molecular relaxation, and there are no drastic changes in the structure of the material as the transition occurs.

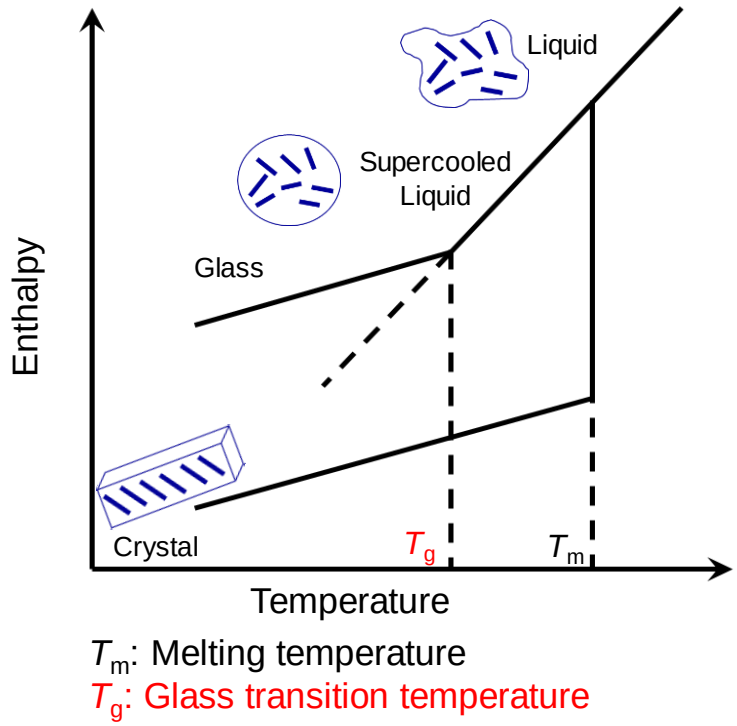

Figure 1. A schematic illustration of the enthalpy of liquids and glasses. The enthalpy depends on the temperature and the state of the material. Adapted from Ref. #5 with permission.

As non-equilibrium materials, glass properties depend on the preparation methods and thermal history along the way to the current state. For example, T_g depends on the cooling rate, where slower cooling usually yields lower T_g.[12, 13] This happens because the slower cooling rate will allow molecules more time to rearrange themselves and remain in the supercooled liquid state at lower temperatures. Once a glass is formed, it will undergo structural relaxation toward the metastable equilibrium state (supercooled liquid) or crystallization.[12, 14] The continuous evolution towards the supercooled-liquid state is called physical aging, which is accompanied by changes in almost all physical properties of glasses, including density, enthalpy, and entropy.

At this point, people may speculate that glasses will eventually crystallize due to the thermodynamic driving force, and if crystallization is the inevitable fate for all glasses, why we still use them? For many glass formers, this concern is unwarranted since this evolution towards crystals can be so slow that the transformation practically “never” happens. For example, o-terphenyl will not crystallize for years in a test tube at room temperature, which probably leaves a graduate student without any chance to observe such a change within their graduate career. The time scale for crystallization of some glasses can be astoundingly long. In a study of an amber that has been aged for 20 million years, the system still remains in the glassy state.[15] These slow dynamics are the foundation of many applications for glasses.

Glasses are frequently compared with their crystalline counterparts, and the amorphous nature does provide some pros and cons. Organic glasses typically have higher solubility and bioavailability, which have important uses in the pharmaceutical industry. However, glasses have lower chemical and thermal stability than crystals. This characteristic usually makes glasses less reliable than crystals. Therefore, preparing glasses that have enhanced stability while maintaining their amorphous nature with useful characteristics would provide an attractive perspective for developing better materials.

1.2 Physical vapor deposition and stable glasses

So far, the only method of preparing a glass that has been discussed is cooling a liquid. In fact, there are several routes to obtain glasses. In a freeze-drying process, rapid freezing favors the formation of an amorphous phase, during which ice or other frozen solvents from a material can be removed through the process of sublimation.[16] Some methods introduce mechanical stress, such as grinding and milling, to destroy the crystalline packing and generate glassy phases.[17] Spin-coating is another glass preparation method commonly used for the fabrication of organic thin films. In this case, the material of interest is dissolved in solvents and cast onto a flat substrate. The substrate is then rotated at high speed to spread the material uniformly by centrifugal force and evaporate the solvent simultaneously.

Physical vapor deposition (PVD) is an important method of glass preparation and has been widely used for the fabrication of organic electronics in applications.[18] Materials of interest are vaporized in a vacuum chamber and deposited onto a substrate. Compared to the above-mentioned methods, PVD has fine control over film thickness and can produce samples with high purity and smooth surface. Solution-based processes (i.e. spin-coating) may also be used for thin film preparation, but they usually suffer from the impurity of residual solvents, and additional annealing processes are generally required. Also, when preparing multi-layer structures it is challenging for solution-based processes to deposit the sequential layers without disrupting the existing ones. Vapor-deposition can prepare glasses with exceptional properties that cannot be accessed by other methods, including enhanced thermal stability, increased density, and anisotropic molecular orientation.[19] Next, I will introduce the vapor-deposition process, exceptional properties of vapor-deposited glasses, and mechanisms underlying the stable glass formation.

1.2.1 Physical vapor deposition

Physical vapor deposition (PVD) transfers molecules of interest into a vapor phase and deposits them onto a substrate in a high-vacuum chamber, as shown in Scheme 1. Depending on how materials are evaporated, PVD can be categorized into several types. For example, sputtering generates a plasma that erodes the source materials and deposit vapors onto a substrate such as a silicon wafer.[20] This method is used for the deposition of metals, as metals usually have high melting points and low vapor pressures. Metals can also be deposited by electron-beam evaporation, which vaporizes materials by using an intense beam of energy applied locally to a target. For small organic molecules, plasmas and high energy beams will destroy chemical bonds, therefore thermal evaporation is commonly used by resistively heating the crucible.[21] Early work found that vapor-deposited organic glasses have higher enthalpy relative to samples prepared by cooling a liquid.[22] Recent work has reported that organic glasses can also be made with extraordinarily high density and low enthalpy if deposition conditions are chosen correctly.

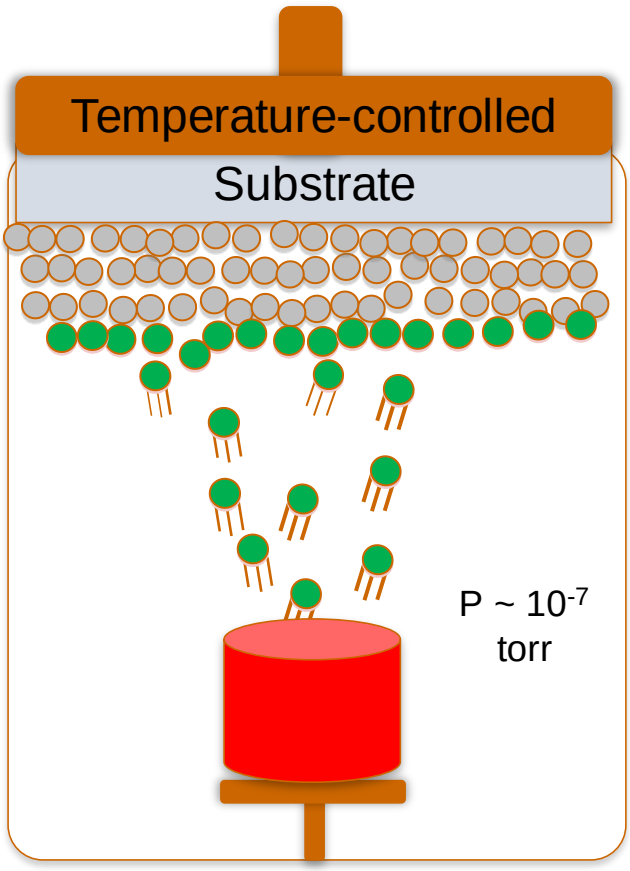

Scheme 1. A schematic illustration of physical vapor deposition. Organic molecules are evaporated or sublimated in a vacuum chamber from a heated crucible. Molecules in the vapor phase condense onto the substrate and form glassy thin films. During the deposition, substrate temperature can be controlled to tune properties of as-deposited glasses.

1.2.2 Exceptional properties of vapor-deposited glasses

In 2007, Swallen and coworkers first reported organic glasses with high thermal stability, low enthalpy, and high-density, for indomethacin and α,α,β-tris-naphthyl benzene (TNB) vapor deposited at substrate temperatures below T_g.[23] Vapor-deposited glasses with these features are called stable glasses. Since then, more than thirty molecules have been reported to produce PVD glasses with such enhanced stability relative to liquid-cooled glasses.[19] Typically, the optimum substrate temperature for preparing stable glasses is about 0.85 T_g.[24] Stable glasses exhibit enhanced thermal stability; upon heating at a constant rate, a stable glass can maintain its glassy packing to a much higher temperature than a liquid-cooled glass. Vapor-deposited glasses also have densities up to 1.4% higher than that of the liquid-cooled glass.

Figure 2 shows an example of α,α,β- TNB vapor-deposited at $T_{substrate}$ = 294 K (0.86 T_g) and provides the context to help us understand some important features of vapor-deposited glasses.[25] The as-deposited material was first heated from 293 to 370 K at 1 K/min and then cooled back to 293 K. During the first heating, the as-deposited material transformed into the supercooled liquid as indicated by the large increase in thickness over a small temperature range. The onset temperature, which characterizes the thermal stability of the as-deposited glass, was determined from the beginning of the transformation into the supercooled liquid (360 K). During the cooling run, the supercooled liquid transformed into the liquid-cooled glass at the normal T_g. There is one more heating and cooling run with the same ramping rate of 1 K/min, which reproduces the behavior of the first cooling run closely enough that the two cannot be distinguished. Two significant features can be seen in Figure 2. A high value of T_{onset} (20 K above T_g) is demonstrated during the first heating run, indicating enhanced thermal stability. Also, the density of the vapor-deposited glass is about 1.3% higher than the liquid-cooled glass, as characterized by the thickness difference before and after transformation. Vapor-deposited glasses with such high density and high thermal stability cannot be accessed by any other

known preparation methods in the lab. Applying external pressure may obtain glasses with similarly increased density and thermal stability, but such enhancement will be lost soon once the pressure is released.[26, 27] In principle, such high density could also be achieved if a liquid-cooled glass was aged for thousands of years, but this is not a practical route for material synthesis.[28-30]

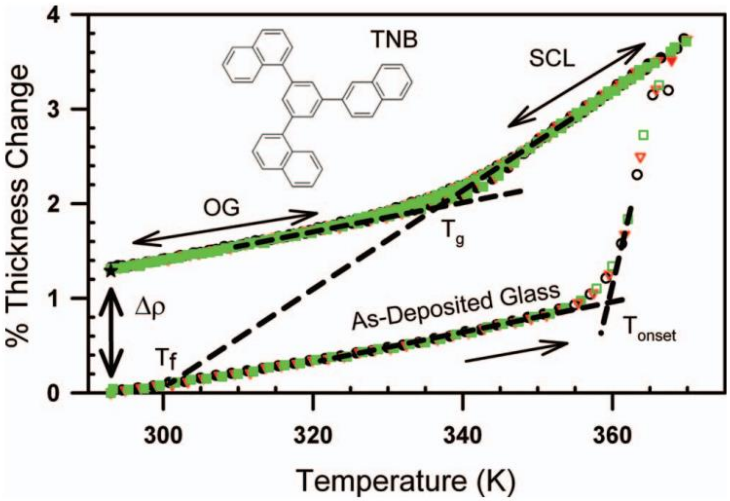

Figure 2. Thickness changes for vapor-deposited glasses of α,α,β- TNB during thermal ramping. Dashed lines are linear extrapolations that schematically demonstrate the calculation of the fictive temperature T_f, the onset temperature T_{onset}, and the ordinary glass transition temperature T_g. Δρ shows the density change between the as-deposited and ordinary glasses. The inset shows the structure of α,α,β-TNB. Adapted from ref. #25 with permission.

Vapor-deposited glasses also have lower enthalpy relative to the liquid-cooled glass. Figure 3 shows an example of indomethacin (IMC) vapor deposited at $T_{substrate}$ = 265 K (0.84 T_g), as characterized by DSC; 0.84 T_g is the optimum substrate temperature for preparing stable glasses of indomethacin.[30] As shown in panel A, the black curve represents the C_p for the liquid-cooled glass and all other curves represent glasses vapor deposited at different rates. Vapor-deposited glasses transform at higher temperatures than the liquid-cooled glass, indicating enhanced thermal stability. The shapes of C_p curves change significantly as a function of deposition rate. As the rate decreases, the peak of the C_p curves shifts to higher temperatures during the DSC scanning.

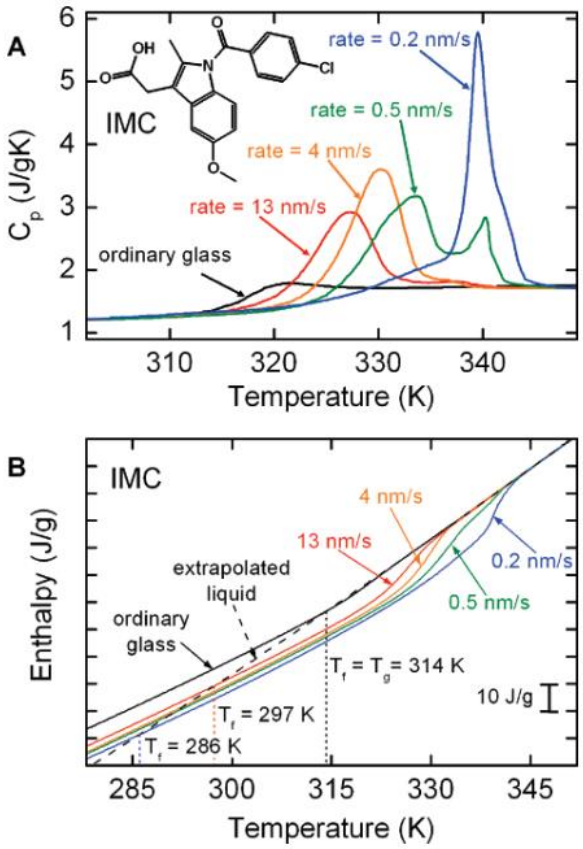

Figure 3. (A) Heat capacity curves observed for vapor-deposited and liquid-cooeld IMC. $T_{substrate}$ was 265 K (0.84 T_g) for each deposition. Depositions were performed at rates of 13 nm/s (red), 4 nm/s (orange), 0.5 nm/s (green), and 0.2 nm/s (blue). Inset: Structure of IMC. (B) Enthalpy curves obtained from integrating the C_p curves in part A. The color of the lines shown in part A corresponds to the curves shown in part B. The temperature at which the extrapolated liquid line (black, dashed) intersects the enthalpy of the vapor-deposited curves defines the fictive temperature T_f as indicated by the dotted vertical lines. Adapted from Ref. #30 with permission.

The dependence of thermal stability on the deposition rate is relevant to the mechanism of stable glass formation, which will be discussed later. Panel B in Figure 3 shows the enthalpy curves that are integrated from the C_p curves shown in the panel A. The enthalpies of all the vapor-deposited glasses are lower than that of the liquid-cooled glass, and the lowest enthalpy is obtained at the slowest deposition rate, 0.2 nm/s.

The DSC measurement of enthalpy gives us an opportunity to estimate the position of vapor-deposited glasses on the energy landscape. The most stable vapor-deposited glass shown in Figure 3 has the enthalpy about 10 J/g lower than the liquid-cooled glass. Considering crystals have enthalpy about 50 J/g lower than the liquid-cooled glass, we can estimate that the most stable glass has progressed about 20% of the way toward the bottom of the energy landscape. As a comparison, natural amber (amorphous) that has been aged for 20-million years has progressed about half way from the energy state of a glass formed by cooling a liquid at 10 K/min toward equilibrium crystals.[15]

The significantly lowered enthalpy of vapor-deposited glasses leaves us with great space of imagination in terms of strengthening chemical stability. At first glance, one may think that 10 J/g or about 3 kJ/mol is a small number for chemical reactions, as most reactions involve the energy activation barrier of about 50-100 kJ/mol. So how can vapor-deposited glasses resist chemical reactions significantly by adding an extra 3 kJ/mol to the energy barrier? However, if we consider the fact that organic crystals are way more stable than glasses for many reactions, and that vapor deposited glasses have explored 20% toward the crystal state, we might have a chance to acquire a significant effect in influencing chemical stability. One main topic of this thesis is to explore the chemical stability of vapor-deposited glasses and its dependence on glass packing.

The formation of stable glass with exceptional properties is attributed to high surface mobility at the glass/vacuum interface.[23] Organic molecules have been found to be more mobile at the free

surface relative to the bulk.[31-34] For example, Zhu et al measured the surface diffusion coefficient of indomethacin near T_g and found that the dynamics at the surface are about six orders of magnitude higher than that in the bulk. Figure 4 shows surface diffusion measurement for several molecules, and both small-molecule and polymeric systems show higher surface mobility near T_g.[31] High surface mobility persists below T_g, and the difference relative to the bulk becomes even larger as temperature decreases. Mobile molecules at the glass/vacuum interface have better opportunity to explore configuration space and reach lower positions on the potential energy landscape, compared to the aging process that happens in the bulk. As the deposition progresses, the molecules deposited at the interface will be highly mobile for a certain amount of time before they are buried and become the bulk. Then, new molecules arrive and rapidly sample configurations at the surface. This process will occur continuously until the end of the deposition when bulk films are formed. The deposition rate dependence of glass stability shown in Figure 3 is consistent with this explanation. As deposition rate decreases, molecules deposited at the interface have a longer time to find low energy configurations, and therefore obtain higher thermal stability, higher density, and lower enthalpy.

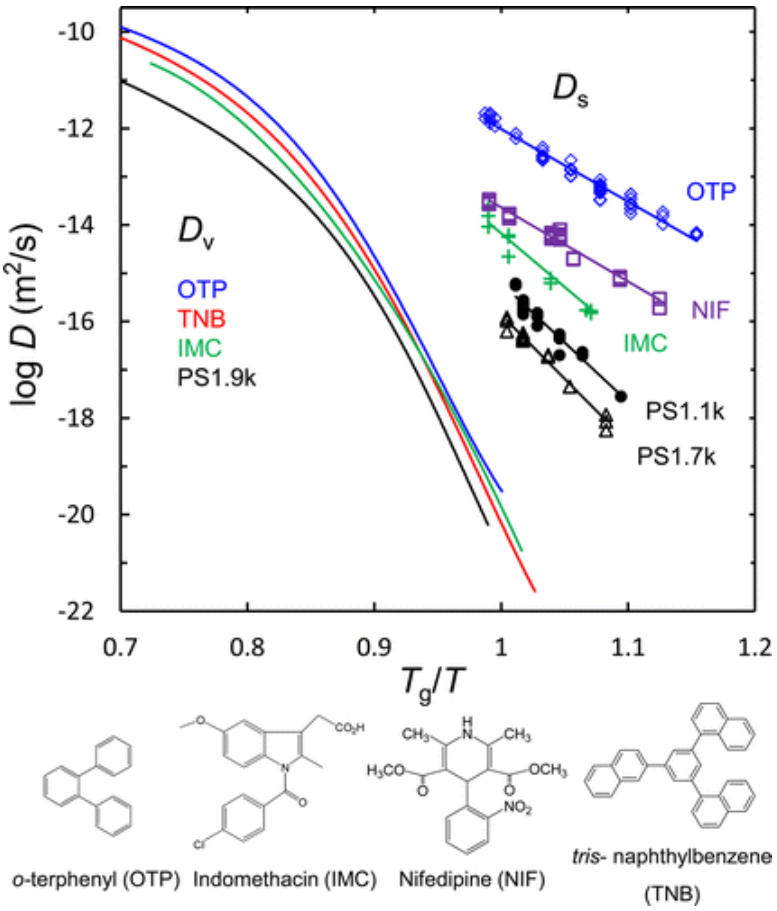

Figure 4. Surface and bulk diffusion coefficients (D_s and D_v) versus inverse temperature. The temperature has been scaled by the DSC T_g (onset): 307 K for PS1.1k, 319 K for PS1.7k, 246 K for OTP, 315 K for IMC and NIF, 347 K for TNB. Near T_g, surface mobility is much higher than the bulk. Bottom shows the molecular structure of four small molecules investigated in the figure. Adapted from Ref. #31 with permission.

More than thirty organic molecules have been reported to prepare stable glasses with exceptional thermal stability and low enthalpy, including simple aromatic hydrocarbons(toluene, ethylbenzene, and so on),[35, 36] pharmaceutical drugs (indomethacin, celecoxib, and so on),[37, 38] molecules with different shapes (linear and disk-shaped molecules),[39] and liquid crystals.[40] Some of the organic molecules have been used for manufacturing of organic electronics.[41] For example, TPD and NPD have been used as charge transport layers and DSA-Ph is a light emitter in OLEDs. The enhanced thermal stability of stable glasses may allow devices using those materials to survive longer at a higher temperature. Besides small organic molecules, vapor-deposition has also been used for polymeric materials. Guo et al. show that matrix-assisted pulsed laser evaporation (MAPLE) can prepare ultrastable and nanostructured glassy polymers which have a T_{onset} 40 K higher than the standard poly(methyl methacrylate) glass formed on cooling a liquid.[42] Recently, Yoon et al. reported stable polymeric glasses of Teflon AF 1600 prepared by vacuum pyrolysis deposition.[43] In this case, the fluoropolymer was thermally evaporated and underwent pyrolysis of the chain and re-polymerization at the substrate. Flash DSC results show that vapor-deposited Teflon had large enthalpy overshoot, consistent with small molecular glass, and fictive temperature of the most stable glass is 57 K lower than T_g. Stable glasses have also been made for metallic materials [44] and inorganic molecules of Sb_2Se_3,[45] both of which were prepared by physical vapor deposition.

Besides high thermal stability, high density, and low enthalpy, there are other outstanding characteristics displayed by vapor-deposited glasses. Examples include but not limited to (1) Vapor deposited indomethacin has enhanced mechanical properties, including higher mechanical moduli[46] and higher longitudinal sound velocities.[24] Utilizing Brillouin light scattering (BLS), stable glasses are found to have the elastic moduli up to 19% higher than the liquid-cooled glass. (2) Vapor-deposited glasses resist uptake of water vapor.[47] The most stable glass of indomethacin in this experiment shows a factor of 5 less water uptake relative to the liquid-

cooled glass. (3) β-relaxation in vapor deposited toluene[48] was reported to be suppressed by 70%; a similar suppression could be reached if a liquid-cooled glass has been physically aged for thousands of years. (4) Transformation of vapor-deposited glasses was found to be heterogeneous, as it initiated from the free surface and propagated into the bulk.[49-51] This is different from the behavior of the liquid-cooled glass, where transformation occurs to the bulk via a homogenous process. (5) Vapor-deposited glasses have shown anisotropic layering and molecular packing, while liquid-cooled glasses inherit the structure of liquids and typically display isotropic molecular orientation (random). The anisotropic packing and layering have been characterized by birefringence measurement,[6] dichroism measurement,[41] UV-Vis spectroscopy,[52] and X-ray scattering.[53]

1.3 Chemical stability in organic materials

Above, we have reviewed some general characteristics of glasses and extraordinary properties of vapor deposited glasses. A common theme running throughout is that all the above-mentioned examples have focused on physical, mechanical, and structural features, and few of them enter into the field of “chemistry”, where real bond rearrangements and electron transfer processes occur. In fact, in most cases when the chemical reaction is investigated in glasses, it comes along with the study of their counterparts, i.e. crystals. As there is a substantial body of evidence showing that amorphous materials are less stable than crystals, many people even believe that the solution to stability problems lies in the exclusion of amorphous forms.[54]

Recently, the development of technology in many areas, including pharmaceuticals and organic electronics, have adopted more and more use of amorphous materials, which raises problems of chemical stability that cannot be overlooked. This situation happens mainly because of two reasons. First, in some cases, amorphous materials are currently the easiest solution for certain purposes. For example, quinapril HCl (shown in Scheme 2), a pharmaceutical that treats high blood pressure, is not readily produced in a crystalline form.[55] Secondly, sometimes the glassy form is purposefully prepared to enhance pharmaceutical properties, such as dissolution and bioavailability,[56] or protein physical stability in lyophilized products.[57]

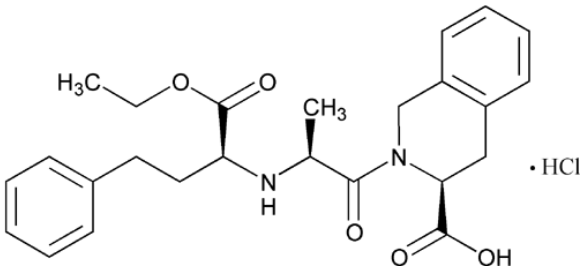

Scheme 2. Molecular structure of quinapril HCl. This molecule is used to treat high blood pressure, and is difficult to crystallize.

1.3.1 Glassy materials against crystallization

There is a substantial interest in developing methods to stabilize glasses in the amorphous phase, and previous efforts mainly focus on decreasing the mobility of drug molecules by mixing them with polymers. For example, furosemide has been reported to mix with Polyvinylpyrrolidone (PVP) by 40% w/w to stabilize the amorphous phase.[58] IR analyses indicated that the intermolecular frusemide-PVP hydrogen bond interaction in the solid state retards or inhibits drug recrystallization by reducing molecular motion in the solid state. PVD provides a new route to prepare materials with slower molecular mobility and enhanced stability against crystallization. For example, Rodriguez-Tinoco et al. reported that vapor-deposited celecoxib shows 30% slower surface crystal growth rate relative to the sample cooled from a melt.[38] They speculate that the surface crystal growth may be influenced by molecules located several molecular diameters deep into the glass, where stable glasses with slower mobility can

inhibit the crystal growth rate. This is the first demonstration that vapor-deposited glasses can resist crystallization with a substantial effect.

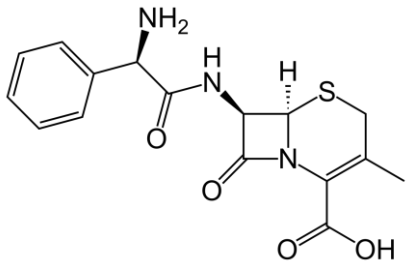

Scheme 3. Molecular structure of cephalexin. This antibiotic molecule is more supcecible to crystallization as humidity increases.

Moreover, PVD glass has less water uptake relative to the liquid-cooled glass, which might provide a further opportunity in suppressing crystal growth. It is well known that the crystal growth rate can be accelerated by the adsorption of water. For example, amorphous cephalexin (Scheme 3) absorbs a large amount of water once the relative humidity is over 75%. The analysis of crystallization of cephalexin shows that the crystal growth rate increases as the humidity increases.[59] This behavior has been explained by Zografi and co-workers who suggested that water acts as a plasticizer that lowers the glass transition temperature.[60] For vapor-deposited indomethacin, it shows that the most stable glass uptakes 20% water relative to the liquid-cooled glass.[47] This study provides a possible method to suppress crystallization of organic glasses by decreasing the water uptake.

1.3.2 Chemical stability of crystals

Organic molecules can have very different chemical reactivity in different crystal polymorphs, and this is known as topochemistry.[61] Depending on how the monomers are situated in the starting matrix and the distance between the bonds, a reaction may or may not proceed. And if it proceeds, the resulting molecules may be different for different polymorphs. Cohen and Schmidt have reported that, after light irradiation of the two polymorphs of *trans*-cinnamic acid, the stable form gives rise to α-truxillic acid whereas the metastable form produces mainly β-truxillic acid.[62] A more striking example was provided by tetrabenzoylethylene, which can undergo unimolecular photoisomerization. Of the two crystalline modifications, one polymorph is light-

stable, while the other photoisomerizes to the furanone (Scheme 4).[61] Schmidt has further suggested the topochemistry principle which states that the reaction will involve nearest-neighbor molecules or functional groups and will occur with minimum atomic and molecular movement.

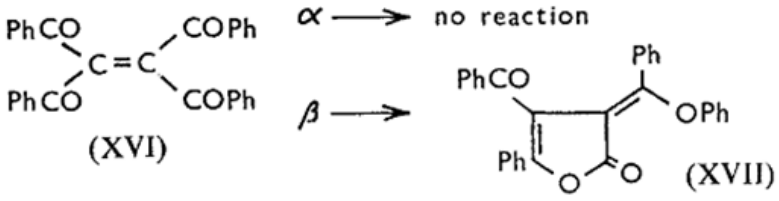

Scheme 4. Photoisomerization of tetrabenzoylethylene. Of the two polymorphs, the α form is light stable, while the β form rearranges to form furanone.

Photodegradation of organic crystals has been found to vary in different polymorphs. For example, for the three crystal polymorphs of carbamazepine, the rates of photodegradation vary by as much as a factor of 5.[63] Carbamazepine can be photodegraded and forms carbamazepine cyclobutane dimer and carbamazepine 10,11-epoxide. As another example, one of the three polymorphs of furosemide photodarkens at a one-sixth the rate of the other polymorphs when subjected to of UV irradiation.[64] These literature precedents indicate that some features of molecular packing can provide stronger resistance to photolytic degradation for one polymorph than the other.

1.3.3 Chemical stability of glasses

As metastable materials with increased enthalpy and molecular mobility, we would expect that glasses are more susceptible to chemical degradation than crystals. Figure 5 shows the photodegradation of nimodipine in both crystalline and glassy phases.[65] Quantification of nimodipine by HPLC analysis indicated that a 50 h irradiation resulted in an approximate 7% degradation of the crystalline phase. The amorphous phase exhibited greater photosensitivity at

approximately 40% degradation for the same irradiation time. Similar trends in chemical stability have also been observed for cyclization of spirapril HCl[55] and oxidation of DL-alanine-DL-methionine[66], where 15 and 3 times faster degradation rates were reported for amorphous forms relative to the crystals respectively. A more comprehensive investigation of the relationship between crystallinity and stability was reported by Pikal et al.[8] By measuring the chemical stability of amorphous cephalothin sodium with different crystallinity, a strong correlation was observed between increased crystalline fraction and decreased reaction rates. Among the investigated crystal/glass mixtures, the sample composed of the highest ratio of glasses (about 50%) degrades about 2 times faster than the neat crystalline sample.

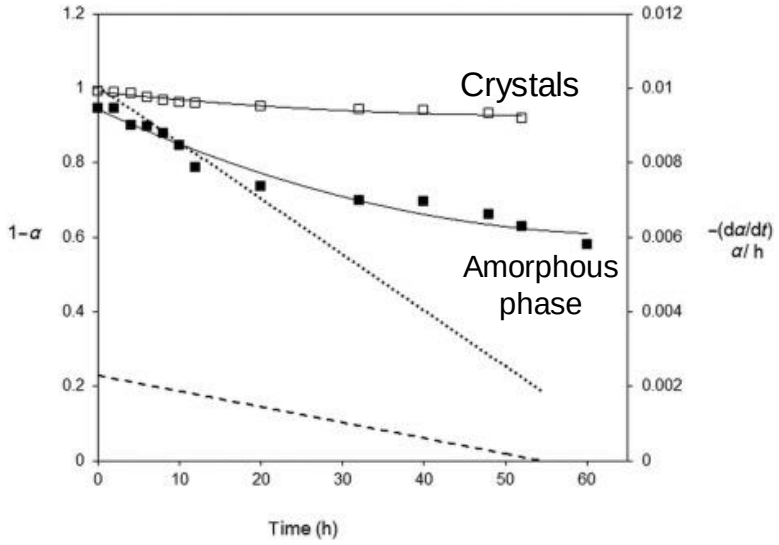

Figure 5. Photodegradation (represented as remaining fraction, 1 − α) of nimodipine samples for crystalline (□) and amorphous nimodipine (▪) as a function of exposure time (h). The solid lines represent the polynomial curve fits to the experimental data. Instantaneous degradation rates (fraction nimodipine degrading, α/h) for the crystalline (▪▪▪▪▪) and amorphous (------) phases are represented on the secondary axis. Adapted from Ref. #65 with permission.

There are several indications that density can play an important role in influencing chemical reactivity in glasses. For example, Royal and Torkelson reported that for 4,4'-diphenyl azobenzene dispersed in amorphous polycarbonate the susceptibility to photoisomerization decreased by about 5% after physical aging over 100 h, aging can increase the glass density slowly.[67] A large extent of density change has been realized by applying high external pressure. In an azobenzene derivative tethered to a PMMA polymer, it was demonstrated that optically induced molecular rearrangement can be hindered in high-density glasses created under high external pressure.[26] The glass density at 150 MPa was increased by 2.4%, and the rate of photo-orientation decreased by a factor of nearly 50. For photo-oxidation reactions in organic photovoltaic materials, it was also demonstrated that molecular packing affects the photo-oxidative stability and a correlation of increased density and decreased degradation rate was observed.[68]

The discovery of stable glasses prepared by vapor deposition provides a great opportunity to address questions of chemical reactivity and stability in glasses. As stable glasses have significantly higher density than the liquid-cooled glass, it worth investigating whether the high density will also lead to significantly enhanced chemical stability. Next, I will introduce several types of chemical reactions that will be investigated in this thesis.

1.4 Related chemical processes in organic materials

1.4.1 Photoisomerization

Azobenzene is a type of photochromic molecule that can undergo *trans-cis* photoisomerization when irradiated by light. The reverse *cis-trans* isomerization can be driven by light or thermal relaxation in the dark. Photochromic properties of azobenzene have been used as a light-triggered switch in many applications, including surface-modified materials,[69] protein probes,[70,

[71] molecular machines,[72, 73] and holographic gratings for recording devices[74, 75]. Unsubstituted azobenzene has two absorption bands in the UV-Vis spectrum. The strong UV band (λ = 320 nm) arises from the symmetry allowed π – π* transition and the much weaker band corresponds to the symmetry forbidden n – π* transition.[75, 76] The half-life of thermal *cis-trans* isomerization is about 2 days at room temperature in solutions, and can be years in the form of crystals.[77]

Substituents on the phenyl ring can produce significant influences on the optical properties and thermal isomerization rates for azobenzene derivatives. Historically, those derivatives have been divided into three categories, depending on the relative energies of the π – π* and n – π*, transitions-azobenzenes (ABn), aminoazobenzenes (aAB), and pseudostilbenes.[77] For example, push-pull azobenzenes (ppABs) is one type of pseudostilbene, which have a strong electron donor and a strong electron acceptor occupying the 4- and 4'- positions of the two phenyl rings. Compared to the unsubstituted azobenzene, ppABs have a large red-shift of the π - π* absorption band from the UV range into the visible spectrum such that it overlaps with the weaker n - π* transition.[78] The half-life of the thermal isomerization of *cis-trans* can be seconds to milliseconds,[79] which is much shorter than in the unsubstituted azobenzene.

Photoisomerization of azobenzenes has been reported to induce density decrease and anisotropic molecular alignment in glasses, which provide observables that can be measured to track the progress of photoreaction. The volume of *cis* azobenzene is larger than the *trans* as the *trans* form is a planer structure while the *cis* form is not. The *trans* → *cis* → *trans* cycling will disrupt packing in the glassy matrix and reduce the density, which is known as the photo-expansion effect.[80] The light-induced density decrease can be monitored by measuring the film thickness. When a *cis* azobenzene returns to the *trans* form after thermal relaxation, it doesn't necessarily have the same molecular orientation as it started with. Repeated photoisomerization with polarized light has the net effect of increasing the fraction of molecules whose transition dipoles are orthogonal to the excitation polarization because these molecules do not have the

opportunity for further photoisomerization. This effect is known as photo-alignment,[81] and the irradiated sample thus becomes anisotropic and birefringent.

1.4.2 Photodegradation

Photodegradation is responsible for the failure of many materials and devices in applications. In the pharmaceutical industry, many drugs have been reported to be susceptible to photodegradation.[63, 64, 82-84] Indomethacin, an anti-inflammatory drug, will undergo photodecarboxylation reaction and generate CO_2 when irradiated by UV light. Photodegradation can cause the drugs to lose efficiency or generate hazardous by-products. This is part of the reason why it is always suggested to avoid direct light exposure when storing drugs.

In the OLEDs, while some photodegradation occurs at the organic – metal electrode interface, there are also many reactions involving interactions within the bulk material. Some charge transport and light emitting molecules, such as α-NPD and TPD, are known to degrade (exhibiting changes in their absorption and photoluminescence emission) after UV irradiation of single layers in the air.[85] Other reports have shown that device degradation can also be induced by a combination of light and electric current. For example, Alq3-based OLED devices illuminated by UV-light show a decrease in the photoluminescence intensity during light exposure.[86] Similarly, Ir(ppy)3 doped into 4,4'-bis(3-methyl-carbazol-9-yl)-2,2'-biphenyl (mCBP) also shows degradation when running the devices under illumination.[87]

1.4.3 Solid-gas reaction

Solid-gas reaction represents a different reaction type than the above-mentioned photoreactions and can shorten the shelf life of pharmaceuticals and induce device failure in organic electronics. For example, the degradation of solid aspirin has been found to accelerate when exposed to high humidity, as aspirin can undergo hydrolysis with water vapor.[88] Also, OLEDs

are capsulated to avoid the direct contact with the water and oxygen in the air. Oxidation reactions have been reported for several OLED molecules.[68, 89].

Previous work has shown that crystal packing can control the reaction of crystal with gases. For example, pharmaceuticals with a carboxylic acid group can react with ammonia and give ammonium salts. Of the two polymorphs of indomethacin, α and γ, α-form reacts readily with ammonia while γ-form is inert to the reaction.[90] Other studies reveal that the crystal-ammonia reaction is anisotropic; ammonia reacts at different rates along different crystallographic directions. For 4-chlorobenzoic acid, the ammonia reacts preferentially on the $(2\bar{1}0)$, $(1\bar{1}0)$, (001) and $(\bar{1}01)$ faces.[91] Scheme 5 shows the crystal packing with respect to the Miller indices of the crystal faces. The anisotropic reaction has been attributed to the fact that penetration into the crystal from these faces allows the ammonia to react with the carboxyl groups. On the other hand, penetration from the (100) face would require the ammonia gas to pass through alternate layers of nonpolar functionalities, as shown in Scheme 5.

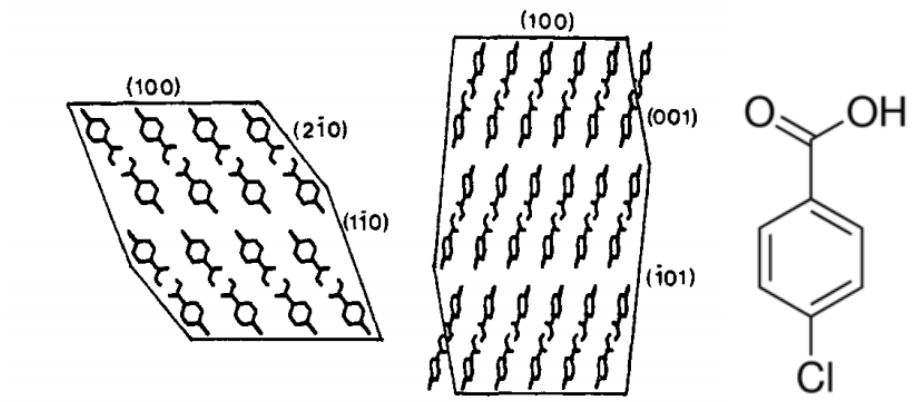

Scheme 5. Drawings of 4-chlorobenzoic acid crystals showing the idealized molecular arrangement at the major faces. Left: view along the c axis (a major zone axis of the crystal); Middle: view looking along b axis (the other major zone axis); Right: molecular structure of 4-chlorobenzoic acid. Adapted from Ref. #91 with permission.

1.5 Characterization methods of chemical reactions in glasses

This section will introduce some experimental methods developed to measure chemical reactions in glasses. Photoisomerization of DO37, an azobenzene derivative that has fast thermal relaxation, has been measured by spectroscopic ellipsometry (Chapter 2). Photoisomerization of 4,4'-diphenyl azobenzene (DPA), an azobenzene derivative with slow thermal relaxation, has been measured by UV-Vis spectroscopy (Chapter 3). Photodegradation and solid-ammonia reaction of indomethacin has been measured by quartz crystal microbalance (Chapter 4 & 5).

Ellipsometry

Ellipsometry is an optical method that can characterize amorphous thin films in the thickness range from nanometers to microns. It has several advantages over other methods of characterizing glassy thin films. First, amorphous materials lack long-range structural order, which renders traditional XRD ineffective here. Amorphous materials have a smooth surface and homogenous packing, which facilitates the precise measurement of sample thickness and refractive index by ellipsometry. Second, ellipsometry is well suits for film thicknesses in the range of application interest, as films used in organic electronics are typically 10-100 nm thick.[6] This can be challenging for methods that need large sample sizes, such as DSC and IR spectroscopy. Third, as an optical method that relies on the interference effect, ellipsometry is non-destructive to materials, which provides convenience for *in situ* experiments. In this thesis, ellipsometry will be employed in multiple tests, including thermal stability, density measurement, and the monitoring of photoisomerization reaction in glassy thin films.

Ellipsometry can precisely measure the interference during the light-material interaction by detecting subtle differences between the incident and reflected light. As shown in Scheme 6, the incident light goes into the thin film sample with a defined linear polarization, where the plane of

the of polarization is usually tilted at 45°. Therefore, the incident light can be divided into two beams of *s*-polarization and *p*-polarization with identical phase and amplitudes. After multiple constructive and destructive interferences in the thin film, the reflected light will have different phase and amplitude between the *s*, *p*-polarized beam, which can be monitored by the detector. The phase shift and amplitude change depend on the thickness and refractive index of the thin film. After an ellipsometry measurement, a model is required to simulate the sample thickness and optical index from the experimental data.

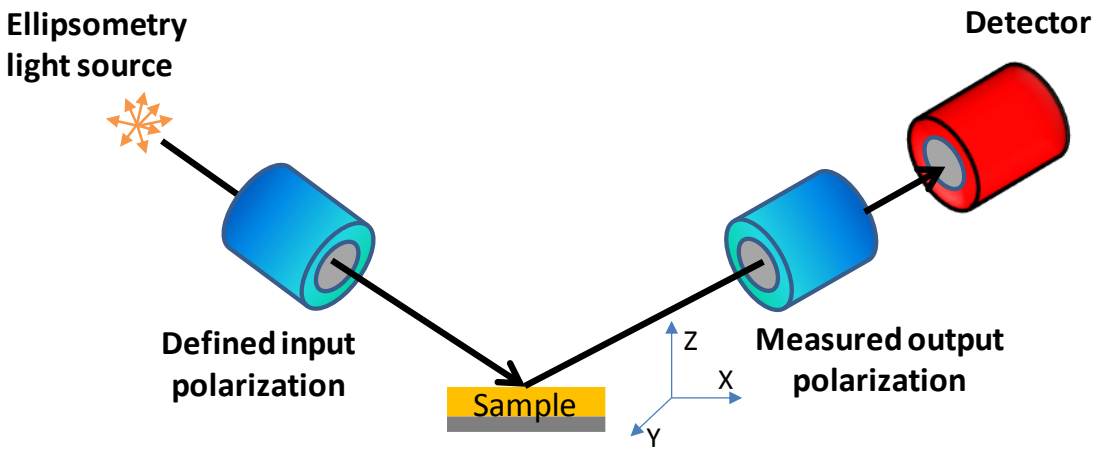

Scheme 6. Experimental test for photoisomerization measurement by ellipsometry. Light with a defined input polarization is reflected by a thin film sample. After constructive and distructive interference with the sample, reflected light with a different phase and polarization from its initial state will be collected and measured by the detector. The thickness, refractive index n, and birefringence are determined by fitting the experimental data to a model.

A model is needed after the ellipsometry measurement to calculate the sample thickness and refractive index. In this thesis, the vapor-deposited glass is described using a Cauchy model. Thickness and refractive index of thin films are fit to predict the phase shifts and polarization changes of light. The good match between predictions and experimental results indicates a successful modeling. Varied Angle Spectroscopic Ellipsometry (VASE) has a broad wavelength range (245 to 1000 nm) and varied angles of incident light (45 to 75°), which allows a systematic modeling for optical information collected at different wavelengths and angles at once. A previous study has reported the effectiveness of the Cauchy model for both isotropic and anisotropic glassy thin films.[37]

UV-Vis spectroscopy

UV-Vis spectroscopy is a common method to measure the electronic absorption of chemicals in solutions and solid states. For organic thin films, UV-Vis spectroscopy is able to non-destructively determine the film thickness and optical properties. Also, UV-Vis can conveniently analyze chemical species and monitor the evolution of chemical concentrations during a reaction, if the absorption characteristics are known. In this thesis, UV-Vis will be used to measure the photoisomerization process directly during light irradiation of 4,4'-diphenyl azobenzene (DPA), a non-push-pull azobenzene. As described in section 1.4.1, non-push-pull azobenzenes can have long thermal relaxations of the *cis* state once the *trans* molecule is photoisomerized, which allows unambiguous characterization of the population of *trans* and *cis* form during photoisomerization.

Figure 6. shows an example of non-push-pull azobenzene BF1AB during light irradiation,[92] where the half-life of BF1AB thermal relaxation is hours. The amorphous thin film started with all *trans*-state and has a maximum absorption at about 460 nm. Upon irradiation of 450 nm light, the *trans* molecule will photoisomerize and become *cis*. At the photostationary state, the equilibrium between the forward photoisomerization and the backward thermal relaxation is

reached, and the final state is a mixture of both *trans/cis*. Inspired by this study, in this thesis, UV-Vis will be used to monitor the photoisomerization of DPA, an azobenzene derivative with slow thermal relaxation.

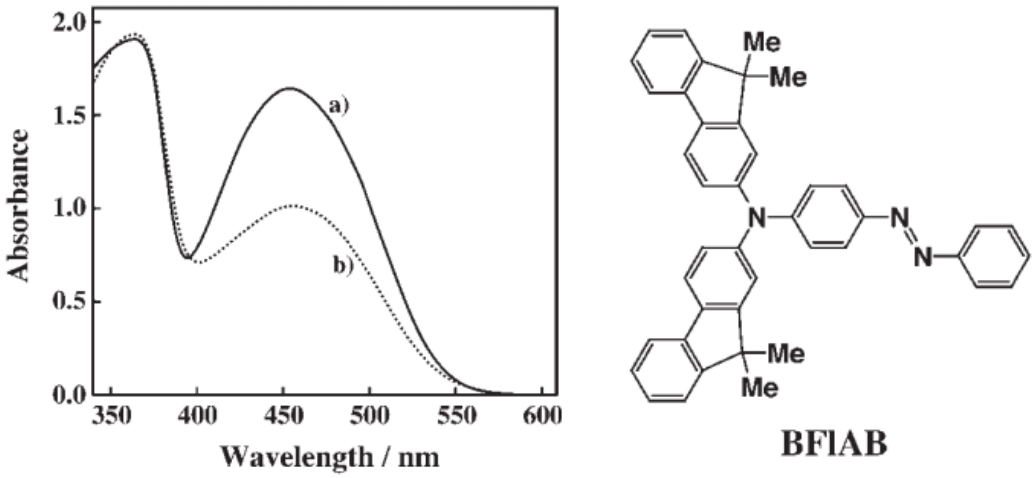

Figure 6. Electronic absorption spectral change of BF1AB amorphous film. Left: (Solid) before photoirradiation, (dotted) photostationary state upon irradiation with 450 nm light. Right: molecular structure of BF1AB. Adapted from Ref. #92 with permission.

Quartz crystal microbalance (QCM)

QCM will be used to measure two reaction types in glasses, photodecarboxylation and solid-ammonia reaction. QCM is widely used as a sensitive mass detector for gas uptake and thin film deposition techniques.[93] For films within the thickness range of 100 nm, the frequency shift of the resonator can be related to the mass change of the sample by the Sauerbrey equation[94]:

$$\Delta f = -\frac{2f_0^2}{A\sqrt{\rho_q \mu_q}}\Delta m \qquad (1)$$

In Equation 1, f_0 is the resonance frequency (Hz), Δf is the frequency change, Δm is the mass change, A is the piezoelectrically active crystal area, ρ_q is the density of quartz (2.648 g/cm^3), and μ_q is the shear modulus of quartz for the AT-cut crystal (2.947 x 10^{11} g·cm^{-1}·s^{-2}). Since f_0, A, ρ_q, and μ_q are all known, Δm can be calculated from Δf.

In a standard QCM measurement, glassy thin films of indomethacin will be vapor deposited at the gold-coated quartz crystal resonators suitable for use in the QCM. Each resonator substrate will have a direct contact with a copper finger, whose temperature can be controlled during deposition. After deposition, the photodecarboxylation reaction will be monitored by the mass loss during irradiation experiments, with CO_2 released during the process; the solid-ammonia reaction experiments will be monitored by the mass increase during the reaction, being an addition reaction that generates ammonium salts.

1.6 Contribution of this work

In this thesis, I investigate the influence of molecular packing in glasses on the chemical reactivity. I show that vapor-deposited glasses can have much stronger resistance against photoisomerization, photodecarboxylation, and solid-gas addition reactions relative to the liquid-

cooled glass. I find that chemical stability correlates with glass density, where high-density glasses are less reactive. Computer simulations performed by my collaborators reproduce many of the features of vapor-deposited glasses, and also show that vapor-deposited glasses are more photostable.

In Chapter 2, I show that photoisomerization of an azobenzene derivative can be suppressed by a factor of 50 relative to the liquid-cooled glass by vapor-depositing molecules at correct substrate temperatures. This is the first demonstration that vapor-deposition can make such an impact on the photostability of amorphous materials. The enhanced photostability was attributed to the extra constraint applied by the tight molecular packing on the chemical rearrangement during photoisomerization. My results are consistent with some recent studies showing that vapor-deposition can prepare organic glass with enhanced chemical stability. For example, in a work that compares the electroluminescence stability of devices made by solution-coating and vapor-deposition, it was found that solution-coated films are more susceptible to degradation relative to vapor-deposited glasses.[95] Faster degradation in the solution-coated films originated primarily from their different molecular packing and not due to chemical impurities.

In Chapter 3, I show that vapor-deposited hosts can also significantly decrease the photoisomerization of azobenzene guest molecules. Photoisomerization was directly monitored by the population of trans azobenzene, as characterized by UV-Vis spectroscopy. Photostability correlates with glass density, and a factor of 10 depression in photoreaction rate was observed in the most stable vapor-deposited glass. This study provides a new route to increase chemical stability by inserting molecules of interest into the tightly packed host.

In Chapter 4, I show that vapor-deposited organic glasses can be about a factor of 2 more resistant against photodecarboxylation reaction. Photostability correlates with glass density. When comparing the effect of enhanced photostability with the previous study in photoisomerization of azobenzene (Chapter 2&3), the same increase in glass density (1.3%)

has a much smaller impact, a factor of 2 vs. a factor of 10 or 50. Such a difference was attributed to the much smaller volume changes required by photodecarboxylation relative to the photoisomerization that involves a large configuration change.

In Chapter 5, I show the first demonstration that the chemical stability of organic glasses in mixtures can be substantially increased against the solid-gas reaction. Chemical stability correlates with glass density, which indicates the important role of density in influencing the solid-gas reactivity. After considering several factors that can be influenced by the glass packing, I suggest that a diminished solubility is most likely to be the reason for enhanced chemical stability.

In summary, my work suggests substrate temperature as a controllable variable during vapor-deposition to modulate the glass packing and substantially increase chemical stability. Consistent with this view, Esaki and coworkers recently reported that the electronic properties of films of organic semiconductors were more stable over time if vapor deposition conditions were optimized to prepare the highest density glasses.[96] Ràfols-Ribé et al. very recently investigated the decay of electroluminescence intensity in OLEDs and found that the optimum vapor-deposited glasses was deposited at the substrate temperature of 0.85 T_g, which is coincident with the glass with the highest density.[97] I hope that my work in this thesis provides a fundamental understanding of the enhanced chemical stability in organic glasses and add insights that allow for the improvement of device lifetimes.

1.7 References

[1] B. Lee, Review of the present status of optical fiber sensors. Opt. Fiber. Technol. **9** (2003) 57.

[2] R. Greco, and L. Nicolais, Glass transition temperature in nylons. Polymer **17** (1976) 1049.

[3] M. Telford, The case for bulk metallic glass. Mater. Today **7** (2004) 36.

[4] H. Mesallati *et al.*, Preparation and characterization of amorphous ciprofloxacin-amino acid salts. Eur. J. Pharm. Biopharm. **121** (2017) 73.

[5] B. C. Hancock, and G. Zografi, Characteristics and significance of the amorphous state in pharmaceutical systems. J. Pharm. Sci. **86** (1997) 1.

[6] D. Yokoyama, Molecular orientation in small-molecule organic light-emitting diodes. J. Mater. Chem. **21** (2011) 19187.

[7] B. C. Hancock, and M. Parks, What is the true solubility advantage for amorphous pharmaceuticals? Pharm. Res. **17** (2000) 397.

[8] M. J. Pikal *et al.*, Quantitative crystallinity determinations for β-lactam antibiotics by solution calorimetry: Correlations with stability. J. Pharm. Sci. **67** (1978) 767.

[9] S. Scholz *et al.*, Degradation mechanisms and reactions in organic light-emitting devices. Chem. Rev. **115** (2015) 8449.

[10] Y. Zhang, J. Lee, and S. R. Forrest, Tenfold increase in the lifetime of blue phosphorescent organic light-emitting diodes. Nat. Comm. **5** (2014) 5008.

[11] Q. Wang, Y. Luo, and H. Aziz, Photodegradation of the organic/metal cathode interface in organic light-emitting devices. Appl. Phys. Lett. **97** (2010) 063309.

[12] M. D. Ediger, C. A. Angell, and S. R. Nagel, Supercooled liquids and glasses. J. Phys. Chem. **100** (1996) 13200.

[13] P. G. Debenedetti, and F. H. Stillinger, Supercooled liquids and the glass transition. Nature **410** (2001) 259.

[14] E. Gruber, L. G. E. Struik: Physical aging in amorphous polymers and other materials. Elsevier sci. Publ. Comp., amsterdam-oxford-new york 1978. 229 seiten, 141 abbildungen, preis: Us $ 42,50, holl. Gulden 97,50. Ber. Bunsenges. Phys. Chem. **82** (1978) 1019.

[15] J. Zhao, S. L. Simon, and G. B. McKenna, Using 20-million-year-old amber to test the super-arrhenius behaviour of glass-forming systems. Nat. Commun. **4** (2013) 1783.

[16] M. J. Pikal, *Freeze-drying of proteins* (American Chemical Society, ACS Symposium Series, 1994), Vol. 567, Formulation and delivery of proteins and peptides, 8.

[17] X. Chen, and T. T. Öpöz, Effect of different parameters on grinding efficiency and its monitoring by acoustic emission. Prod. & Manuf. Res. **4** (2016) 190.

[18] D. M. Mattox, in *Handbook of physical vapor deposition (pvd) processing (second edition)*, edited by D. M. Mattox (William Andrew Publishing, Boston, 2010), pp. 195.

[19] M. D. Ediger, Perspective: Highly stable vapor-deposited glasses. J. Chem. Phys. **147** (2017) 210901.

[20] S. M. Rossnagel, Thin film deposition with physical vapor deposition and related technologies. J. Vac. Sci. Technol. A **21** (2003) S74.

[21] H. Hikawa, M. Oguni, and H. Suga, Construction of an adiabatic calorimeter for a vapor-deposited sample and thermal characterization of amorphous butyronitrile. J. Non-Cryst. Solids **101** (1988) 90.

[22] K. Takeda *et al.*, Calorimetric study on structural relaxation of 1-pentene in vapor-deposited and liquid-quenched glassy states. The Journal of Physical Chemistry **99** (1995) 1602.

[23] S. F. Swallen *et al.*, Organic glasses with exceptional thermodynamic and kinetic stability. Science **315** (2007) 353.

[24] S. S. Dalal, Z. Fakhraai, and M. D. Ediger, High-throughput ellipsometric characterization of vapor-deposited indomethacin glasses. J. Phys. Chem. B **117** (2013) 15415.

[25] S. S. Dalal *et al.*, Density and birefringence of a highly stable α,α,β-trisnaphthylbenzene glass. J. Chem. Phys. **136** (2012) 204501.

[26] Z. Sekkat, G. Kleideiter, and T. Knoll, Optical orientation of azo dye in polymer films at high pressure. J. Opt. Soc. Am. B-Opt. Phys. **18** (2001) 1854.

[27] C. Rodríguez-Tinoco *et al.*, Ultrastable glasses portray similar behaviour to ordinary glasses at high pressure. Sci. Rep. **6** (2016) 34296.

[28] T. Liu *et al.*, The effect of chemical structure on the stability of physical vapor deposited glasses of 1,3,5-triarylbenzene. J. Chem. Phys. **143** (2015) 084506.

[29] K. L. Kearns, P. Krzyskowski, and Z. Devereaux, Using deposition rate to increase the thermal and kinetic stability of vapor-deposited hole transport layer glasses via a simple sublimation apparatus. J. Chem. Phys. **146** (2017) 203328.

[30] K. L. Kearns *et al.*, Hiking down the energy landscape: Progress toward the kauzmann temperature via vapor deposition. J. Phys. Chem. B **112** (2008) 4934.

[31] W. Zhang, and L. Yu, Surface diffusion of polymer glasses. Macromolecules **49** (2016) 731.

[32] J. A. Forrest *et al.*, Effect of free surfaces on the glass transition temperature of thin polymer films. Phys. Rev. Lett. **77** (1996) 2002.

[33] C. W. Brian, and L. Yu, Surface self-diffusion of organic glasses. J. Phys. Chem. A **117** (2013) 13303.

[34] L. Zhu *et al.*, Surface self-diffusion of an organic glass. Phys. Rev. Lett. **106** (2011) 256103.

[35] E. Leon-Gutierrez *et al.*, Stability of thin film glasses of toluene and ethylbenzene formed by vapor deposition: An in situ nanocalorimetric study. PCCP **12** (2010) 14693.

[36] M. Ahrenberg *et al.*, In situ investigation of vapor-deposited glasses of toluene and ethylbenzene via alternating current chip-nanocalorimetry. J. Chem. Phys. **138** (2013) 024501.

[37] S. S. Dalal, and M. D. Ediger, Molecular orientation in stable glasses of indomethacin. J. Phys. Chem. Lett. **3** (2012) 1229.

[38] C. Rodriguez-Tinoco *et al.*, Highly stable glasses of celecoxib: Influence on thermo-kinetic properties, microstructure and response towards crystal growth. J. Non-Cryst. Solids **407** (2015) 256.

[39] D. M. Walters *et al.*, Influence of molecular shape on the thermal stability and molecular orientation of vapor-deposited organic semiconductors. J. Phys. Chem. Lett. **8** (2017) 3380.

[40] J. Gómez *et al.*, Nematic-like stable glasses without equilibrium liquid crystal phases. J. Chem. Phys. **146** (2017) 054503.

[41] S. S. Dalal *et al.*, Tunable molecular orientation and elevated thermal stability of vapor-deposited organic semiconductors. Proc. Natl. Acad. Sci. U.S.A. **112** (2015) 4227.

[42] Y. Guo *et al.*, Ultrastable nanostructured polymer glasses. Nat. Mater. **11** (2012) 337.

[43] H. Yoon *et al.*, An ultrastable polymeric glass: Amorphous fluoropolymer with extreme fictive temperature reduction by vacuum pyrolysis. Macromolecules **50** (2017) 4562.

[44] P. Luo *et al.*, Ultrastable metallic glasses formed on cold substrates. Nat. Comm. **9** (2018) 1389.

[45] K. Zhang *et al.*, Ultrastable amorphous Sb2Se3 film. J. Phys. Chem. B **121** (2017) 8188.

[46] K. L. Kearns *et al.*, High-modulus organic glasses prepared by physical vapor deposition. Adv. Mater. **22** (2010) 39.

[47] K. J. Dawson *et al.*, Highly stable indomethacin glasses resist uptake of water vapor. J. Phys. Chem. B **113** (2009) 2422.

[48] H. B. Yu *et al.*, Suppression of β relaxation in vapor-deposited ultrastable glasses. Phys. Rev. Lett. **115** (2015) 185501.

[49] D. M. Walters, R. Richert, and M. D. Ediger, Thermal stability of vapor-deposited stable glasses of an organic semiconductor. J. Chem. Phys. **142** (2015) 134504.

[50] A. Sepúlveda *et al.*, Stable glasses of indomethacin and α,α,β-tris-naphthylbenzene transform into ordinary supercooled liquids. J. Chem. Phys. **137** (2012) 204508.

[51] S. F. Swallen *et al.*, Stable glass transformation to supercooled liquid via surface-initiated growth front. Phys. Rev. Lett. **102** (2009) 065503.

[52] S. Yoshiya, S. Maki, and Y. Daisuke, Simple model-free estimation of orientation order parameters of vacuum-deposited and spin-coated amorphous films used in organic light-emitting diodes. Appl. Phys. Express **8** (2015) 096601.

[53] A. Gujral *et al.*, Structural characterization of vapor-deposited glasses of an organic hole transport material with x-ray scattering. Chem. Mater. **27** (2015) 3341.

[54] S. R. Byrn, R. R. Pfeiffer, and J. G. Stowell, *Solid-state chemistry of drugs* (SSCI, Inc., 3065 Kent Avenue, West Lafayette, Indiana 47906-1076, 1999), Second edn., 256.

[55] Y. Guo, S. R. Byrn, and G. Zografi, Physical characteristics and chemical degradation of amorphous quinapril hydrochloride. J. Pharm. Sci. **89** (2000) 128.

[56] A. Newman, G. Knipp, and G. Zografi, Assessing the performance of amorphous solid dispersions. J. Pharm. Sci. **101** (2012) 1355.

[57] J. J. Hill, E. Y. Shalaev, and G. Zografi, Thermodynamic and dynamic factors involved in the stability of native protein structure in amorphous solids in relation to levels of hydration. J. Pharm. Sci. **94** (2005) 1636.

[58] C. Doherty, and P. York, Accelerated stability of an x-ray amorphous frusemide-polyvinylpyrrolidone solid dispersion. Drug Dev. Ind. Pharm. **15** (1989) 1969.

[59] M. Otsuka, and N. Kaneniwa, Hygroscopicity and solubility of noncrystalline cephalexin. Chem. Pharm. Bull **31** (1983) 230.

[60] C. Ahlneck, and G. Zografi, The molecular basis of moisture effects on the physical and chemical stability of drugs in the solid state. Int. J. Pharm **62** (1990) 87.

[61] M. D. Cohen, and G. M. J. Schmidt, 383. Topochemistry. Part i. A survey. J. Chem. Soc. (1964) 1996.

[62] G. M. J. Schmidt, Photodimerization in the solid state. Pure Appl. Chem. **27** (1971) 647.

[63] Y. Matsuda *et al.*, Pharmaceutical evaluation of carbamazepine modifications: Comparative study for photostability of carbamazepine polymorphs by using fourier-transformed reflection-

absorption infrared spectroscopy and colorimetric measurement. J. Pharm. Pharmacol. **46** (1994) 162.

[64] Y. Matsuda, and E. Tatsumi, Physicochemical characterization of furosemide modifications. Int. J. Pharm. **60** (1990) 11.

[65] D. Grooff *et al.*, Photostability of crystalline versus amorphous nifedipine and nimodipine. J. Pharm. Sci. **102** (2013) 1883.

[66] W. Xu, Investigation of solid-state stability of selected bioactive compounds (Purdue University, West Lafayette, IN, 1997).

[67] J. S. Royal, and J. M. Torkelson, Photochromic and fluorescent probe studies in glassy polymer matrices. 5. Effects of physical aging on bisphenol a polycarbonate and poly(vinyl acetate) as sensed by a size distribution of photochromic probes. Macromolecules **25** (1992) 4792.

[68] W. R. Mateker *et al.*, Molecular packing and arrangement govern the photo-oxidative stability of organic photovoltaic materials. Chem. Mater. **27** (2015) 6345.

[69] F. Violetta *et al.*, Light-powered electrical switch based on cargo-lifting azobenzene monolayers. Angew. Chem. Int. Ed. **47** (2008) 3407.

[70] M. R. Banghart *et al.*, Photochromic blockers of voltage-gated potassium channels. Angew. Chem. Int. Ed. **48** (2009) 9097.

[71] Y. Kim *et al.*, Using photons to manipulate enzyme inhibition by an azobenzene-modified nucleic acid probe. Proc. Natl. Acad. Sci. U.S.A. **106** (2009) 6489.

[72] T. Muraoka, K. Kinbara, and T. Aida, Mechanical twisting of a guest by a photoresponsive host. Nature **440** (2006) 512.

[73] H. Murakami *et al.*, A light-driven molecular shuttle based on a rotaxane. J. Am. Chem. Soc. **119** (1997) 7605.

[74] X. L. Jiang *et al.*, Unusual polarization dependent optical erasure of surface relief gratings on azobenzene polymer films. Appl. Phys. Lett. **72** (1998) 2502.

[75] K. Kreger *et al.*, Stable holographic gratings with small-molecular trisazobenzene derivatives. J. Am. Chem. Soc. **132** (2010) 509.

[76] T. Cusati *et al.*, Oscillator strength and polarization of the forbidden n→π* band of trans-azobenzene: A computational study. J. Chem. Phys. **128** (2008) 194312.

[77] H. M. D. Bandara, and S. C. Burdette, Photoisomerization in different classes of azobenzene. Chem. Soc. Rev. **41** (2012) 1809.

[78] B. Schmidt *et al.*, Femtosecond fluorescence and absorption dynamics of an azobenzene with a strong push−pull substitution. J. Phys. Chem. A **108** (2004) 4399.

[79] G. Kathrin, K. Helmut, and Q. Konrad, Rate constants of the thermal cis-trans isomerization of azobenzene dyes in solvents, acetone/water mixtures, and in microheterogeneous surfactant solutions. Int. J. Chem. Kinet. **31** (1999) 337.

[80] O. M. Tanchak, and C. J. Barrett, Light-induced reversible volume changes in thin films of azo polymers: The photomechanical effect. Macromolecules **38** (2005) 10566.

[81] Z. Sekkat *et al.*, in *Optical Science, Engineering and Instrumentation '97* (SPIE, 1997), p. 25.

[82] J. O. Williams, Structural imperfections in solid state chemistry. Sci. Prog. **64** (1977) 247.

[83] N. J. Karch *et al.*, X-ray and electron paramagnetic resonance structural investigation of oxygen discrimination during the collapse of methyl-benzoyloxy radical pairs in crystalline acetyl benzoyl peroxide. J. Am. Chem. Soc. **97** (1975) 6729.

[84] K. L. Camera *et al.*, Photopatterning of indomethacin thin films: A solvent-free vapor-deposited photoresist. ACS Appl. Mater. Interfaces **7** (2015) 23398.

[85] Y. Qiu, and J. Qiao, Photostability and morphological stability of hole transporting materials used in organic electroluminescence. Thin Solid Films **372** (2000) 265.

[86] X. Z. Wang *et al.*, Photodegradation of organic light-emitting devices observed in nitrogen-filled environment. Thin Solid Films **516** (2008) 2171.

[87] N. C. Giebink *et al.*, Direct evidence for degradation of polaron excited states in organic light emitting diodes. J. Appl. Phys. **105** (2009) 124514.

[88] L. J. Leeson, and A. M. Mattocks, Decomposition of aspirin in the solid state. J. Am. Pharm. Assoc. (Scientific ed.) **47** (1958) 329.

[89] Z. Kin, H. Kajii, and Y. Ohmori, Patterning of organic light-emitting diodes utilizing a sputter deposited amorphous carbon nitride buffer layer. Thin Solid Films **499** (2006) 392.

[90] X. Chen *et al.*, Reactivity differences of indomethacin solid forms with ammonia gas. J. Am. Chem. Soc. **124** (2002) 15012.

[91] R. S. Miller, I. C. Paul, and D. Y. Curtin, Reactions of molecular crystals with gases. Ii. X-ray structure of crystalline 4-chlorobenzoic acid and the anisotropy of its reaction with ammonia gas. J. Am. Chem. Soc. **96** (1974) 6334.

[92] H. Nakano *et al.*, Formation of a surface relief grating using a novel azobenzene-based photochromic amorphous molecular material. Adv. Mater. **14** (2002) 1157.

[93] L. Banda, M. Alcoutlabi, and G. B. McKenna, Errors induced in quartz crystal mass uptake measurements by nongravimetric effects: Considerations beyond the eernisse caution. J. Polym. Sci. B **44** (2006) 801.

[94] G. Sauerbrey, Verwendung von schwingquarzen zur wägung dünner schichten und zur mikrowägung. Z. Phys. **155** (1959) 206.

[95] Y. J. Cho, and H. Aziz, Root causes of the limited electroluminescence stability of organic light-emitting devices made by solution-coating. ACS Appl. Mater. Interfaces **10** (2018) 18113.

[96] Y. Esaki *et al.*, Enhanced electrical properties and air stability of amorphous organic thin films by engineering film density. J. Phys. Chem. Lett. **8** (2017) 5891.

[97] J. Ràfols-Ribé *et al.*, High-performance organic light-emitting diodes comprising ultrastable glass layers. Sci. Adv. **4** (2018) eaar8332.

Chapter 2

Photostability can be significantly modulated by molecular packing in glasses

Yue Qiu, Lucas W. Antony, Juan J. de Pablo, M. D. Ediger

Published in *J. Am. Chem. Soc.*, 2016, **138**, 11282–11289

Abstract

While previous work has demonstrated that molecular packing in organic crystals can strongly influence photochemical stability, efforts to tune photostability in amorphous materials have shown much smaller effects. Here we show that physical vapor deposition can substantially improve the photostability of organic glasses. Disperse Orange 37 (DO37), an azobenzene derivative, is studied as a model system. Photostability is assessed through changes in the density and molecular orientation of glassy thin films during light irradiation. By optimizing the substrate temperature used for deposition, we can increase photostability by a factor of 50 relative to the liquid-cooled glass. Photostability correlates with glass density, with density increases of up to 1.3%. Coarse-grained molecular simulations, which mimic glass preparation and the photoisomerization reaction, also indicate that glasses with higher density have substantially increased photostability. These results provide insights that may assist in the design of organic photovoltaics and light emission devices with longer lifetimes.

2.1 Introduction

Glasses are amorphous materials that have wide usage in modern technology, including polymers,[1] pharmaceuticals,[2] solar cells[3] and organic electronics.[4,5] For many applications, organic materials prepared as amorphous states are preferred over crystalline solids. For example, in the pharmaceutical industry, some drugs are formulated as glasses due to their higher solubility and bioavailability.[6,7] In the organic electronics field, glasses are frequently used in device fabrication to provide smooth and homogeneous layers.[4] One important issue for organic glasses is photochemical stability. Photodegradation can cause the failure of organic electronics in both display and light harvesting technologies, and this is sometimes a more limiting factor than device efficiency.[8,9] As photodegradation can be caused by light in the environment or by self-emission,[9,10] photochemically robust materials are in demand.[10,11]

Previous work has shown that modification of local packing in glasses has a negligible effect on photostability in comparison to what has been observed for crystalline materials. Organic molecules can have very different photoreactivities in different crystal polymorphs. In pioneering work in topochemistry, Schmidt *et al.* studied the [2+2] photodimerization of cinnamic acid in the solid state. This compound crystallizes in three polymorphic forms which exhibit different photochemical reactivity upon irradiation.[12] An even more striking example is provided by tetrabenzoylethylene, which can undergo unimolecular photoisomerization. Of the two crystalline modifications, one polymorph is light stable while the other photoisomerizes to the furanone.[13] In contrast, for amorphous materials, it has been found that photoreactivity depends only slightly on the manner in which the glass is prepared. Torkelson *et al.* reported that, for 4,4'-diphenyl azobenzene dispersed in amorphous polycarbonate, the susceptibility to photoisomerization decreased by about 5% after physical aging for 100 hours; aging generally increases the density of a glass.[14] We are not aware of a literature precedent showing significant tuning of photoreactivity in organic glasses through control of local packing.

Recently, physical vapor deposition (PVD) has been used to prepare glasses with exceptional properties that are not accessible by any other preparation method.[15-20] By properly controlling processing conditions such as deposition rate and substrate temperature, vapor deposition can form *stable glasses* that have higher density and enhanced kinetic stability relative to that of traditional liquid-cooled glasses. Typically, the optimal substrate temperature for preparing these PVD glasses is about 0.85 T_g, where T_g is the glass transition temperature. Vapor-deposited glasses can exhibit enhanced kinetic stability; upon heating at a constant rate a stable glass can maintain its glassy packing to a much higher temperature than a liquid-cooled glass. Vapor-deposited glasses also have densities up to 1.4% higher than the corresponding liquid-cooled glass.[21] It has been estimated that a liquid-cooled glass would have to be physically aged for thousands to millions of years to achieve a glass with the same density.[22] Many of the features observed in experimental PVD glasses, including high density and high kinetic stability, have also been observed in computer simulations that mimic the vapor deposition process.[20,23,24]

In this work, we test whether the extraordinary kinetic stability and high density of PVD glasses also lead to extraordinary photostability. As a model system, we investigate the photostability of vapor-deposited and liquid-cooled glasses of 3-[[4-(2,6-dichloro-4-nitrophenyl)azo]-*N*-ethylanilino]-propionitrile (also known as Disperse Orange 37 or DO37), an azobenzene derivative. Azobenzenes can undergo *trans*->*cis* photoisomerization reactions when irradiated by light; the *cis* state will relax back to the *trans* state spontaneously, as the *trans* state is thermodynamically more stable. We vapor-deposited DO37 onto substrates held at different temperatures and successfully obtained glasses with different initial densities and a wide range of kinetic stabilities. Using spectroscopic ellipsometry, the photostability of the different DO37 glasses during light irradiation was characterized by changes in the glass density and birefringence. In this way, the photostability of a series of glasses with identical composition but different densities could be easily compared.

We find that photostability of vapor-deposited DO37 glasses can be significantly modulated through the choice of substrate temperature. The most photostable PVD glass is 50 times more resistant to light irradiation than the liquid-cooled glass. We observe that photostability is highly correlated with the density of the vapor-deposited glasses. Molecular simulations of photoisomerization in vapor-deposited glasses are able to capture the key features observed in the experiments, and provide further molecular-level insight into the mechanism of stability. In particular, the tight molecular packing of the denser glass creates higher energy barriers for molecular rearrangement which then inhibit the photoisomerization reaction. We expect that enhanced photostability is a general property of dense vapor-deposited glasses that may also be exploited with other molecular systems, including those used in organic electronics.

2.2 Results and Discussion

2.2.1 Vapor-deposited DO37 forms glasses with high kinetic stability

As an initial step in these experiments, we used spectroscopic ellipsometry to characterize the kinetic stability and density of PVD glasses of DO37. Figure 1 shows an example of a temperature-ramping experiment for a DO37 glass vapor-deposited at $T_{substrate}$ = 260 K (0.88 T_g). Three different ramping cycles were performed. In the first cycle, the as-deposited sample was first heated from 288 K to 320 K and then cooled back to 288 K. Subsequent heating and cooling cycles between 288 K to 310 K are also shown, and all heating/cooling rates were 1 K/min. During the first cycle of heating, the initial increase in thickness (below 303 K) is due to thermal expansion of the as-deposited glass. At the onset temperature (T_{onset}), the as-deposited glass begins to transform into a super-cooled liquid. During subsequent cooling, the super-cooled liquid falls out of equilibrium and transforms into a glass at T_g. As expected, the second and third cooling runs shown in Figure 1 are indistinguishable from the first cooling since they all started in the equilibrium supercooled liquid.

The as-deposited glass of DO37 in Figure 1 shows high kinetic stability and high density relative to the liquid-cooled glass. The high T_{onset} (12 K above T_g) required to transform the as-deposited glass into the supercooled liquid is an indication of enhanced kinetic stability. The change in thickness between the first heating and cooling cycles is used to determine the density of the as-deposited glass relative to the liquid-cooled glass ($\Delta\rho$). In this case, the as-deposited glass is 1.3% more dense, consistent with more efficient local packing and higher kinetic stability. Vapor-deposited glasses of DO37 have properties similar to other PVD glasses with high kinetic stability.[15,16,18,19,25-28] For comparison, indomethacin, an extensively studied system, has been reported to form glasses with T_{onset} as high as 18 K above T_g, along with density increases of up to 1.4%.[21]

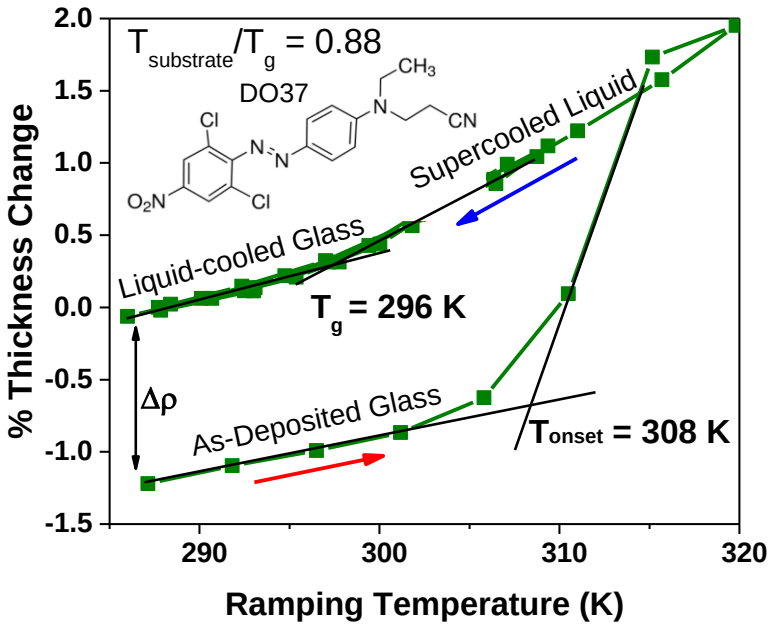

Figure 1. Thickness changes for a vapor-deposited glass of DO37 during temperature ramping at 1 K/min. The green symbols represent experimental data for a sample prepared at $T_{substrate}$ = 0.88 T_g. Black lines are linear extrapolations that demonstrate the determination of T_g (for the liquid-cooled glass) and the onset temperature T_{onset} (for the as-deposited glass). $\Delta\rho$ shows the density difference between the as-deposited and liquid-cooled glass. The inset shows the molecular structure of DO37.

The kinetic stability of vapor-deposited DO37 glasses depends on the choice of substrate temperature during PVD. As indicated by the inset in Figure 2, DO37 glasses were prepared on a substrate that had an imposed temperature gradient ranging from 0.75 T_g to above T_g. In this way, a library of glasses was prepared in one deposition. The detailed method of sample preparation is presented in the Methods section. For glasses deposited above T_g (296 K), the as-deposited sample had the same onset temperature as the liquid-cooled glass. For $T_{substrate}$ lower than T_g, enhanced kinetic stability was obtained. The optimal $T_{substrate}$ for kinetic stability is 0.88 T_g (Figure 2), which is similar to indomethacin and other molecular systems.[22] The increased kinetic stability and density of vapor-deposited films is attributed to enhanced surface mobility during film formation.[24,29,30] Freshly deposited molecules have enough mobility to efficiently sample packing arrangements, resulting in near-equilibrium local packing well below T_g; subsequent deposition locks this efficient packing into the glassy film. The optimal stability obtained by deposition onto substrates near 0.88 T_g is a result of the competition between kinetic and thermodynamic control.[22] At lower temperature surface mobility is not high enough to allow access to better packing arrangements even though the thermodynamic driving force is larger.

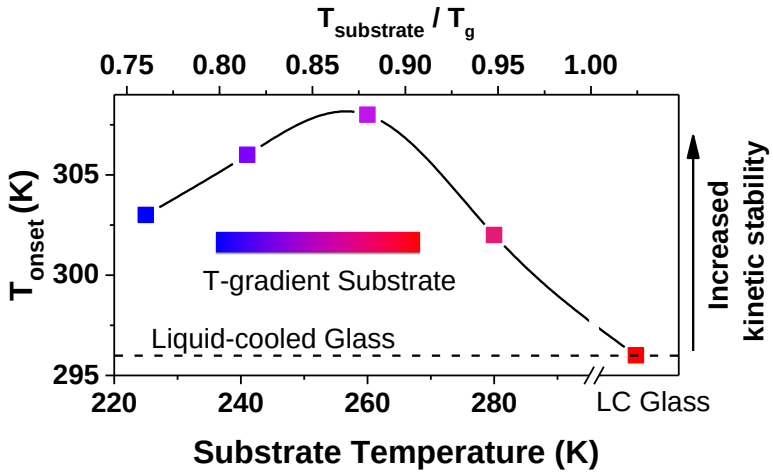

Figure 2. Kinetic stability of DO37 glasses vapor-deposited at different substrate temperatures. T_{onset} represents the onset of glass transformation during heating of 1 K/min. All glasses were prepared during one deposition on a temperature gradient substrate. The inset schematically indicates a temperature-gradient across the substrate. The solid black line is a guide to the eye.

2.2.2 PVD glasses exhibit enhanced photostability

The photostability of DO37 glasses was monitored by spectroscopic ellipsometry during light irradiation. Density and birefringence, representing molecular packing and molecular orientation respectively, can be obtained by ellipsometry and were used to characterize photostability of the glassy thin films. As shown in Scheme 1, a 532 nm laser was used to irradiate the thin glass samples and induce photoisomerization. Simultaneously, spectroscopic ellipsometry measured the thickness and birefringence changes in the irradiated area. Since the in-plane sample dimensions are fixed, density is inversely related to thickness.

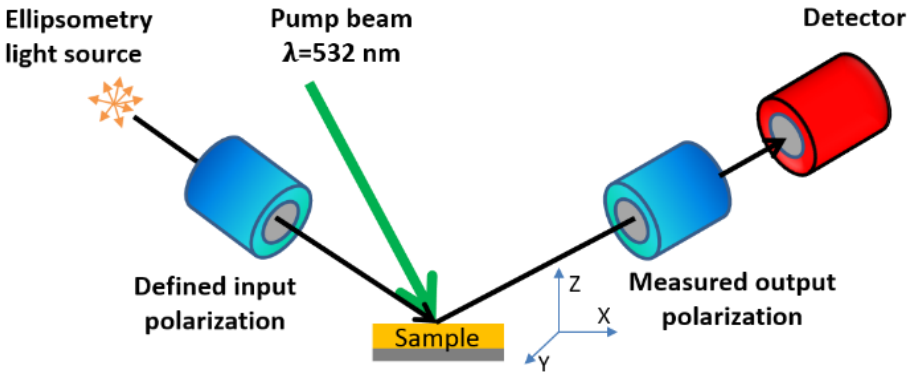

Scheme 1. Experimental test of photostability for glassy thin films. A 532 nm laser is used to irradiate the DO37 thin film inducing photoisomerization. Simultaneously, spectroscopic ellipsometry is used to measure thickness and birefringence changes in the film.

A comparison of the light-induced density and birefringence changes for PVD and liquid-cooled glasses, as shown in Figure 3, reveals that the PVD glasses display significantly enhanced photostability. The density of the liquid-cooled glass decreases immediately after irradiation begins and reaches steady-state in tens of seconds. In contrast, PVD glasses can maintain their original density for hundreds to thousands of seconds, depending on the substrate temperature at which the sample was deposited. The birefringence measurements also show that vapor-deposited glasses are more photostable; molecules in PVD glasses are more resistant to light-driven changes in molecular orientation. Both *s*-polarized and *p*-polarized irradiation result in similar trends. Results for *s*-polarized irradiation are shown in Figure 3 while results for *p*-polarized irradiation are given in the Supporting Information (SI), Figure S1.

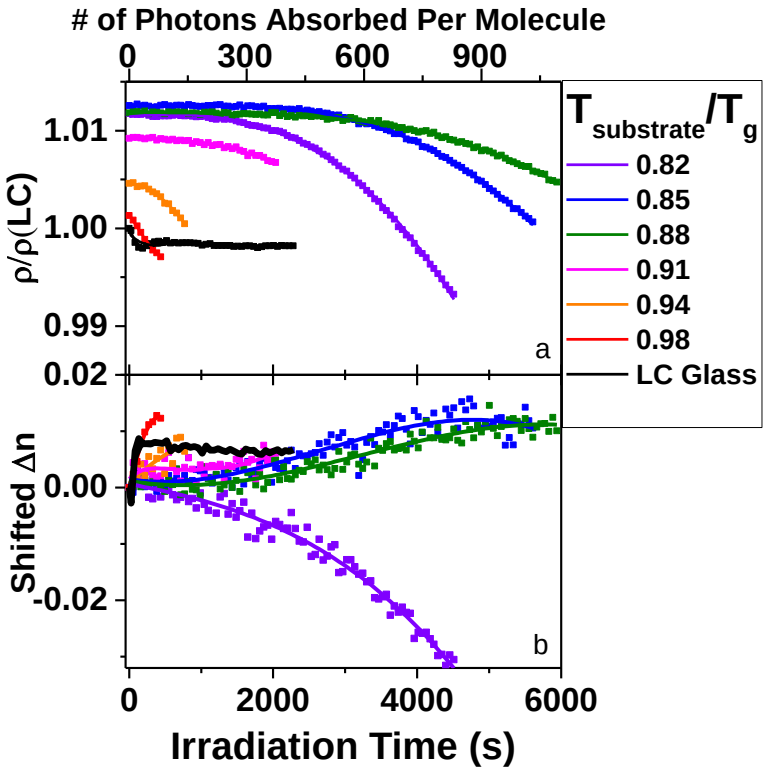

Figure 3. Density and birefringence changes for vapor-deposited and liquid-cooled (LC) glasses of DO37 as a function of irradiation time. (a) Glass density relative to initial density of the liquid-cooled glass. (b) Birefringence Δn relative to as-deposited glass. Lines are guides to the eye.

Previous studies of azobenzene-containing glasses under irradiation have proposed mechanisms which qualitatively explain the density and birefringence changes shown in Figure 3.[31-34] *Trans->cis->trans* cycling disrupts packing in the glassy matrix due to changes in molecular shape and molecular volume.[35,36] Because of the very long relaxation time of the glass, molecules have little opportunity to re-optimize their local packing during irradiation. Changes in birefringence during irradiation can be attributed to the photoalignment effect.[33] When a molecule returns to the *trans* state after isomerization, it need not have the same orientation as it had initially. Repeated photoisomerization with polarized light has the net effect of increasing the fraction of molecules whose transition dipoles are orthogonal to the excitation polarization, since these molecules do not have the opportunity for further photoisomerization; the sample thus becomes anisotropic and birefringent. We note that most as-deposited glasses of DO37 showed negative initial birefringence (SI, Figure S2). In Figure 3b, the birefringence is shifted so that the initial value is zero for all glasses for easier comparison.

2.2.3 Photostability correlates with glass density

To quantitatively compare photostability of vapor-deposited and liquid-cooled glasses, we analyze the experimental results presented in Figure 3. Figure 4a shows the irradiation times required to achieve small changes in density and birefringence. These small changes in density (0.1%) and birefringence (0.005) represent the initial structural alteration of the glasses, at a stage where the glasses have not yet lost their initial material properties. Photostabilities deduced from these two observables are highly consistent. For comparison, Figure 4b shows the density for DO37 glasses vapor-deposited at different substrate temperatures relative to the liquid-cooled glass. All glasses deposited with $T_{substrate} < T_g$ show higher densities than the liquid-cooled glass. The maximum density is observed for a substrate temperature of 0.86 T_g, which is consistent with previously reported vapor-deposited glasses of indomethacin.[21]

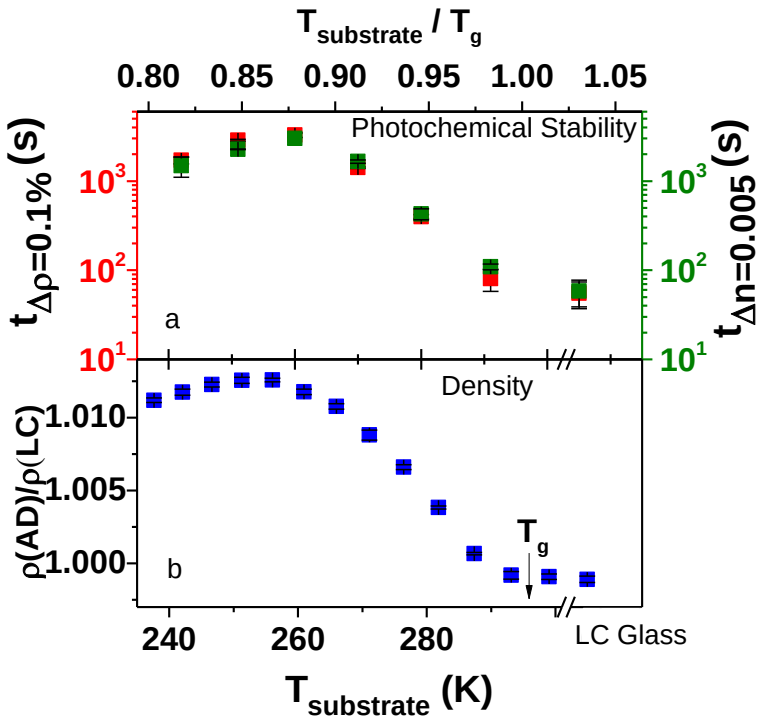

Figure 4. Photostability and density of PVD glasses of DO37, with comparison to the liquid-cooled (LC) glass. A strong correlation is observed between photostability and density. (a) Irradiation time required to achieve a 0.1% density change (red) and 0.005 birefringence change (green). (b) Density of as-deposited (AD) glasses relative to the LC glass. For substrate temperature below T_g, vapor-deposited glasses show increased density, and the maximum density occurs at 255K (0.86 T_g).

By comparing Figure 4a and 4b, it is evident that there is a strong correlation between photostability and glass density, and that the higher density of the PVD glasses is associated with a 50-fold increase in photostability. As we discuss further below, there is no precedent for such a large effect of glass packing at ambient pressure. In a study of an azobenzene derivative tethered to a PMMA polymer, it was demonstrated that optically induced molecular orientation can be hindered by density increases caused by high pressure;[37] compared to ambient pressure, the glass density at 150 MPa was increased by 2.4% and the rate of photo-orientation decreased by a factor of nearly 50. This high-pressure work demonstrated a correlation between density and photostability that is qualitatively consistent with the results in Figure 4. However, in the work of ref 37, enhanced photostability was only observed at high pressure and the rate of photoisomerization became fast again when the pressure was released. In contrast, the present work provides a method to increase the photostability of ambient-pressure materials.

To test the generality of the effect of enhanced photostability, we performed additional experiments at a lower irradiation temperature and found that PVD glasses of DO37 become even more photostable relative to the liquid-cooled glass. In the field of organic electronics, materials are usually used at temperatures at least 30-40 K below T_g. In contrast, for experiments described in Figure 3 and 4, the measurement temperature was 287 K, only 9 K below the T_g for DO37. For a few experiments, we lowered the measurement temperature to 278 K (T_g-18 K) to get closer to the conditions for many applications. For PVD glasses, the photostability results are nearly the same at 278 K and 287 K (SI, Figure S4). For the liquid-cooled glass, however, photoinduced density and birefringence changes occurred more quickly at lower temperature (SI, Figure S5), such that the PVD glasses are even more photostable at lower temperature, relative to the liquid-cooled glass. This behavior of the liquid-cooled glass can be attributed to the competition between photoinduced changes and structural relaxation back towards equilibrium.[38] At lower

temperatures, structural relaxation becomes slower, allowing illumination to more quickly drive the system away from equilibrium.

2.2.4 Molecular simulations of PVD glasses

Molecular simulations of the vapor deposition and photoisomerization processes were performed to understand the mechanism of enhanced photostability in PVD glasses. In order to focus on the key physics responsible for the packing effects observed in our experiments, we propose a simple model to examine isomerization, namely a linearly-connected molecule of four beads that serves as a coarse-grained representation of DO37 (Figure 5, inset). During the vapor deposition portion of the simulations, which utilized a procedure employed in previous simulations of PVD glasses,[23,24,39,40] these molecules were held in the *trans* state. Glass films were deposited onto substrates at temperatures ranging from 0.76 T_g to 0.97 T_g, where T_g was determined to 0.66 (in reduced Lennard-Jones units) by simulations in which the liquid was cooled into the glass. (SI, Figure S6). Consistent with the experimental results in Figure 4b, all the simulated PVD glasses had higher density than the liquid-cooled glass (SI, Table S1). During the photoisomerization portion of the simulations, an iterative method mimicking the stochastic process of photoexcitation, described in the Methods section, was then used to test the photostability of each of the glasses formed. In brief, a few molecules are “photoexcited” by instantaneously switching the dihedral potential from the initial state (where *trans* is the stable state) to a new potential (where *cis* is the stable state). Molecular dynamics simulations are then continued with the local packing environment of each molecule determining whether or not the *cis* state can actually be reached. After a period of time (mimicking the excited state lifetime), the potential is switched back to the original one favoring the *trans* state. This process is repeated many times with molecules randomly selected for photoexcitation.

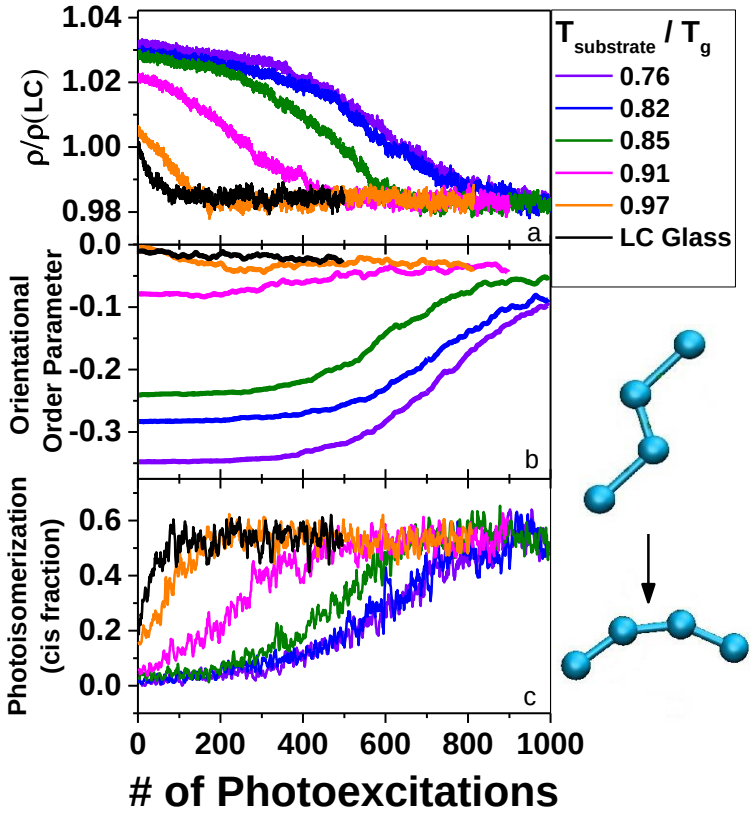

Figure 5. Simulations of photo-stability for vapor-deposited and liquid-cooled (LC) glasses, as a function of photoexcitation cycle. (a) Glass density relative to LC glass (ρ/ρ(LC)). (b) Orientation order parameter (c) Fraction of successful *trans*->*cis* conversions in each photo-excitation. Representative structures of the coarse-grained model in *trans* and *cis* states are shown on the right panel.

Figure 5 shows that the simulated PVD glasses have substantially increased photostability relative to the liquid-cooled glass, in qualitative agreement with the experimental results shown in Figure 3. The top panel of Figure 5 shows that the PVD glasses, which have higher initial densities than the liquid-cooled glass, maintain their initial density for a greater number of photoexcitation cycles. The middle panel of Figure 5 shows the orientation order parameter, S_z, of the simulated glasses as a function of the number of photoexcitation steps; S_z represents the average orientation of transition dipoles for simulated molecules and can be qualitatively compared with the experimentally measured birefringence. Although only small changes in orientation occur for the liquid-cooled glass, they occur much more quickly than for the PVD glasses. Figure S3 (SI) quantifies photostability using these results, and shows that the simulated PVD glasses are at least 10 times more photostable than the liquid-cooled glass. In addition, the simulation results display a strong correlation between photostability and glass density, in agreement with experiment (SI, Figure S3).

The simulation trajectories indicate that the initial molecular packing of higher density glasses restricts excited molecules from reaching the *cis* state, even though their molecular potential strongly favors the *cis* state. The fraction of successful isomerization events is shown as a function of photoexcitation cycles for each glass in Figure 5c. This is loosely equivalent to the quantum yield for the actual photoisomerization reaction. For the highest density glasses, there is a very low probability for a successful isomerization event and this explains the very slow initial changes in the density and S_z parameter.

2.2.5 Mechanism for enhanced photostability

We considered two possible mechanisms for the enhanced photostability of high density PVD glasses shown in Figures 3 and 4. According to one possible mechanism, photoisomerization to the *cis* state occurs only rarely in the highest density PVD glasses (due to efficient packing) but occurs much more frequently in lower density glasses. For the second possible mechanism, we

imagine that photoisomerization to the *cis* state occurs efficiently in all glasses, but that only the low density glasses are restructured as a result. We favor the first mechanism and our simulation results strongly support this view. Figure 5c shows that, for the highest density vapor-deposited glasses, the isomerization from *trans* to *cis* is nearly completely prevented in the simulations. In the simulation, photoexcitation provides an intramolecular driving force to leave the *trans* state, but in high density glasses, most molecules are unable to reconfigure due to efficient packing. For lower density glasses, the intermolecular barrier for rearrangement will be lower, allowing molecules to achieve the *cis* state with higher probability.

We performed additional experiments to directly test the hypothesis that molecules in a dense glass rarely reach the *cis* state as a result of photoexcitation. DO37 is a “push-pull” azobenzene, and consistent with other azobenzene derivatives of this type, the lifetime of the *cis* state for DO37 is reported to be less than one second.[41] Our efforts to directly detect depletion of the *trans* state in the absorption spectrum during irradiation were unsuccessful, even for the liquid-cooled glass. A reasonable interpretation of these results is that the steady-state population of the *cis* state in our experiments is always quite low. While we expect that the *cis* state population during irradiation is lower for denser glasses than for the liquid-cooled glass, we have not directly established this.

Our proposed mechanism is consistent with literature evidence that the local packing environment can influence the ability of photoexcited azobenzenes to reach the *cis* state. For example, in a glass of 4,4’-diphenyl azobenzene dispersed in amorphous polycarbonate, it was shown that physical aging for 100 hours caused a ~5% decrease in the photoisomerization quantum yield relative to the glass prepared by liquid-cooling;[14] because a symmetric azobenzene with a long *cis* lifetime was used in this study, this result could be seen directly as depletion of *trans* state absorption. 100 hours of aging likely increases density by much less than 1.3% and this provides a way to understand the much larger effects on photostability obtained in our study with PVD

glasses. In another study, azobenzene derivatives were incorporated into different DNA sequences, so that the local packing could be tuned by changing the neighboring base pairs.[42] In this system, it was demonstrated that the quantum yield of azobenzene photoisomerization decreased with increased restriction of molecular packing, varying by a factor of four. Additionally, the photoisomerization of crystalline *trans*-azobenzene is severely hindered in the bulk crystal.[43] These studies all support the idea that the quantum yield for photoisomerization to the *cis* state decreases with increasing intermolecular barriers for molecular rearrangement.

Considering that literature precedents and our simulations both support the view that denser glasses can prevent photoisomerization, it is useful to estimate the magnitude of the intermolecular barriers for rearrangement in PVD and liquid-cooled glasses. Figure 6 shows the energy diagram for photoisomerization of an azobenzene in the gas phase and provides background for our discussion. After a 532 nm photon causes excitation to the S_1 state, the molecule relaxes to a twisted configuration ($\theta = 90°$). Upon transition to the ground state, the molecule either twists forward to the *trans* state or back to the *cis* state, with roughly equal probability.[44] In a glass, in order for an azobenzene molecule to transition from *trans* to *cis*, it must additionally overcome intermolecular barriers in an environment that is quite rigid and essentially static on the time scale of photoexcitation. Using measurements and estimates of the structural relaxation times, we can estimate the activation free energies for cooperative rearrangements in the liquid-cooled and PVD glasses to be 34 kT and 51 kT, respectively (see SI). We now imagine adding an intermolecular potential favoring the *trans* state to the diagram in Figure 6. As the barrier for rearrangement in the high density glass is a large fraction of the photon energy (94 kT at the experimental temperature), it is plausible that the intermolecular packing blocks any significant progress toward the *cis* state in the dense glass while this mechanism would be less efficient in the liquid-cooled glass. A weakness of this argument is that we have no experimental estimate of the intermolecular barrier associated with photoisomerization, but given the size of the molecular

rearrangement required to reach the *cis* state, it is reasonable that it will be not too much smaller than the barrier for structural relaxation. A more detailed theoretical study will be required to examine our proposed mechanism more rigorously.

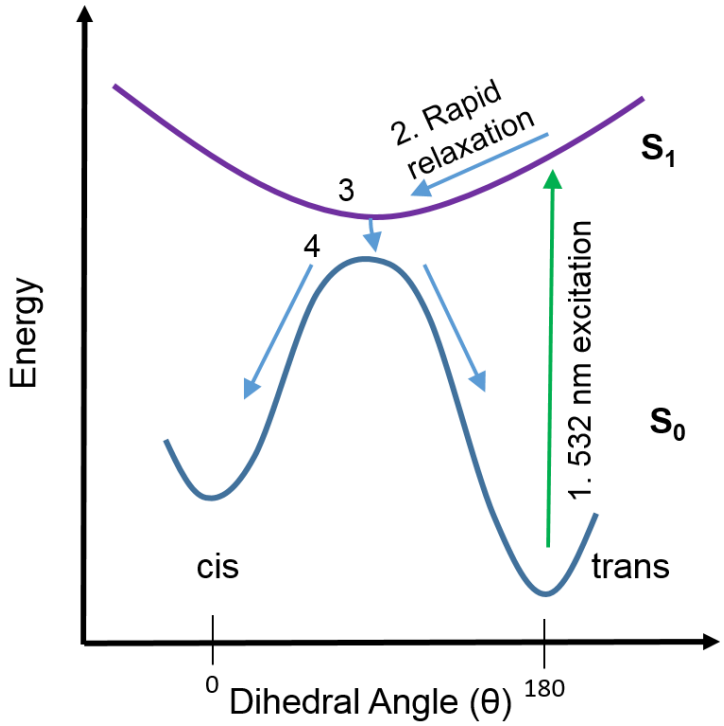

Figure 6. Energy diagram of photoisomerization for DO37.

2.3 Conclusion

In this study, we have established that vapor-deposited organic glasses can be much more photostable than liquid-cooled glasses. While previous work on crystals indicated the important influence of local packing, this is the first demonstration of a significant impact of different amorphous packing arrangements on the photostability of organic molecules. We showed that high density glasses of DO37 can be made by PVD and that the density can be systematically varied through controlling the substrate temperature. The highest density glass was 50 times more photostable than the liquid-cooled glass and we find a strong correlation between photostability and glass density. We attribute this effect to the high intermolecular barriers for rearrangement that are present in the highest density PVD glasses. This view is supported by molecular simulations of coarse-grained DO37 molecules that successfully reproduced the high density and high photostability of the PVD glasses. The simulations show that, in the highest density glasses, the local packing environment prevents photoexcited molecules from escaping the *trans* configuration.

We expect that enhancement in photostability for vapor-deposited glasses is a general effect that will be observed for many molecular systems beyond the azobenzenes. To date, PVD has prepared glasses with high kinetic stability from more than thirty organic molecules, including several molecules used in the active layers of organic light emitting diodes (OLEDs).[20] In every case where it has been checked, glasses with high kinetic stability also have high density relative to the liquid-cooled glass. Thus we expect that PVD glasses of many organic molecules will show an increased energy barrier for molecular rearrangements that will slow photoreactions. This may be particularly useful in applications where photodegradation leads to deterioration of performance, as in OLEDs and organic photovoltaics. For example, operational lifetime is considered to be a bottleneck to the further improvement of OLED display performance, especially for blue emitters.[45] It has been found that degradation of OLEDs can be caused by self-

luminescence,[9] electrochemical reaction[46] and hole injection[47]. We speculate that high density PVD glasses might delay degradation of OLED molecules as a result of any of these processes, as our results indicate that efficient packing can inhibit chemical processes. As OLEDs are already produced by PVD, optimizing the substrate temperature to produce the densest glass might thus increase device lifetime. We do not expect that all organic glasses will show a two order of magnitude enhancement in photostability as a result of optimal vapor deposition. Azobenzenes require a particularly large rearrangement for photoisomerization and it is likely that photodegradation processes that require smaller rearrangements will be less impacted by the local packing. Future work should investigate the impact of glass packing on a range of different chemical and photochemical processes.

2.4 Experiment and simulation methods

Materials:

Disperse Orange 37 (99% purity) was obtained from Santa Cruz Biotechnology and used as received. DO37 was selected for these experiments because it has a T_g higher than room temperature; it is a reasonably good glass former, which facilitates glassy thin film preparation via the PVD process. Differential scanning calorimetry (DSC) measurements show that the glass transition temperature (T_g) for DO37 is 296 K, with a 10 K/min cooling and heating rate, which is in good agreement with ellipsometry results. Prior to performing the DSC measurements, the material was first melted then quenched into liquid nitrogen.

Physical vapor deposition (PVD):

PVD was performed in a vacuum chamber with a base pressure of 10^{-7} *torr*. Crystalline DO37 was placed in a crucible that was resistively heated. The deposition rate was controlled by tuning the heater power and monitored by a quartz crystal microbalance (QCM). The deposition rate was kept at a constant value of 2 Å /s for all experiments. The final sample thicknesses were about

300 nm. A high throughput method was utilized to prepare a library of glasses with different densities and kinetic stabilities.[21] The substrate (Si wafer) was suspended between two copper fingers; different temperatures were imposed at each finger to create a temperature gradient across the sample during deposition. The substrate temperature range was from 240 K to 305 K.

Kinetic stability and density measurements:

Kinetic stability and density of vapor-deposited thin films were characterized by spectroscopic ellipsometry, an optical technique that measures thickness and refractive indices of thin films. For all ellipsometry measurements, three incident angles were used (50°, 60° and 70°), and wavelengths from 370-1000 nm were utilized. To measure kinetic stability, ellipsometry was performed on samples placed on a custom-built hot stage, and the temperature was increased at 1 K/min from near room temperature to 25 K above T_g. The onset temperature, which characterizes the kinetic stability of a glass, was determined from the beginning of the transformation into the supercooled liquid, as shown in Figure 1. Immediately after heating, the supercooled liquid was cooled at 1 K/min into the liquid-cooled glass. By comparing sample thickness before and after temperature-cycling, the density of the vapor-deposited glass relative to the liquid-cooled glass can be determined.

Photostability measurement:

The light irradiation experiment used to test photostability of PVD glasses is shown in Scheme 1. A linearly-polarized 532 nm laser was used as the light source to induce the photoisomerization reaction, at a power level of 11 mW/cm^2. During irradiation, spectroscopic ellipsometry was used to characterize the glass thickness and birefringence, at the same spot where the 532 nm laser irradiated the sample. In this way, photoinduced structural changes of the thin glassy films were monitored in real time. The photostability tests shown in the main text were performed at 287 K (T_g – 9 K). To model the ellipsometric data observed during light irradiation, a biaxial anisotropic

Cauchy model was used. This model allows three independent refractive indices, which is necessary since irradiation generates anisotropy in the glass sample along a different axis than the anisotropy generated in the deposition process. In the measurement of photostability, birefringence is defined as the refractive index difference n_z-n_x at 980 nm, where n_z and n_x represent refractive indices for light polarized along the substrate normal and the x direction in the plane of the substrate, respectively; see Scheme 1 for coordinate system.

Computer simulations:

Molecular dynamics simulations of a coarse-grained (CG) model of DO37 were performed to study photoisomerization of vapor-deposited glasses at a molecular level. The model consists of four linearly connected Lennard-Jones (LJ) particles (Figure 5) with parameters σ_{bb} = 1.0 and ε_{bb} = 1.0. (All units reported for the simulations are reduced LJ units.) The cutoff distance for the potential is r_c = 2.5 with a smooth decay starting at r = 2.4. To mimic the structure of azobenzene, the four particles were held together by three stiff harmonic bonds with the inner bond shorter than the two outer bonds (l_{inner} = 1.0, l_{outer} = 1.5, k_b = 1000). The two bond angles were controlled by a harmonic potential with values that mimic sp^2 hybridization (θ = 120°, k_{angle} = 1000). As described below, the dihedral angle potential was switched in order to mimic the photoexcitation process. The dihedral angles for the *trans* and *cis* potentials were defined by:

$$U_{dihedral} = \frac{1}{2}k_1(1 + \cos\theta) + \frac{1}{2}k_2(1 - \cos 2\theta)$$

where k_1 = 20 and k_2 = 8 for the *trans* state and k_1 = -25 and k_2 = 6.25 for the *cis* state.

Vapor-deposited glasses were generated in a simulation box with dimensions of 20 σ_{bb} by 20 σ_{bb} in the plane of the substrate (xy-plane), and at least 10 σ_{bb} larger than the deposited film thickness in the normal direction to the substrate (z-dimension). Periodic boundary conditions were applied to the x and y-dimensions. The substrate was generated from 1,000 randomly placed smaller particles. The potential parameters for the substrate are chosen to minimize any ordering effect

on the deposited material while still being able to anchor the growing film.[39] The interaction parameters for substrate atoms are σ_{ss} = 0.6, ε_{ss} = 0.1, and the interaction parameters for the deposited molecules with the substrate are σ_{sb} = 0.75 and ε_{sb} = 1.0, with a cutoff distance of 2.5 $\sigma_{\alpha\beta}$, where $\alpha,\beta \in$ (s,b). The substrate atoms are fixed to their initial position by harmonic springs. The simulated vapor deposition process is analogous to that reported earlier.[23,24,39,40] At least 850 deposition steps were performed for each glass film in order to achieve a film thickness of at least 40 σ_{bb}. The middle section of the film (15 σ_{bb} to 28 σ_{bb} in the z-dimension) was used to calculate bulk glass properties to avoid the influence of the substrate or the free surface. The deposition cycle consists of four repeated steps: (i) introduction of four randomly oriented molecules above, but in close proximity to, the film surface, (ii) equilibration of the newly introduced molecules at high temperature (T=1.25), (iii) linear cooling over 2000 time-units of these molecules to the substrate temperature, and finally (iv) minimization of the energy for the entire system. A separate thermostat is used to maintain the previously deposited molecules and substrate particles at the desired substrate temperature throughout the cycle. For the entire film preparation process described above, the *cis* dihedral potential was utilized. All simulations were performed using the Large-Scale Atomic/Molecular Massively Parallel Simulator (LAMMPS) package[48] in the canonical ensemble with a simulation time step of 0.001 LJ time units. The orientation order parameter, S_z, was used to characterize the average orientation of the simulated films. S_z is defined as:

$$S = \frac{3}{2} < cos^2 \delta_z > -1$$

where δ_z is the angle of the molecular end-to-end vector relative to the substrate normal.

An iterative process was used to simulate the photoisomerization reaction. To mimic photoexcitation, a small group of selected molecules have their dihedral angle potential temporarily switched from *trans* to *cis*. During the short molecular dynamics trajectory that follows

(mimicking the excited state lifetime), these selected molecules may transition to the *cis* state or their environment may trap them with a dihedral angle close to the *trans* state, i.e., although their dihedral angle potentials were changed to favor the *cis* state, the selected molecules were not forced to the *cis* state. To avoid influences from the interfaces, only the bulk region of the simulated film was considered for the photoisomerization process. In order to capture the directionality of the polarized light, a director vector was used as a proxy, which pointed 30° off the substrate normal. All photoexcitation simulations were carried out at T=0.6 (0.9 T_g). Each cycle included the following steps: 1) Select a molecule at random; 2) Accept or reject for excitation with probability $\cos^2(\gamma)$, where γ is the angle between the director vector and the end-to-end vector of the molecule; 3) Continue first two steps until 1% of the bulk molecules have been accepted; 4) Switch the dihedral potential for the selected molecules from *trans* to *cis*; 5) Run molecular dynamics for 100 time units; 6) Return all dihedral potentials to the *trans* potential.

ACKNOWLEDGMENT

We thank Trisha Andrew and Lian Yu for helpful discussions, and Men Zhu for help with DSC experiments. In addition, MDE acknowledges a conversation with the late Paul Barbara that stimulated these experiments. We acknowledge support from NSF DMR-1234320. Instrumentation was supported by the US Department of Energy, Office of Basic Energy Sciences, Division of Materials Sciences and Engineering, Award DE-SC0002161.

2.5 References

(1) Soutis, C. *Mater. Sci. Eng. A* **2005**, *412*, 171.

(2) Yu, L. *Adv. Drug Deliv. Rev.* **2001**, *48*, 27.

(3) Chen, Y. H.; Lin, L. Y.; Lu, C. W.; Lin, F.; Huang, Z. Y.; Lin, H. W.; Wang, P. H.; Liu, Y. H.; Wong, K. T.; Wen, J. G.; Miller, D. J.; Darling, S. B. *J. Am. Chem. Soc.* **2012**, *134*, 13616.

(4) Yokoyama, D. *J. Mater. Chem.* **2011**, *21*, 19187.

(5) Shirota, Y.; Kageyama, H. *Chem. Rev.* **2007**, *107*, 953.

(6) Hancock, B. C.; Parks, M. *Pharm. Res.* **2000**, *17*, 397.

(7) Kushida, I.; Ichikawa, M.; Asakawa, N. *J. Pharm. Sci.* **2002**, *91*, 258.

(8) Holmes, R. J.; Forrest, S. R.; Tung, Y. J.; Kwong, R. C.; Brown, J. J.; Garon, S.; Thompson, M. E. *Appl. Phys. Lett.* **2003**, *82*, 2422.

(9) Wang, Q.; Luo, Y. C.; Aziz, H. *Appl. Phys. Lett.* **2010**, *97*, 063309.

(10) Seifert, R.; de Moraes, I. R.; Scholz, S.; Gather, M. C.; Lussem, B.; Leo, K. *Org. Electron.* **2013**, *14*, 115.

(11) Rezzonico, D.; Jazbinsek, M.; Gunter, P.; Bosshard, C.; Bale, D. H.; Liao, Y.; Dalton, L. R.; Reid, P. J. *J. Opt. Soc. Am. B-Opt. Phys.* **2007**, *24*, 2199.

(12) Schmidt, G. M. J. *Pure. Appl. Chem.* **1971**, *27*, 647.

(13) Cohen, M. D.; Schmidt, G. M. J. *J. Chem. Soc.* **1964**, 1996.

(14) Royal, J. S.; Torkelson, J. M. *Macromolecules* **1992**, *25*, 4792.

(15) Swallen, S. F.; Kearns, K. L.; Mapes, M. K.; Kim, Y. S.; McMahon, R. J.; Ediger, M. D.; Wu, T.; Yu, L.; Satija, S. *Science* **2007**, *315*, 353.

(16) Leon-Gutierrez, E.; Garcia, G.; Clavaguera-Mora, M. T.; Rodriguez-Viejo, J. *Thermochim. Acta* **2009**, *492*, 51.

(17) Sepulveda, A.; Tylinski, M.; Guiseppi-Elie, A.; Richert, R.; Ediger, M. D. *Phys. Rev. Lett.* **2014**, *113*, 045901.

(18) Rodriguez-Tinoco, C.; Gonzalez-Silveira, M.; Rafols-Ribe, J.; Garcia, G.; Rodriguez-Viejo, J. *J. Non-Cryst. Solids* **2015**, *407*, 256.

(19) Ramos, S.; Chigira, A. K.; Oguni, M. *J. Phys. Chem. B* **2015**, *119*, 4076.

(20) Dalal, S. S.; Walters, D. M.; Lyubimov, I.; de Pablo, J. J.; Ediger, M. D. *Proc. Natl. Acad. Sci. USA* **2015**, *112*, 4227.

(21) Dalal, S. S.; Fakhraai, Z.; Ediger, M. D. *J. Phys. Chem. B* **2013**, *117*, 15415.

(22) Kearns, K. L.; Swallen, S. F.; Ediger, M. D.; Wu, T.; Sun, Y.; Yu, L. *J. Phys. Chem. B* **2008**, *112*, 4934.

(23) Lyubimov, I.; Antony, L.; Walters, D. M.; Rodney, D.; Ediger, M. D.; de Pablo, J. J. *J. Chem. Phys.* **2015**, *143*, 094502.

(24) Lyubimov, I.; Ediger, M. D.; de Pablo, J. J. *J. Chem. Phys.* **2013**, *139*, 144505.

(25) Tylinski, M.; Sepulveda, A.; Walters, D. M.; Chua, Y. Z.; Schick, C.; Ediger, M. D. *J. Chem. Phys.* **2015**, *143*, 244509.

(26) Zhu, L.; Yu, L. A. *Chem. Phys. Lett.* **2010**, *499*, 62.

(27) Dawson, K.; Zhu, L.; Kopff, L. A.; McMahon, R. J.; Yu, L.; Ediger, M. D. *J. Phys. Chem. Lett.* **2011**, *2*, 2683.

(28) Walters, D. M.; Richert, R.; Ediger, M. D. *J. Chem. Phys.* **2015**, *142*, 10.

(29) Zhu, L.; Brian, C. W.; Swallen, S. F.; Straus, P. T.; Ediger, M. D.; Yu, L. *Phys. Rev. Lett.* **2011**, *106*, 4.

(30) Zhang, W.; Brian, C. W.; Yu, L. *J. Phys. Chem. B* **2015**, *119*, 5071.

(31) Tanchak, O. M.; Barrett, C. J. *Macromolecules* **2005**, *38*, 10566.

(32) Hagen, R.; Bieringer, T. *Adv. Mater.* **2001**, *13*, 1805.

(33) Sekkat, Z.; Wood, J.; Knoll, W. *J. Phys. Chem.* **1995**, *99*, 17226.

(34) Bennani, O. R.; Al-Hujran, T. A.; Nunzi, J. M.; Sabat, R. G.; Lebel, O. *New J. Chem.* **2015**, *39*, 9162.

(35) Harada, J.; Ogawa, K. *J. Am. Chem. Soc.* **2004**, *126*, 3539.

(36) Mostad, A.; Rømming, C. *Acta Chem. Scand.* **1971**, *25*, 3561.

(37) Sekkat, Z.; Kleideiter, G.; Knoll, T. *J. Opt. Soc. Am. B-Opt. Phys.* **2001**, *18*, 1854.

(38) Tanino, T.; Yoshikawa, S.; Ujike, T.; Nagahama, D.; Moriwaki, K.; Takahashi, T.; Kotani, Y.; Nakano, H.; Shirota, Y. *J. Mater. Chem.* **2007**, *17*, 4953.

(39) Singh, S.; Ediger, M. D.; de Pablo, J. J. *Nat. Mater.* **2013**, *12*, 139.

(40) Lin, P. H.; Lyubimov, I.; Yu, L.; Ediger, M. D.; de Pablo, J. J. *J. Chem. Phys.* **2014**, *140*, 9.

(41) Dokic, J.; Gothe, M.; Wirth, J.; Peters, M. V.; Schwarz, J.; Hecht, S.; Saalfrank, P. *J. Phys. Chem. A* **2009**, *113*, 6763.

(42) Yan, Y. Q.; Wang, X.; Chen, J. I. L.; Ginger, D. S. *J. Am. Chem. Soc.* **2013**, *135*, 8382.

(43) Nakayama, K.; Jiang, L.; Iyoda, T.; Hashimoto, K.; Fujishima, A. *Jpn. J. Appl. Phys. 1* **1997**, *36*, 3898.

(44) Crecca, C. R.; Roitberg, A. E. *J. Phys. Chem. A* **2006**, *110*, 8188.

(45) Zhang, Y. F.; Lee, J.; Forrest, S. R. *Nature Communications* **2014**, *5*.

(46) Papadimitrakopoulos, F.; Zhang, X. M.; Higginson, K. A. *IEEE J. Sel. Topics Quantum Electron.* **1998**, *4*, 49.

(47) Aziz, H.; Popovic, Z. D.; Hu, N. X.; Hor, A. M.; Xu, G. *Science* **1999**, *283*, 1900.

(48) Plimpton, S. *J. Comput. Phys.* **1995**, *117*, 1.

2.6 Supporting Information

Effect of light polarization on photo-stability of PVD glasses of DO37

In the main text, we demonstrated that PVD glasses of DO37 display significantly enhanced photo-stability in experiments that utilized *s*-polarized irradiation. Here we show that similar photo-stability results in experiments using *p*-polarized light. Figure S1 shows the density (ρ) and birefringence (Δn) changes of both vapor-deposited and liquid-cooled glasses as a function of time during *p*-polarized irradiation. For liquid-cooled glasses (black curves), ρ and Δn change immediately after irradiation, on the time scale of tens of seconds. In contrast, PVD glasses change much more slowly. For example, for glasses vapor-deposited at 0.88 T_g (green curves), it takes thousands of seconds for significant changes to occur.

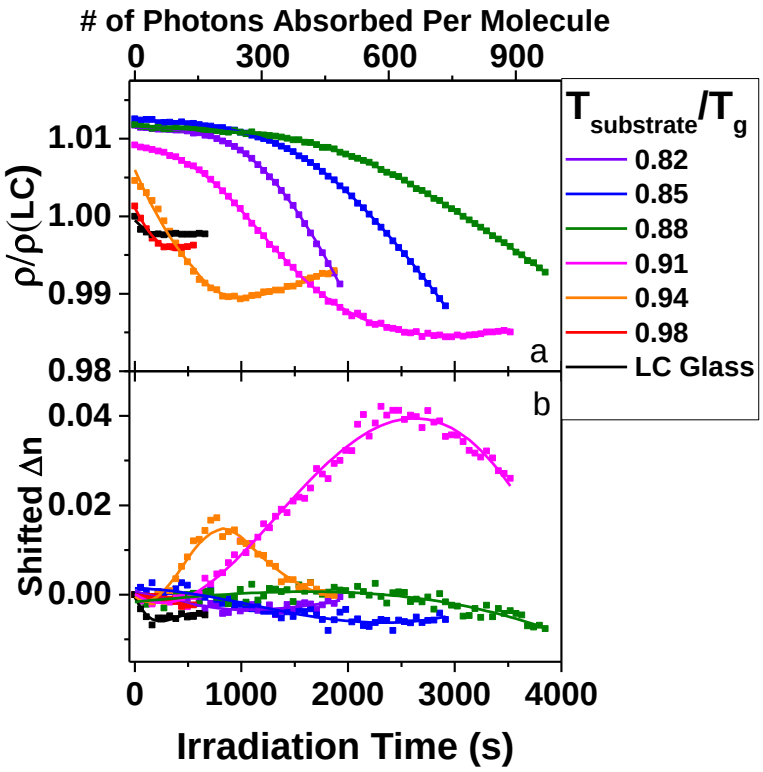

Figure S1. *P*-polarized light measurements of photo-stability as a function of irradiation time for vapor-deposited and liquid-cooled (LC) glasses of DO37. (a) Relative density (ρ/ρ(LC)) in comparison to the LC glass. (b) Changes in the birefringence Δn. Lines are guides to the eye.

Initial birefringence of PVD glasses of DO37

For DO37 PVD glasses, initial birefringence depends on the substrate temperature ($T_{substrate}$). This phenomenon is not unique for DO37, and has been reported for PVD glasses of other molecules.[1-3] At $T_{substrate} > T_g$, the initial birefringence is nearly zero, consistent with the random molecular orientation inherited from the super-cooled liquid. At $T_{substrate} < T_g$, the birefringence of the as-deposited glass is less than zero, which indicates that the molecular axis with maximum polarizability tends to lie in the plane of the substrate. Here birefringence is defined as the difference in refractive index between the extraordinary and ordinary direction of the thin films.

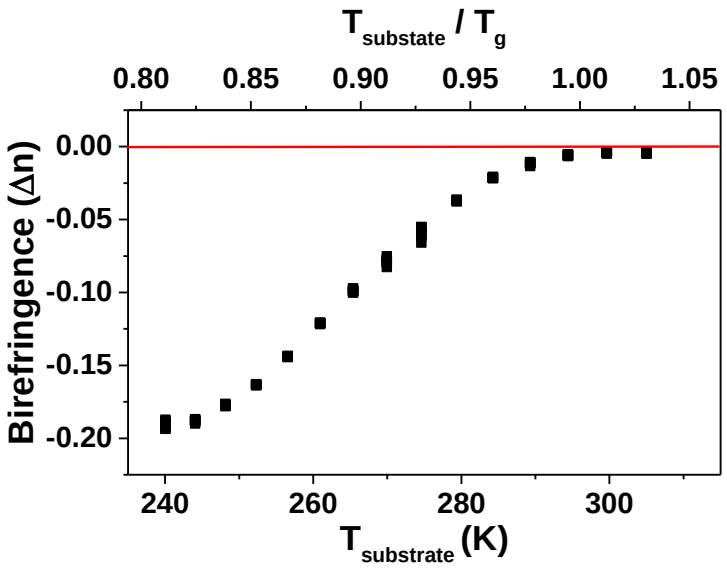

Figure S2. Initial birefringence as a function of substrate temperature ($T_{substrate}$) for vapor-deposited glasses of DO37, as determined by ellipsometry.

Simulation results for the correlation of photostability with glass density

The molecular simulations described in the text show a strong correlation between glass density and photo-stability, similar to the correlation observed in the experiments. Figure S3a shows the number of excitation iterations required for 1% density (ρ) and 5% orientational order parameter (S_z) changes, respectively. The most photo-stable glass changes its properties about a factor of 20 slower than the liquid-cooled glass. The density for glasses vapor-deposited at different substrate temperatures relative to the liquid-cooled glass is shown in Figure S3b. At $T_{substrate} < T_g$, the density of vapor-deposited glasses is greater than that of the liquid-cooled glass.

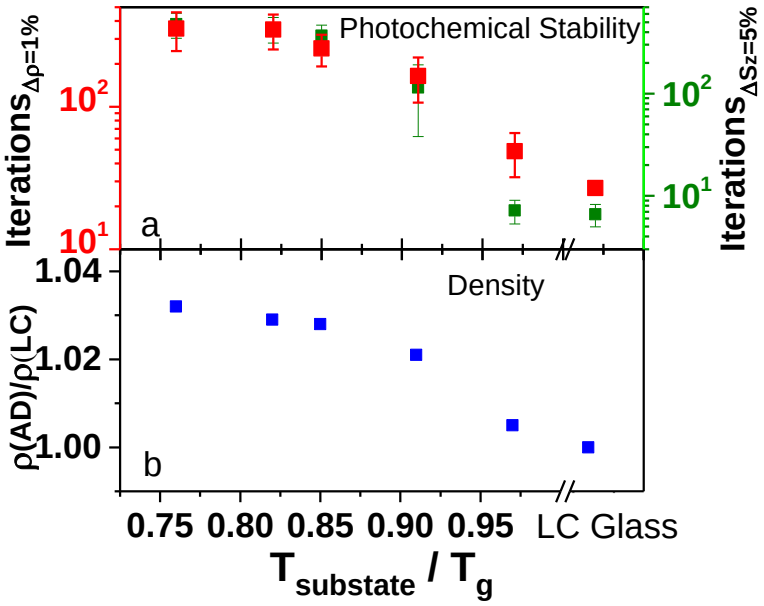

Figure S3. Correlation of photo-stability with glass density as a function of normalized substrate temperature for vapor-deposited and liquid-cooled (LC) glasses in computer simulations. (a) # of photoexcitation iterations required for 1% density change (red) and 5% order parameter change (green). (b) Density of as-deposited (AD) glasses relative to the LC glass.

PVD glass photo-stability at a lower irradiation temperature

In the main text, all the photo-stability data presented was collected during irradiation at 287 K, which is 9 K below T_g. Here we show that, when the measurement temperature is lowered to 278 K, the PVD glass shows almost no difference in photo-stability. Figure S4 shows the density (ρ) and birefringence changes (Δn) during light irradiation for DO37 films vapor-deposited at $T_{substrate}$ = 0.91 T_g. The time required for changes of 0.1% in density, and 0.005 in birefringence, are nearly the same for the two irradiation temperatures.

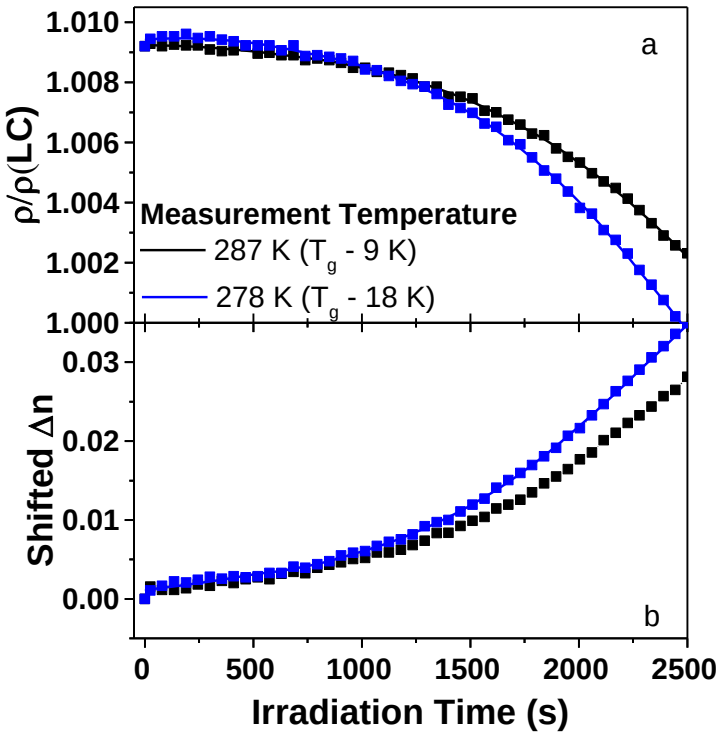

Figure S4. Photo-stability as a function of irradiation time for glasses vapor-deposited at $T_{substrate}$ = 0.91 T_g at different irradiation temperatures. (a) Relative density (ρ/ρ(LC)) changes (b) Birefringence (Δn) changes. Lines are guides to the eye.

Liquid-cooled glass photo-stability at different irradiation temperatures

The photo-stability of liquid-cooled glasses was assessed at different irradiation temperatures. We observe in Figure S5 that photo-induced changes in ρ and ∆n are accelerated at lower temperatures. Lowering the temperature from 287 K to 278 K speeds photo-induced changes in liquid-cooled glasses by about a factor of two.

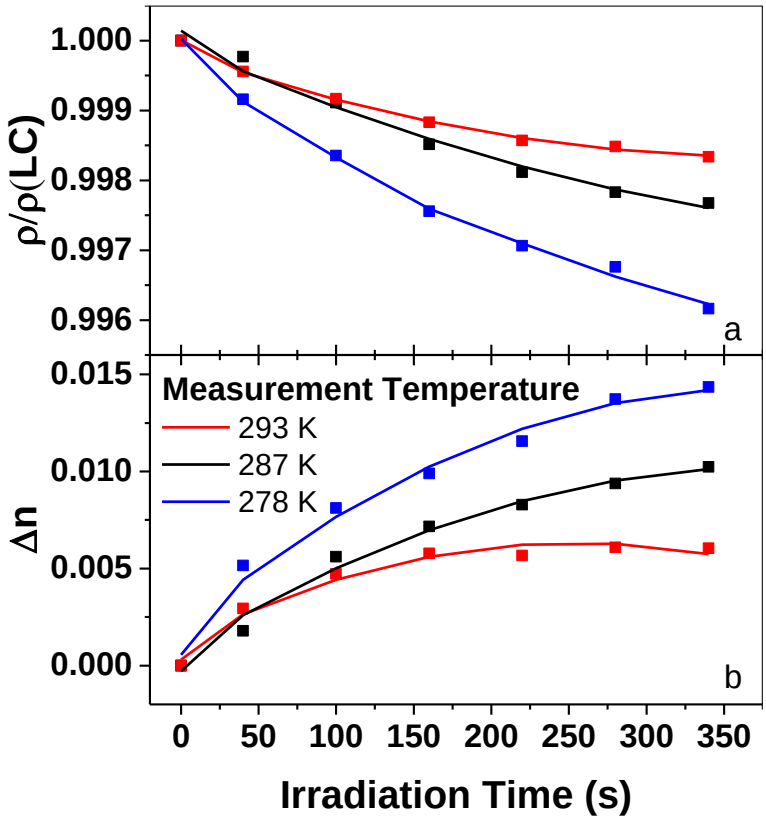

Figure S5. Photo-stability as a function of irradiation time for liquid-cooled (LC) glasses at different irradiation temperatures. (a) Change in relative density. (b)Change in birefringence ∆n. Lines are guides to the eye.

Simulated liquid-cooled glass transition at different cooling rates

For comparison with the experiments, the glass transition temperature of a film of coarse-grained DO37 molecules was determined in the simulations as shown in Figure S6. In the figure, one can see the cooling rate dependence of T_g. The T_g corresponding to the slowest cooling rate is used in the main text and elsewhere in the supporting information. The cooling rates (q_c) are presented in units of LJ temperature/LJ time-unit.

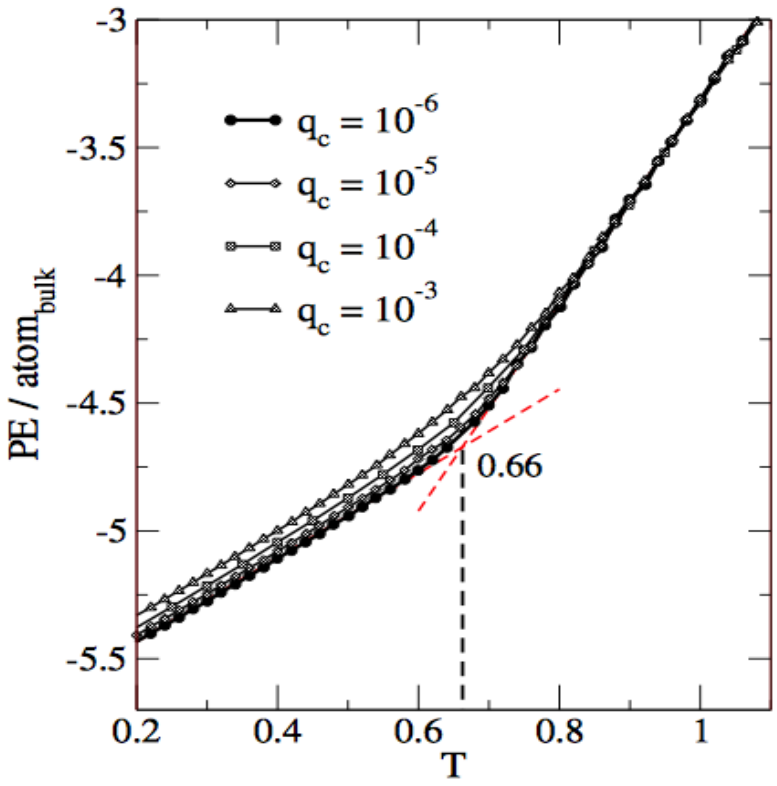

Figure S6. The intensive potential energy calculated for the bulk region of the film as a function of temperature. Four different cooling rates (q_c) were used. The glass transition temperature (T_g) was calculated from intersection of the liquid and glass lines as shown.

Properties of simulated vapor-deposited glasses

Simulated vapor depositions were performed at various substrate temperatures ranging from 0.76 T_g to 0.97 T_g as described in the main text. For each substrate temperature, five sample films were produced. To compare the properties of the vapor-deposited films to the liquid-cooled glass, the average inherent structure energy and the average density are calculated; both of these quantities are evaluated in the bulk portion of the film. Table S1 compares these properties with the liquid-cooled glasses prepared at the three lowest cooling rates. All the vapor deposited glasses have higher density and lower inherent structure energies. The liquid-cooled glass at the lowest cooling rate is used as a reference point.

Table S1 Comparison of Vapor-deposited and Liquid-cooled Glasses of the Coarse-grained DO37 System.

$T_{substrate}/T_g$	E_{IS}	ρ/ρ_{LC}
0.76	-0.244 ±0.010	1.037 ±0.001
0.82	-0.229 ±0.002	1.032 ±0.002
0.85	-0.210 ±0.010	1.027 ±0.003
0.91	-0.139 ±0.013	1.017 ±0.002
0.97	-0.004 ±0.008	0.997 ±0.003
q_c		
10^{-6}	0.000 ±0.002	1.000 ±0.002
10^{-5}	0.026 ±0.006	0.997 ±0.002
10^{-4}	0.056 ±0.002	0.993 ±0.002

The substrate temperatures $T_{substrate}$ are all relative to T_g (0.66) and there are three different cooling rates (q_c). The inherent structure energies (E_{IS}) are all shifted such that the lowest q_c is the zero energy point. The densities (ρ) are reported relative to the lowest q_c. Errors are reported by calculating the standard deviation for five independent films.

Estimation of the activation free energy associated with molecular rearrangements in glasses:

We estimate the activation free energy for molecular rearrangements in the glass by utilizing the temperature dependence of the structural relaxation or alpha relaxation time (τ_α). τ_α is the characteristic time for intermolecular rearrangements in supercooled liquids and glasses. At T_g, the supercooled liquid has a τ_α that is equal to 10^2 s. At infinitely high temperature, $\tau_{a,\infty}$ is estimated to be about 10^{-13} s, which represents the fastest movement that a molecule can achieve in the condensed phase. From the following equation,

$$\ln \tau_\alpha(T_g) = \ln \tau_{\alpha,\infty} + E_a/kT_g$$

we estimate the activation free energy for the supercooled liquid at T_g to be about 34 kT_g. Since the liquid-cooled glass inherits its structure from the supercooled liquid at T_g, 34 kT_g ($\cong$ 34 kT at the irradiation temperature) is also a good estimate of the activation free energy for molecular rearrangements in the liquid-cooled glass.

For the highest density glass of DO37, we use previous measurements on indomethacin to estimate the activation free energy. Both DO37 and indomethacin have the same optimum deposition temperature (0.85 T_g) and show similar density increases compared to the liquid-cooled glass. For indomethacin, τ_α at the temperature of preparation (0.85 T_g) can be estimated to be 10^{13} seconds.[4] Using this value and the following equation,

$$\ln \tau_\alpha(0.85\ T_g) = \ln \tau_{\alpha,\infty} + E_a/(0.85\ kT_g)$$

we estimate the activation free energy for the highest density PVD glass at about 51 kT_g ($\cong$ 51 kT at the irradiation temperature.)

References:

(1) Dalal, S. S.; Walters, D. M.; Lyubimov, I.; de Pablo, J. J.; Ediger, M. D. *Proc. Natl. Acad. Sci. USA* **2015**, *112*, 4227.

(2) Dalal, S. S.; Fakhraai, Z.; Ediger, M. D. *J. Phys. Chem. B* **2013**, *117*, 15415.

(3) Yokoyama, D. *J. Mater. Chem.* **2011**, *21*, 19187.

(4) Dawson, K.; Kopff, L. A.; Zhu, L.; McMahon, R. J.; Yu, L.; Richert, R.; Ediger, M. D. *J. Chem. Phys.* **2012**, *136*, 094505.

Chapter 3

Tenfold increase in the photostability of an azobenzene guest in vapor-deposited glass mixtures

Yue Qiu, Lucas W. Antony, John M. Torkelson, Juan J. de Pablo, M. D. Ediger

To be submitted to *J. Chem. Phys.*

Abstract

Improvements to the photostability of organic glasses for use in electronic applications have generally relied on modification of chemical structure. We show here that the photostability of a guest molecule can also be significantly improved - without chemical modification - by using physical vapor deposition to pack molecules more densely. Photoisomerization of the substituted azobenzene, 4,4'-diphenyl azobenzene (DPA), was studied in a vapor-deposited glass matrix of celecoxib. We directly measure photoisomerization of *trans*- to *cis*- states via UV-Vis spectroscopy and show that the rate of photoisomerization depends upon the substrate temperature used during co-deposition of the glass. Photostability correlates with the density of the glass, where the optimum glass is about tenfold more photostable than the liquid-cooled glass. Molecular simulations, which mimic photoisomerization, also demonstrate that photoreaction of a guest molecule can be suppressed in vapor-deposited glasses. From the simulations, we estimate that the region that is disrupted by a single photoisomerization event encompasses approximately 5 molecules.

3.1 Introduction

Organic glasses are amorphous materials that have been widely used in modern technologies, including pharmaceuticals,[1] organic light emitting diodes (OLEDs),[2, 3] polymers,[4, 5] and organic solar cells.[6] For many applications, glassy materials are preferred over their crystalline counterparts. For example, in the pharmaceutical industry, drugs are formulated into amorphous solids to achieve higher solubility and

bioavailability than can be attained with crystals.[7] In OLEDs, vapor-deposited organic glasses are frequently the active layers that transport charge and emit light. For OLEDs, smooth surfaces and lack of grain boundaries are key advantages of vapor-deposited glasses.[2] One potential concern when using organic materials is photochemical stability. Photodegradation can cause the failure of organic electronic devices,[8, 9] and this is sometimes a more limiting factor than device efficiency.[10]

Recently, physical vapor deposition (PVD) has been used to prepare single-component glasses that are highly photostable relative to liquid-cooled or spin-coated glasses prepared from the same molecules.[11] It was reported that photoisomerization of an azobenzene derivative (Disperse Orange 37 or DO37) could be slowed by a factor of 50 by using the correct substrate temperature during vapor deposition.[12] In another example, it was shown that vapor-deposited glasses of indomethacin suppress photodecarboxylation rates by a factor of 2 relative to the liquid-cooled glass.[13] The highly photostable glasses prepared by PVD also have high density[11, 14-17] and exceptionally high thermal stability[14, 18-21].For example, a glass prepared by vapor deposition onto a substrate near 0.85 T_g (where T_g is the glass transition temperature) can have a density as much as 1.3% higher than the liquid-cooled glasses. In principle, such high density (and high photostability) could also be achieved if a liquid-cooled glass was annealed for thousands of years,[16, 20, 22] but this is obviously not a practical route for materials synthesis. For the two examples above,[12, 13] enhanced photostability was found to correlate with glass density and explained by the constraint applied by tight molecular packing on the local molecular rearrangements needed for photoreaction. These examples from the literature for single component systems raise

the question of whether high density and high thermal stability glasses prepared by PVD can also lead to increased photostability for glass mixtures.

For many applications in organic electronics, glassy mixtures are utilized instead of single component glasses, and photostability is also a concern for these mixtures. For example, in the typical OLED, the light emitting molecule is diluted in a charge transport layer.[3] This arrangement both increases emission efficiency and facilitates tuning of the emission wavelength (by changing emitters) without changing the electrical characteristics of the device.[23, 24] It is known that switching to a more rigid host matrix can increase the photostability of guest emitters,[25,26] but often there are numerous constraints on the choice of the host material – such that this is impractical. Therefore, it would be ideal if photostability could be improved without changing the chemical identity of the guest or the host. As mentioned above, annealing a glass can increase density and rigidity. Royal and Torkelson reported that, for 4,4'-diphenyl azobenzene dispersed in amorphous polycarbonate, the susceptibility to photoisomerization decreased by 5% after annealing the glass for 100 hours.[27] While this example supports the principle that tighter glass packing can improve photostability of a guest molecule (without changing the guest or host identity), we are not aware of literature precedents that show a large increase in photostability by annealing a liquid-cooled glass.

In this study, we test whether PVD can be used to prepare mixed glasses in which the photostability of a guest molecule is substantially increased relative to that of the liquid-cooled glass. As a model system, we investigate the photoisomerization of the guest molecule 4,4'- diphenyl azobenzene (DPA) in vapor-deposited and liquid-cooled glasses of celecoxib. Azobenzene molecules can undergo *trans->cis* photoisomerization when

irradiated by light, as shown in Scheme 1. We first deposited pure celecoxib onto substrates held at different temperatures and successfully obtained glasses with different initial densities and a wide range of thermal stabilities. This result was expected on the basis of recent calorimetric work showing that PVD glasses of celecoxib had low enthalpy and high thermal stability.[21] We then co-deposited 5% DPA with 95% celecoxib and prepared glass mixtures that have similar thermal stability and packing as with the neat films. UV-Vis spectroscopy was used to measure the photoisomerization process directly during light irradiation. The long lifetime of the thermal relaxation from *cis* to *trans* (~10 hrs.) allows unambiguous characterization of the initial rate of photoisomerization.

We find that, relative to the liquid-cooled glass, the photoisomerization rate of the guest DPA can be decreased tenfold by controlling the packing in co-deposited PVD glasses. We observe that photostability is highly correlated with the density of the glass. To the best of our knowledge, this result represents a first demonstration that photostability of a dilute guest can be significantly increased via tighter glass packing, without changing the guest or host chemical identity. Molecular simulations of photoisomerization in vapor-deposited glasses capture the key features of the experiments and provide further molecular-level insight into the mechanism of photostability. In particular, the effect of dilution relative to neat films and the impact of an isomerization event on the

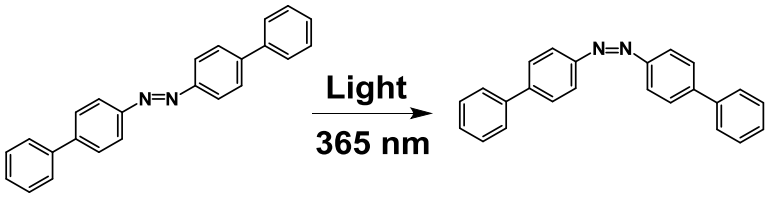

Scheme 1. Photoisomerization of 4,4’-diphenylazobenzene (DPA) under UV irradiation.

surrounding host molecules were investigated. From the simulations, we estimate that the region that is disrupted by a single photoisomerization event contains about 5 molecules.

3.2 Experiments

3.2.1 Materials

DPA was synthesized as described elsewhere.[27] Celecoxib (99%) was purchased from AvaChem Scientific and used as received. Celecoxib was selected as the host for these experiments because it is a good glass former that facilitates glassy thin film preparation via PVD.[21] Celecoxib absorbs light in the deep UV region and has no electronic absorbance above 300 nm. Thus, the absorbance of DPA at 370 nm can be observed by UV-Vis spectroscopy without interference, allowing convenient characterization of the *trans-cis* isomerization.

3.2.2 Preparation of DPA and celecoxib glass mixtures via PVD

PVD was performed in a vacuum chamber with the base pressure of 10^{-7} Torr. DPA and celecoxib were simultaneously evaporated from two different crucibles and thus co-deposited onto substrates. The total deposition rate was 2 Å/s, as monitored by the quartz crystal microbalance (QCM). The deposition rate for each component was controlled by tuning the heating power for each crucible independently. DPA was deposited at a rate of 0.1 Å/s in order to prepare a 5% mixture with the celecoxib host. A high throughput method was utilized to prepare a library of glasses with different densities and thermal stabilities in a single deposition. The substrate was suspended between two copper fingers; each finger was kept at a different temperature to create a

temperature gradient across the sample during deposition. The substrate temperature range was from 240 to 340 K. Fused silica substrates were used for photostability measurements (by UV-Vis) and silicon wafers were used for density and thermal stability measurement (by ellipsometry). Film thicknesses were about 1000 nm for films on silica and 300 nm for films on silicon.

3.2.3 Photostability measurement

A 365 nm UV lamp (Spectroline ENF-240C, 20 nm bandwidth) was used as the light source to induce photoisomerization of DPA. Samples were intermittently illuminated at normal incidence with an irradiance of 40 μW/cm^2 at room temperature. Immediately after each illumination period, a UV-Vis absorbance spectrum was recorded. The rate of photoisomerization was analyzed from the changes in the absorbance with illumination time. For the 1000 nm thick films with 5% DPA that we utilized, 60-70% of the 365 nm light is absorbed.

3.2.4 Density and thermal stability measurement

The density and thermal stability of vapor-deposited glasses were characterized by spectroscopic ellipsometry (J. A. Woollam, M-2000). (See Figure 5 below for sample data.) For all ellipsometry measurements, three incident angles were used (50°, 60°, and 70°), and wavelengths from 500 to 1000 nm were used to fit the measurements to an anisotropic Cauchy model. To measure density and thermal stability, ellipsometry was performed on samples placed on a custom-built hot stage, and the temperature was increased at 1 K/min from near room temperature to 350 K (28 K above T_g of celecoxib). The onset temperature, which characterizes the thermal stability of a glass,

was determined from the beginning of the transformation into the supercooled liquid. Immediately after heating, the supercooled liquid was cooled at 1 K/min to room temperature to form the liquid-cooled glass. By comparing the sample thickness before and after heating/cooling runs, the density of the vapor-deposited glass relative to that of the liquid-cooled glass was determined.

We also measured the density changes during light irradiation at an isothermal condition. Spectroscopic ellipsometry was used to characterize the glass thickness at the spot where the 365 nm UV irradiated the sample. Relative density was determined by the inversed thickness changes induced by light. Sample data are shown in Figure 4.

3.2.5 Computer simulations

In order to better understand photoisomerization in vapor-deposited glasses, molecular simulations were performed using a coarse-grained model of a glass forming host and a photoactive guest. We used a previous simulation study[12] as our starting point, and made two important changes in order to make the simulations more realistic for the current experiments. In this paragraph, we briefly recap the simulations of Reference 12 in order to provide context for the current work. The goal of Reference 12 was to simulate the photoisomerization of vapor-deposited glasses of neat DO37 (an azobenzene derivative). The simulations began with the vapor deposition of a coarse-grained molecule with four linearly-connected beads (as shown in Figure 8) onto a temperature-controlled substrate. At several different substrate temperatures, films were deposited up to a thickness of approximately 40 σ_{bb}, where σ_{bb} is the Lennard-Jones interaction radius of each bead in the molecule. After the film was prepared with all molecules in the *trans* state, the response of the film to photoexcitation was investigated

in the “bulk” region of the film, defined as the section of the film between 15 σ_{bb} to 28 σ_{bb} in the z-dimension. During the entire simulation, the dihedral angle potentials had the following functional form:

$$U_{dihedral} = \frac{1}{2}k_1(1+\cos\theta) + \frac{1}{2}k_2(1-\cos 2\theta).$$

During deposition, the parameters used for the dihedral potential were $k_1 = 20$ and $k_2 = 8$; this potential strongly favors the *trans* state. In Reference 12, photoexcitation was simulated by randomly selecting a small fraction of the molecules and instantaneously switching the dihedral potential to one that favored the *cis* state ($k_1 = -25$ and $k_2 = 6.25$).

In comparison to the procedure used in Reference 12, the simulation of the photoexcitation process was modified in two respects in order to describe the photoisomerization of the guest DPA in a celecoxib matrix. First, after the deposition stage, we randomly selected a subset of the molecules to be “guests”; only this subset could be photoexcited in subsequent stages of the simulation. Second, to account for the much longer *cis*- lifetime of DPA as compared to DO37, the dihedral potential describing the resting state for the guest molecules was changed ($k_1 = 10$ and $k_2 = 25$) to have a minimum in the *cis* configuration ($\theta = 0$) as well as the *trans* configuration ($\theta = \pm 180°$). For one set of simulations (described below as “original potential”), when a photoexcitation event occurred we switch to the same potential used for photoexcitation in Reference 12 ($k_1 = -25$ and $k_2 = 6.25$). For a second set of simulations, we increased the driving force for isomerization by a factor of 1.5; for these simulations (described below as “1.5x original potential”), we utilized $k_1 = -37.5$ and

$k_2 = 9.375$ when a photoexcitation event occurred. In this way, the effect of isomerization driving force, which mimics photon energy, on reaction kinetics was investigated.

For the simulations reported here, the photoexcitation procedure was adjusted such that, on average, only 1 out of the approximately 1000 bulk molecules were excited within each iteration. For each photoexcitation iteration, the dihedral potential for a selected guest molecule was switched temporally from the resting state with minima for *cis* and *trans* states to the designated excitation potential with a minimum only in the *cis* state. A short molecular dynamics simulation of a 100 LJ time units was then performed, which allowed the excited molecules to isomerize to the *cis* state if the local packing arrangement allowed it. The dihedral potential was then switched back to the resting potential and the procedure was repeated with new excited molecules randomly selected from the guest molecules. Due to the *cis* state minimum in the resting dihedral potential, once a molecule successfully isomerized to the *cis* configuration it remained *cis* for the duration of the simulation. (This was not the case in Reference 12, where the resting dihedral potential favored the *trans* state.) For the x-axes in Figures 8 and 9, the "Number of photoexcitations" was calculated by using the number of iterations of the photoexcitation process times the average number of photoexcitations per iteration.

All other aspects of the simulations that are not discussed above were performed as described in Reference 12.

3.3 Results

3.3.1 Photoisomerization in PVD and liquid-cooled glasses

The photostability of mixed glasses of DPA in celecoxib was monitored by UV-Vis spectroscopy. Figure 1 shows the absorption spectra of a glass vapor-deposited at 273 K and the liquid-cooled glass. Upon irradiation with 365 nm light, the absorbance at the peak near 370 nm for both glasses decreased due to photoisomerization from the *trans* to *cis* states. The absorbance of the liquid-cooled glass decayed faster at the initial stages relative to the sample deposited at 273 K, indicating less resistance to light-induced photoisomerization.

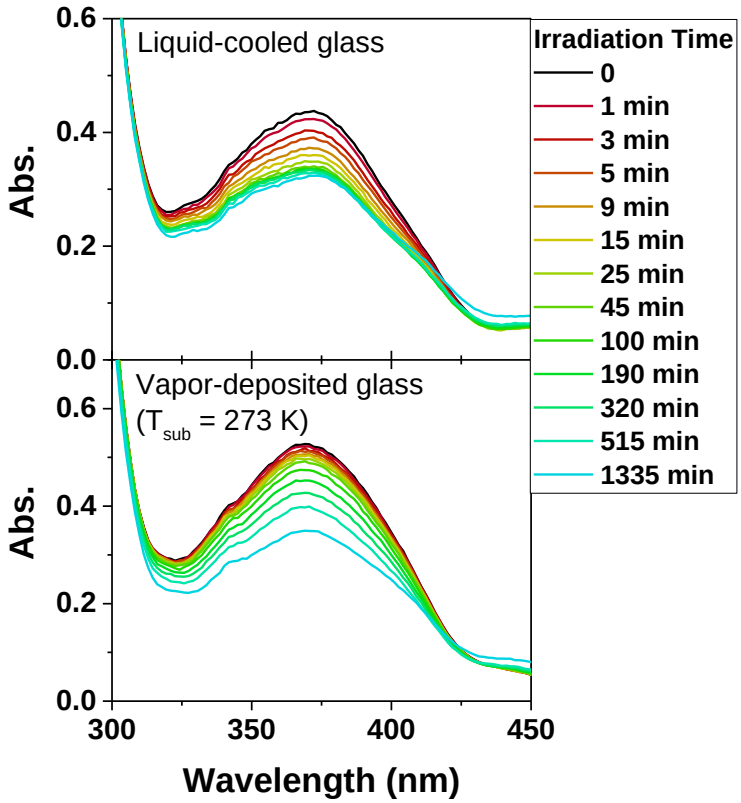

Figure 1. Photoisomerization of glasses containing 5% DPA guest in a matrix of celecoxib as monitored by absorbance after light irradiation at 365 nm; irradiation times are specified in the legend. Top panel shows results for a liquid-cooled glass and the bottom panel shows results for a glass vapor-deposited at 273 K. At early times, photoisomerization is much

Figure 2 shows the comparison of DPA photoisomerization in vapor-deposited and liquid-cooled glasses and reveals that PVD glasses display significantly lower reaction rates, *i.e.* enhanced photostability. Immediately after irradiation begins, the normalized absorbance at 370 nm starts to decrease for all glasses, indicating *trans to cis* isomerization. For the liquid-cooled glass, as represented by the black curve, the reaction half-life is about 10 minutes and the reaction reaches a stationary state after about 100 min irradiation. In contrast, photoisomerization in vapor-deposited glasses occurs more slowly with the reaction rate depending upon the substrate temperature during deposition. For the optimum PVD glass (T_{sub} = 273 K = 0.85 T_g), the reaction half-life is about 200 min, which is about 20 times longer than for the liquid-cooled glass with the same composition.

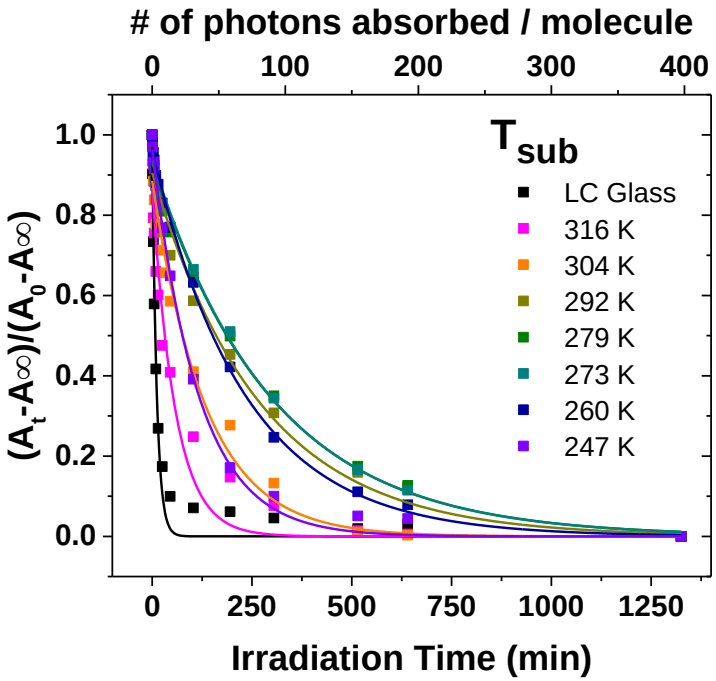

Figure 2. Time dependence of photoisomerization for vapor-deposited and liquid-cooled (LC) glasses of 5% DPA in celecoxib as determined from normalized absorbance at 370 nm. The glasses were prepared at a range of substrate temperatures as indicated. PVD glasses exhibit much slower photoisomerization than the liquid-cooled glass. Solid lines are exponential fits.

The kinetics of DPA photoisomerization in mixed glasses with celecoxib are summarized in Figure 3, showing that the photoisomerization rate varies by a factor of ten depending upon the substrate temperature used during deposition. The rate constant k was obtained from exponential fits of the data shown in Figure 2; for these fits, we only utilized the first 45 minutes of the data to ensure that we obtained an accurate description of the initial reaction rate. The liquid-cooled glass, which has the highest reaction rate among the glasses, was prepared by vapor-deposition at a temperature above 322 K (T_g) and cooled back to the room temperature at 1 K/min. The most photostable glasses were prepared between 247 to 292 K, which corresponds to glasses with the highest initial densities (see discussion below). As a control experiment, the photoisomerization rate of a liquid-cooled glass was measured before and after aging for 140 hours at 273 K. As shown in Figure 3, 140 hours of aging leads to a very small increase in photostability. This result indicates that, as a practical matter, the aging of a liquid-cooled glass cannot achieve the large increases in photostability observed for the PVD glasses. The photoisomerization rate of DPA was also measured in ethanol and is shown in Figure 3. All of these results are consistent with the idea that a well-packed glassy environment can inhibit the photoreaction of a guest molecule.

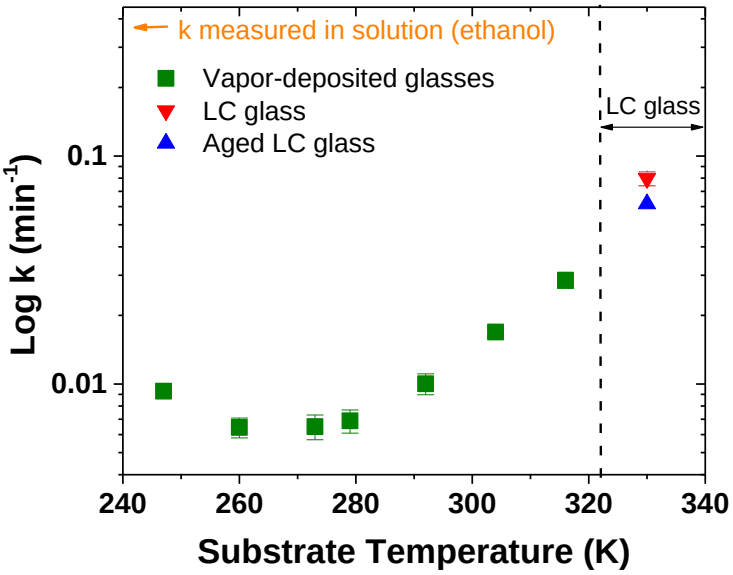

Figure 3. Photostability of vapor-deposited glasses, with comparison to the liquid-cooled (LC) glass and DPA in solution. The logarithm of the photoisomerization rate constant k is plotted against substrate temperature. Blue and red triangles show the influence of aging on a liquid-cooled glass over 140 hours at 273 K. The photoisomerization rate in ethanol solution is also indicated for reference (orange).

The impact of DPA photoisomerization on the mixed glass structure was also investigated by using ellipsometry to measure the density changes induced by light irradiation, demonstrating that PVD glasses resist density changes more strongly than the liquid-cooled glass. As shown in Figure 4, vapor-deposited glasses initially have a higher density than the liquid-cooled glass (see below). For all glasses, upon light irradiation, the glass density decreases immediately after irradiation due to the photo-expansion effect.[28] The liquid-cooled glass expands quickly after irradiation and reaches a stationary state at about 100 min, after which no further expansion can be observed. Compared to that, vapor-deposited glasses photo-expand more slowly, which can be found by measuring the time required for the density to change by 0.1%. A density change of this magnitude requires about 10 min for the liquid-cooled glass and about 100 min for the glass deposited at 272 K.

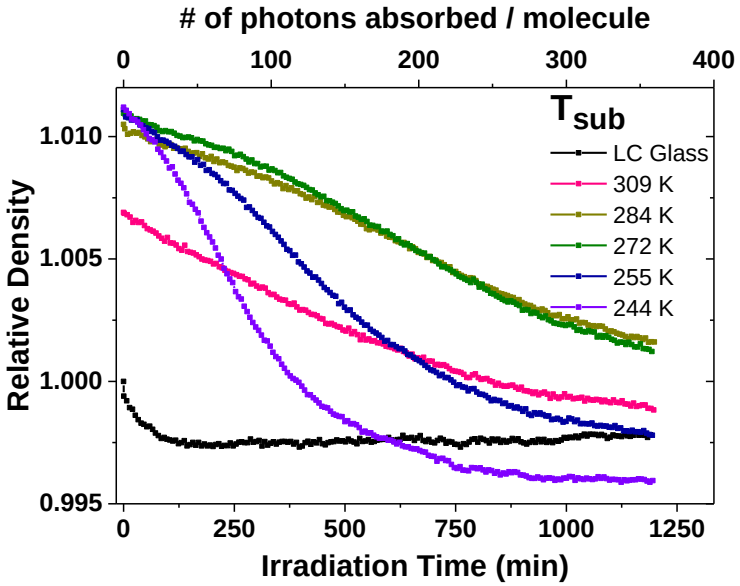

Figure 4. Density changes during illumination for vapor-deposited and liquid-cooled glasses of celecoxib with 5% DPA, as a function of irradiation time. Density is normalized to the initial density of the liquid-cooled glass. Relative to the liquid-cooled glass, density changes much more slowly during illumination for the most stable PVD glasses.

3.3.2 Density and thermal stability of PVD glasses

For comparison with the photostability results presented above, the density and thermal stability of PVD glasses of neat celecoxib and DPA/celecoxib mixtures were investigated by spectroscopic ellipsometry. Figure 5 shows an example of a temperature-ramping experiment for celecoxib deposited at T_{sub} = 276 K (0.86 T_g), as characterized by ellipsometry. Three temperature ramping cycles were performed. In the first cycle, the as-deposited celecoxib was heated from 295 K to 350 K at 1 K/min and then cooled back to 295 K. The subsequent heating/cooling runs were performed at the same rate from 295 K to 340 K. During the first heating, the as-deposited sample transforms into the supercooled liquid as indicated by the large increase in thickness over a small temperature range. The onset temperature, which characterizes the thermal stability of the as-deposited glass, was determined from the beginning of the transformation into the supercooled liquid (334 K). During the subsequent cooling, the liquid-cooled glass was formed at the glass transition temperature (T_g) of 322 K. Thickness data from the second and third cooling runs reproduced closely the data from the first cooling run, since the preparation details of the deposition process are erased during transformation to the supercooled liquid.

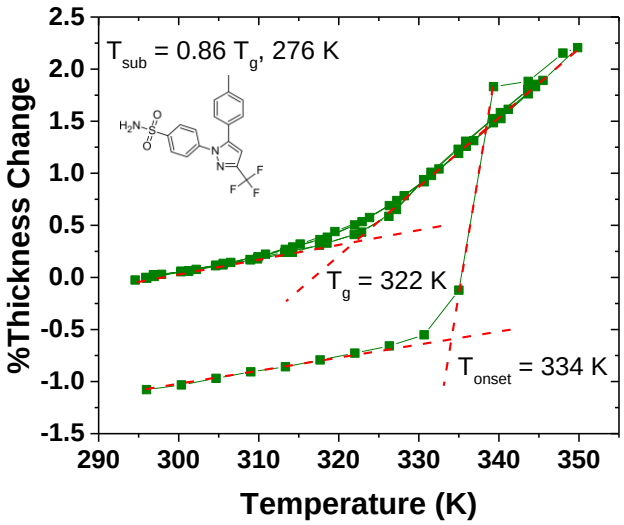

Figure 5. Thickness changes obtained by ellipsometry for a vapor-deposited glass of celecoxib during temperature cycling at 1 K/min. Data is shown for a glass vapor-deposited at T_{sub} = 276 K (0.86 T_g). This PVD glass is more dense than the liquid-cooled glass (formed by heating/cooling) and has greater thermal stability (since T_{onset} is greater than T_g). The sample thickness is about 300 nm. Inset shows the molecular structure of celecoxib.

The PVD glass of celecoxib illustrated in Figure 5 shows high density and high thermal stability. The change in thickness between the first heating and cooling runs is used to determine the density of the as-deposited glass relative to the liquid-cooled glass. In this case, the as-deposited glass is 1.1% more dense. A high value of T_{onset} (12 K above T_g) is demonstrated during the first heating run, indicating enhanced thermal stability. PVD glasses of celecoxib have properties similar to PVD glasses of other molecules.[15] For comparison, indomethacin has been reported to form PVD glasses with T_{onset} as much as 18 K above T_g and a density increase of up to 1.3% relative to the liquid-cooled glass.[18] Figure 6a shows the density for celecoxib glasses vapor-deposited at different substrate temperatures relative to the liquid-cooled glass. All the glasses deposited at $T_{sub} < T_g$ show higher density than the liquid-cooled glass. We attempted to measure the density of DPA/celecoxib mixtures by the method described in Figure 5 but could not, as the thickness of the transformed sample was not stable in the second and third heating cycles; this is possibly due to desorption of DPA during the ramping experiment. Given the small amount of DPA present in the mixed glasses, we assume that the relative densities of the mixtures are the same as the neat films shown in Figure 6a. This assumption was used in the construction of Figure 4.

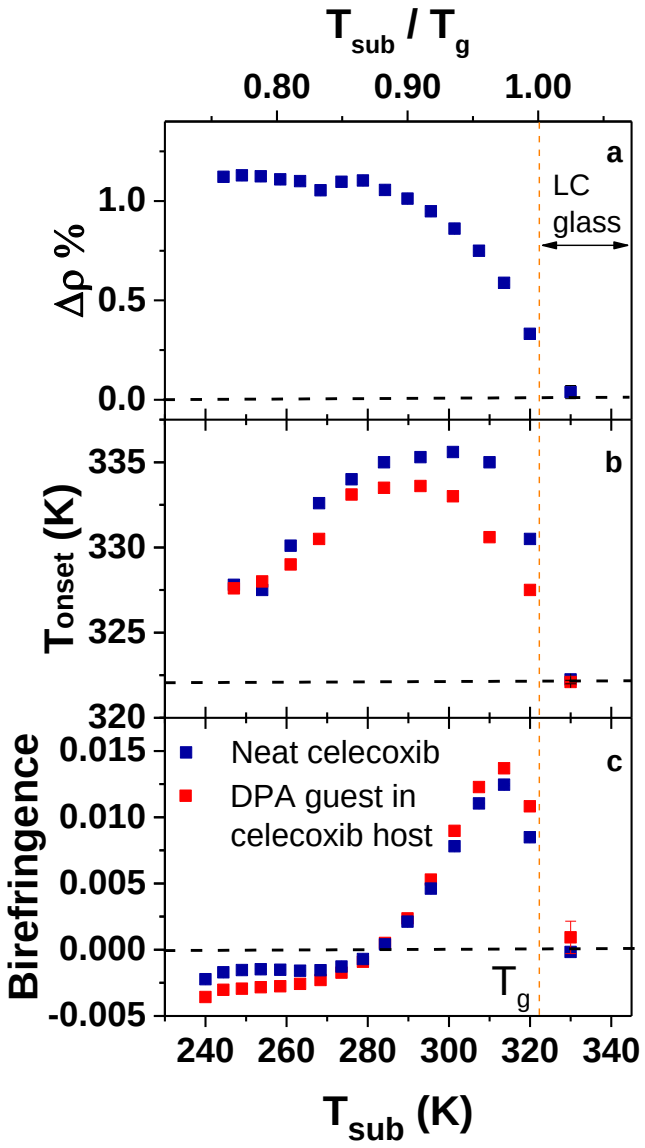

Figure 6. Summary of (a) relative density, (b) onset temperature, and (c) birefringence (n_z – n_{xy}) of vapor-deposited neat films of celecoxib (blue points) and mixtures with 5% DPA (red points), as characterized by ellipsometry. Liquid-cooled (LC) glasses were deposited at a substrate temperature higher than T_g and then cooled into the glassy state. Horizontal black dashed lines in each panel represent the corresponding measurement for the LC glass.

We find that co-deposition of 5% DPA with celecoxib does not significantly change the thermal stability and structure of PVD glasses in comparison with pure celecoxib glasses. To illustrate this, comparisons of the onset temperature and birefringence for vapor-deposited glasses of celecoxib and DPA/celecoxib mixtures are shown in Figures 6b and 6c. Glasses deposited above T_g (and subsequently cooled to room temperature) are regarded as liquid-cooled glasses and this is consistent with the observation that $T_{onset} = T_g = 322$ K for these materials. For T_{sub} lower than T_g, enhanced thermal stability was observed. Glasses with the optimum thermal stability were prepared at T_{sub} between 0.85 to 0.96 T_g. The increased thermal stability and enhanced density of these vapor-deposited glasses are attributed to enhanced surface mobility during glass formation.[29, 30] Birefringence of vapor-deposited glasses, indicative of molecular orientation, is shown in Figure 6c. Above T_g, the zero birefringence indicates random molecular orientation, which is consistent with the isotropic structure that a liquid-cooled glass inherits from the supercooled liquid. Below T_g, birefringence is not zero and depends upon the value of T_{sub}. This non-zero birefringence has been reported for many other PVD glasses.[17, 20, 31, 32] Both onset temperatures and birefringence data indicate that glass packing of neat celecoxib films and DPA/celecoxib mixtures is similar.

We can now compare the DPA photoisomerization rates (Figure 3) with the densities for different glasses (Figure 6a). Figure 7 shows a strong correlation between the photostability of the DPA guest and the glass density. Increased glass density is associated with a decreased photoisomerization rate. DPA in the liquid-cooled glass photoisomerizes about 10 times faster than it does in the glasses with the highest

density. As discussed later, this result is consistent with the view that higher density plays an important role in suppressing photoreaction. The behavior of the aged liquid-cooled glass is qualitatively consistent with this finding. The density change after 140 hours of aging was not measured but is expected to be a few tenths of a percent; this small density change would be consistent with the trend shown in Figure 7, given the slightly lower isomerization rates for the aged sample shown in Figure 3.

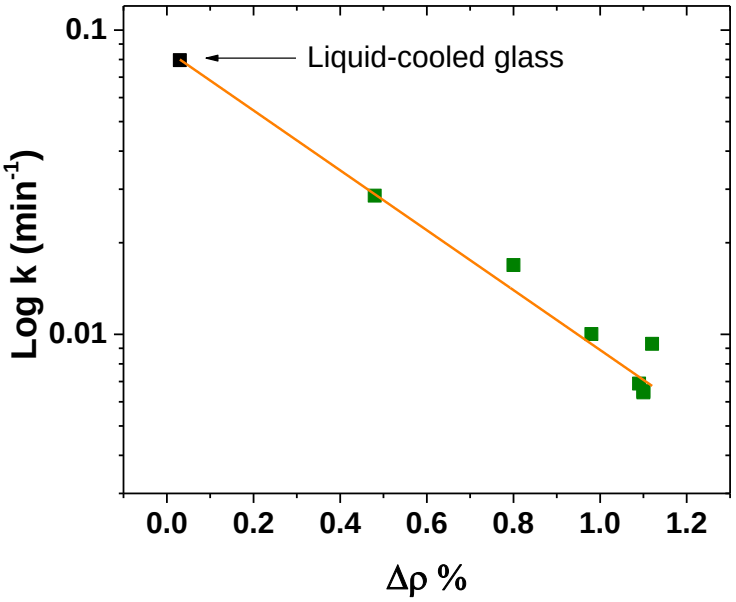

Figure 7. Correlation of photoisomerization rate constant with the density of vapor-deposited glasses of the celecoxib host. The orange solid line is the linear fit.

3.3.3 Simulations of vapor-deposited guest/host glasses

Molecular simulations of vapor-deposition and photoisomerization were performed to provide insight to the enhanced photostability in co-deposited PVD glasses. As explained earlier, the vapor deposition and photoisomerization aspects of the simulation are similar to the method used in a previous study of DO37[12] where, to examine the packing effect on photoisomerization process, DPA was represented by a coarse-grained linearly connected molecule with four beads (Figure 8, inset). During the vapor deposition process, coarse-grained DPA molecules were held in the *trans* state and deposited onto substrates at temperatures ranging from 0.76 to 0.97 T_g, where T_g was determined to be 0.66 in reduced Lennard-Jones (LJ) units. Consistent with the experimental results, the simulated PVD glasses had a higher density than the corresponding liquid-cooled glass (SI, Figure S1) when deposited at substrate temperatures below T_g. For the photoisomerization process, we mimic the dilution of DPA in the experiments by randomly selecting 5% of deposited molecules to be guests; only this subset can photoreact. For each photoexcitation cycle, guest molecules are selected with a small probability to be excited; this occurs by switching dihedral potentials such that a force acts to push the molecule from *trans* to *cis*. On average, only one guest is selected for excitation during each photoexcitation cycle. Whether or not the *cis* state is actually attained is determined by the local packing environment. Guest molecules that reach the *cis* state during photoexcitation remain there for the duration of the simulation, consistent with the long thermal relaxation time for the *cis* state of DPA.

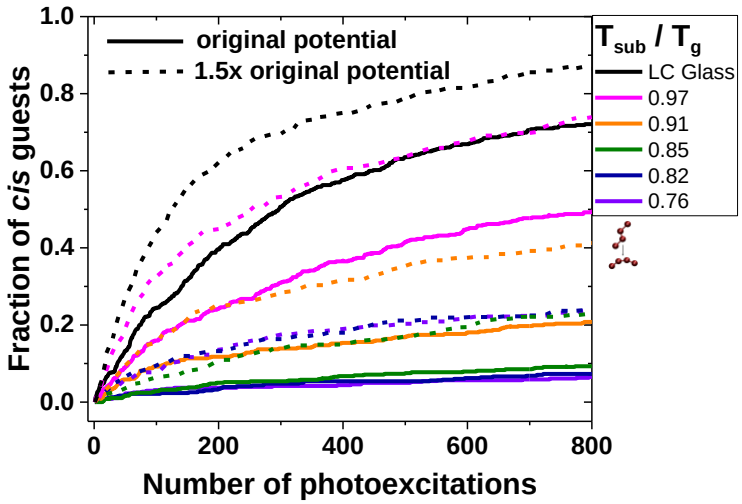

Figure 8. Photoisomerization from *trans* to *cis* states as observed in molecular simulations for a mixed glass (5% isomerizable guests), for glasses vapor-deposited at different substrate temperatures. Two different driving forces for isomerization were studied: the solid lines were obtained with the potential utilized in Reference 12 and the dashed lines represent results for a dihedral potential that has a 50% larger driving force for photoisomerization. Representative structures of the coarse-grained model in *trans* and *cis* states are shown in the inset. For both dihedral potentials, vapor-deposited glasses show much slower *trans-cis* photoisomerization.

Figure 8 shows that simulated glasses prepared by PVD are substantially more photostable than the liquid-cooled glass. For each glass, the fraction of guests isomerized is shown as a function of the number of photoexcitation events. We performed these simulations using two different dihedral potentials for the photoexcitation step, in order to investigate the effect of the driving force on the photoisomerization kinetics. Figure 8 shows results both for the potential utilized in reference 12 (the “original potential”) and one in which the driving force is 50% larger (“1.5x original potential”).

For the liquid-cooled glass driven by the original potential, the *cis* fraction of the guest molecules increased from zero to 0.7 after 800 photoexcitations. After the same number of photoexcitations, the fraction of guests that successfully reached *cis* for the most photostable glass (T_{sub} = 0.76 T_g) was only 0.04. The simulation result indicates that the initial molecular packing of the vapor-deposited glasses suppresses the ability of excited molecules to change from *trans* to *cis*, and that the substrate temperature during deposition has a strong impact on photostability. Both of these observations are qualitatively consistent with the experimental results in Figure 2.

By comparing results from the two different dihedral potentials used in the photoexcitation step, we find that the rate of photoisomerization is significantly increased when a stronger driving force is utilized. As shown in Figure 8, the optimum glass has a *cis* fraction of 0.24 after 800 photoexcitation events with the stronger driving force; this is 6 times the *cis* fraction resulting from the original potential from Reference 12. We use this result below to compare experiments on azobenzene derivatives that are excited with different photon energies.

The effect of the concentration of guest molecules in mixtures was also investigated in the simulations revealing that, for a given number of photoexcitations, a higher guest concentration leads to greater disruption of glass packing. As shown in Figure 9, glass density decreases as the number of photoexcitations increases due to the photo-expansion effect, which is consistent with the experimental results in Figure 4. The density decrease is faster when the concentration of isomerizable guests is larger. For example, after 800 photoexcitations, the sample with the lowest azobenzene concentration (0.03) only photo-expands by 0.35%, while density of the film in which every molecule is photoisomerizable decreases by 3.4%. Note that in this comparison the total number of photoexcitation events is the same for glasses with different guest concentrations. Figure 9 shows that when these photoexcitation events are concentrated in a small number of guest molecules, the overall glass density is minimally affected.

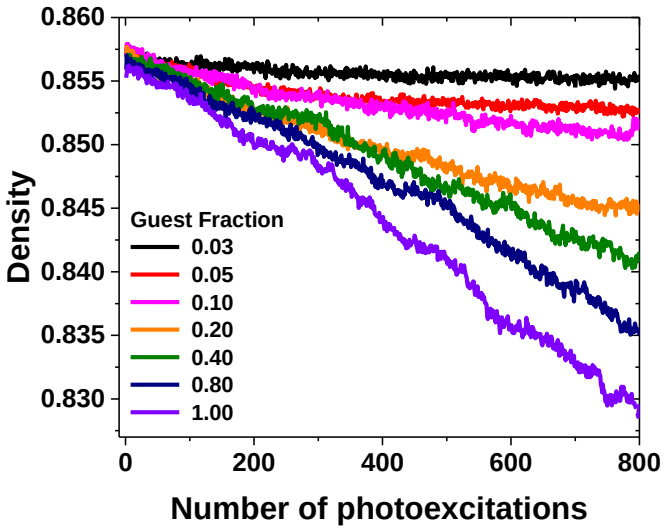

Figure 9. Simulation results showing photo-induced density changes for glasses with different fractions of isomerizable guests. All glasses were deposited at $T_{sub} = 0.76\ T_g$. For the same number of excitation events, the density of the glass changes more quickly when the guest fraction is larger.

By comparing the light-induced density decrease for films in which a different fraction of the molecules is photoisomerizable, we can estimate the extent to which a photoisomerization event disrupts the packing of its surroundings. Figure 10 shows how the density change after 800 photoexcitation events varies as a function of the fraction of photoisomerizable guests. Two regimes of linear dependence can be observed, with the rate of increase becoming slower when the guest fraction surpasses 0.2. We interpret the transition of density disruption to indicate the size of the region that can be influenced by each photoisomerizing guest. At the guest/host ratio of 1:4, the local regions that have been influenced by photoisomerization start to overlap and each isomerizing guest molecule starts to feel the existence of its neighbors.

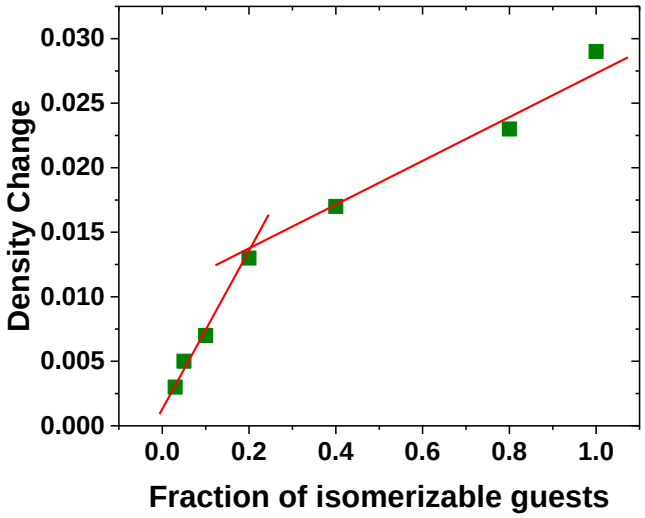

Figure 10. Density change in simulations after 800 photoexcitation events for glasses with different guest fractions. Solid lines are guide to the eye. Density disruption becomes larger as DPA fraction increases, and the transition point indicates the size of the region that can be influenced by each photoisomerizing guest. All the glasses shown were prepared at T_{sub} = 0.76 T_g.

3.4 Discussion

We have shown that photoreaction of a guest molecule can be substantially suppressed in a glass mixture by more densely packing the glass, without altering the chemical structures of the guest or host. The strong correlation between glass density and photostability in a two-component system identified here had not been established before, and we therefore anticipate that the results reported in this work will help guide future studies of efficiency in organic electronics. In these experiments, photostability is highly dependent on the substrate temperature used during vapor deposition. For substrate temperatures lower than T_g, the photostability of PVD glasses can be increased by up to a factor of 12 in the systems considered here. We also show that photostability correlates with glass density, with higher density glasses being more resistant to reactions. Molecular simulations reproduce important features observed in our experiments, such as enhanced photostability for guests in high-density PVD glasses. Moreover, simulations provide an opportunity to investigate the effect of driving force (photon energy) and guest concentration and provide insight into the mechanism by which glass packing can suppress photoisomerization.

Previous literature has suggested that density can play an important role in modulating the photoreaction rate of a guest molecule in a two-component glass. For example, in a glass of DPA dispersed in amorphous polycarbonate, it was shown that physical aging for 100 hours led to an ~5% decrease in the extent of photoisomerization; physical aging for this period of time can increase glass density slightly.[27] Compared to aging, PVD provides a route to obtain glasses with substantially increased photostability and density within reasonably short sample preparation times.

In previous studies of one-component PVD glasses, it has been observed that photostability is correlated with glass density. Photostability of vapor-deposited DO37, an azobenzene derivative, was characterized by measuring density and molecular orientation changes during irradiation.[12] It was observed that structural changes associated with photoisomerization were suppressed by a factor of 50 by a density increase of 1.3%. In a second example, that of an azobenzene derivative tethered to a PMMA polymer, it was demonstrated that optically induced molecular rearrangement can be hindered by high-density glasses created by high external pressure.[33] The glass density at 150 MPa was increased by 2.4% and the rate of photo-orientation decreased by a factor of nearly 50. These two examples show a strong correlation between glass density and photostability for single-component glasses. The work presented here extends this conclusion to guest stability in a two-component glass.

A significant improvement in our current experiment relative to previous work on vapor-deposited DO37 glasses is that here we provide direct experimental evidence that photoisomerization is blocked by dense packing. In the earlier work on DO37, photostability was assessed by measuring the density and molecular orientation changes induced by light; the impact of glass packing on the *trans* to *cis* reaction rate could not be directly monitored.[12] The work presented here allows us to directly observe the *trans-cis* photoreaction by measuring UV-Vis absorbance. In light of these new results, we think that *trans-cis* isomerization was also blocked in the previous study of DO37, and this conclusion is consistent with the computer simulations reported for that system.[12] We imagine that this result is quite general and so we expect that photoreactions in both one and two components glasses can generally be suppressed

by preparing high-density glasses by PVD. An issue not resolved by this work is whether density is the glass property that best correlates with increased photostability. For example, for cases where it has been investigated, high-density PVD glasses also have high moduli.[34] It is possible that the moduli might correlate with enhanced photostability even better than the density. This would be reasonable as a high modulus glass would be expected to better resist the driving force for *trans* to *cis* isomerization.

This study provides an important opportunity to investigate the effect of different excitation wavelengths on photoisomerization in glasses. For the DPA/celecoxib experiments presented here, we observe immediate photoisomerization and photo-expansion in Figures 2 and 4, respectively. In contrast, in our previous DO37 experiment, for the most stable glass, hardly any change in density was observed even after all the molecules had been excited 300 times. In part, we attribute these observations to the fact that DPA was excited by 365 nm light while DO37 was excited by 532 nm light. Since 365 nm photons are 45% more energetic than 532 nm photons, this provides a larger driving force for photoisomerization. Simulation results in Figure 8 are consistent with this conclusion. When the driving force used to mimic the photoexcitation increases by a factor of 1.5, much larger rates of photoisomerization are observed for the most stable glass.

When a molecule in a glass isomerizes, we expect that the packing of the surrounding molecules is altered and these simulation results provide an opportunity to estimate the size of this disrupted region. Figure 10 shows that the impact of guest concentration on the disruption of glass structure undergoes a transition when the guest fraction exceeds 20%. We interpret this result to indicate that, when the guest concentration is less than

20%, each photoisomerization of a guest molecule occurs nearly independently of the other guests. When the guest fraction is larger, the regions that are disrupted by photoisomerization overlap, and therefore the impact of each photoisomerizing guest on the overall density will be diminished. From this interpretation, we infer that each photoisomerizing guest molecule influences a region of the glass that, on average, also includes four host molecules. We speculate that there may be some connection between the size of this region and the cooperatively rearranging regions (CRR) described in various theories of the glass transition. [35-37] In these theories, the size of the CRRs is typically connected to the configuration restrictions associated with glass packing that can be described by the configurational entropy. This is an interesting issue for exploration by future simulations and experiments.

Finally, we note that this study builds upon previous vapor-deposition studies of neat celecoxib by Rodriguez-Viejo and coworkers.[21] Using calorimetry, these authors reported that glasses of celecoxib with the very high thermal stability and low enthalpy were obtained for substrate temperatures near 275 K. These results are in reasonable accord with the ellipsometry results presented in Figure 6.

3.5 Concluding Remarks

We have shown that photoisomerization of guest molecules can be significantly inhibited by improving the packing in a glass without any changes in the chemical identity of the guest or host. Photoisomerization of the guest DPA in a matrix of celecoxib can be suppressed tenfold relative to the liquid-cooled glass by selecting the optimum conditions for vapor deposition. Photostability is observed to correlate

reasonably with density, where the tighter packing exerts stronger constraints on the molecular rearrangements required for *trans*-*cis* isomerization.

Our work suggests that substrate temperature is an important control variable for optimizing the performance of the multicomponent glassy layers used in organic electronic devices. Previous study has revealed that, for emitters doped in the host materials used for OLEDs, solution-coated films are more susceptible to degradation relative to vapor-deposited glasses.[38] Our work has demonstrated that the photostability of two-component vapor-deposited glasses can be further improved by optimizing the glass density. So far, more than thirty molecules have been made into single component high-density glasses by PVD, and several of these molecules are used as host materials for OLEDs.[15] Thus, we expect that the suppression of photoreaction shown in the current work will also be observed for emitter/host glassy layers used in OLEDs. This method for increasing resistance to photodegradation could be important as operational lifetime is considered to be a bottleneck to the further improvement of OLED display performance, especially for blue emitters.[10] There are recent reports that the electronic and optical properties of films of organic semiconductors can be more stable over time if vapor deposition conditions are optimized to prepare the highest density glasses.[39, 40] Our results clearly show the importance of glass density in suppressing photoreactions, and with these other recent results, suggest that optimizing the substrate temperature utilized in PVD is an effective method of extending device lifetime.

Acknowledgments

The experimental work was supported by the U.S. Department of Energy (DOE), Office of Basic Energy Sciences (BES), Division of Materials Sciences and Engineering, Award DE-SC0002161 (to M.D.E. and Y.Q.) and by funds associated with a Walter P. Murphy Professorship (to J.M.T.). The simulations were also supported by the Department of Energy, Basic Energy Sciences, Materials Sciences and Engineering Division. Additional support from the US Army Research Office through the MURI program W911NF-15-1-0568 for development of light-responsive materials is gratefully acknowledged (J.J.dP).

3.6 References

[1] B. C. Hancock, and G. Zografi, Characteristics and significance of the amorphous state in pharmaceutical systems. J. Pharm. Sci. **86** (1997) 1.

[2] D. Yokoyama, Molecular orientation in small-molecule organic light-emitting diodes. J. Mater. Chem. **21** (2011) 19187.

[3] K. Sei-Yong *et al.*, Organic light-emitting diodes with 30% external quantum efficiency based on a horizontally oriented emitter. Adv. Funct. Mater. **23** (2013) 3896.

[4] G. B. McKenna, and S. L. Simon, 50th anniversary perspective: Challenges in the dynamics and kinetics of glass-forming polymers. Macromolecules **50** (2017) 6333.

[5] Y. Joo *et al.*, A nonconjugated radical polymer glass with high electrical conductivity. Science **359** (2018) 1391.

[6] M. Helgesen, R. Sondergaard, and F. C. Krebs, Advanced materials and processes for polymer solar cell devices. J. Mater. Chem. **20** (2010) 36.

[7] B. C. Hancock, and M. Parks, What is the true solubility advantage for amorphous pharmaceuticals? Pharm. Res. **17** (2000) 397.

[8] Q. Wang, Y. Luo, and H. Aziz, Photodegradation of the organic/metal cathode interface in organic light-emitting devices. Appl. Phys. Lett. **97** (2010) 063309.

[9] P. Cheng, and X. Zhan, Stability of organic solar cells: Challenges and strategies. Chem. Soc. Rev. **45** (2016) 2544.

[10] Y. Zhang, J. Lee, and S. R. Forrest, Tenfold increase in the lifetime of blue phosphorescent organic light-emitting diodes. Nat. Commun. **5** (2014) 5008.

[11] M. D. Ediger, Perspective: Highly stable vapor-deposited glasses. J. Chem. Phys. **147** (2017) 210901.

[12] Y. Qiu *et al.*, Photostability can be significantly modulated by molecular packing in glasses. J. Am. Chem. Soc. **138** (2016) 11282.

[13] Y. Qiu, S. S. Dalal, and M. D. Ediger, Vapor-deposited organic glasses exhibit enhanced stability against photodegradation. Soft Matter **14** (2018) 2827.

[14] S. F. Swallen *et al.*, Organic glasses with exceptional thermodynamic and kinetic stability. Science **315** (2007) 353.

[15] S. S. Dalal *et al.*, Tunable molecular orientation and elevated thermal stability of vapor-deposited organic semiconductors. Proc. Natl. Acad. Sci. U.S.A. **112** (2015) 4227.

[16] K. L. Kearns, P. Krzyskowski, and Z. Devereaux, Using deposition rate to increase the thermal and kinetic stability of vapor-deposited hole transport layer glasses via a simple sublimation apparatus. J. Chem. Phys. **146** (2017) 203328.

[17] T. Liu *et al.*, Birefringent stable glass with predominantly isotropic molecular orientation. Phys. Rev. Lett. **119** (2017) 095502.

[18] S. S. Dalal, Z. Fakhraai, and M. D. Ediger, High-throughput ellipsometric characterization of vapor-deposited indomethacin glasses. J. Phys. Chem. B **117** (2013) 15415.

[19] M. S. Beasley *et al.*, Glasses of three alkyl phosphates show a range of kinetic stabilities when prepared by physical vapor deposition. J. Chem. Phys. **148** (2018) 174503.

[20] T. Liu *et al.*, The effect of chemical structure on the stability of physical vapor deposited glasses of 1,3,5-triarylbenzene. J. Chem. Phys. **143** (2015) 084506.

[21] C. Rodriguez-Tinoco *et al.*, Highly stable glasses of celecoxib: Influence on thermo-kinetic properties, microstructure and response towards crystal growth. J. Non-Cryst. Solids **407** (2015) 256.

[22] K. L. Kearns *et al.*, Hiking down the energy landscape: Progress toward the kauzmann temperature via vapor deposition. J. Phys. Chem. B **112** (2008) 4934.

[23] J. Vygintas *et al.*, Highly efficient tadf oleds: How the emitter–host interaction controls both the excited state species and electrical properties of the devices to achieve near 100% triplet harvesting and high efficiency. Adv. Funct. Mater. **24** (2014) 6178.

[24] Y. Tao, C. Yang, and J. Qin, Organic host materials for phosphorescent organic light-emitting diodes. Chem. Soc. Rev. **40** (2011) 2943.

[25] G. Valverde-Aguilar, Photostability of laser dyes incorporated in formamide sio2 ormosils. Opt. Mater. **28** (2006) 1209.

[26] R. Sastre, and A. Costela, Polymeric solid-state dye lasers. Adv. Mater. **7** (1995) 198.

[27] J. S. Royal, and J. M. Torkelson, Photochromic and fluorescent probe studies in glassy polymer matrices. 5. Effects of physical aging on bisphenol a polycarbonate and poly(vinyl acetate) as sensed by a size distribution of photochromic probes. Macromolecules **25** (1992) 4792.

[28] J. Harada, and K. Ogawa, X-ray diffraction analysis of nonequilibrium states in crystals: Observation of an unstable conformer in flash-cooled crystals. J. Am. Chem. Soc. **126** (2004) 3539.

[29] L. Zhu *et al.*, Surface self-diffusion of an organic glass. Phys. Rev. Lett. **106**, 256103 (2011) 4.

[30] S. Ruan *et al.*, Surface diffusion and surface crystal growth of tris-naphthyl benzene glasses. J. Chem. Phys. **145** (2016) 064503.

[31] D. M. Walters *et al.*, Influence of molecular shape on the thermal stability and molecular orientation of vapor-deposited organic semiconductors. J. Phys. Chem. Lett. **8** (2017) 3380.

[32] J. Gómez *et al.*, Nematic-like stable glasses without equilibrium liquid crystal phases. J. Chem. Phys. **146** (2017) 054503.

[33] Z. Sekkat, G. Kleideiter, and T. Knoll, Optical orientation of azo dye in polymer films at high pressure. J. Opt. Soc. Am. B-Opt. Phys. **18** (2001) 1854.

[34] K. L. Kearns *et al.*, High-modulus organic glasses prepared by physical vapor deposition. Adv. Mater. **22** (2010) 39.

[35] V. Lubchenko, and P. G. Wolynes, Theory of structural glasses and supercooled liquids. Annual Review of Physical Chemistry **58** (2007) 235.

[36] G. Adam, and J. H. Gibbs, On the temperature dependence of cooperative relaxation properties in glass-forming liquids. J. Chem. Phys. **43** (1965) 139.

[37] L. Berthier *et al.*, Direct experimental evidence of a growing length scale accompanying the glass transition. Science **310** (2005) 1797.

[38] Y. J. Cho, and H. Aziz, Root causes of the limited electroluminescence stability of organic light-emitting devices made by solution-coating. ACS Appl. Mater. Interfaces **10** (2018) 18113.

[39] Y. Esaki *et al.*, Enhanced electrical properties and air stability of amorphous organic thin films by engineering film density. J. Phys. Chem. Lett. **8** (2017) 5891.

[40] J. Ràfols-Ribé *et al.*, High-performance organic light-emitting diodes comprising ultrastable glass layers. Sci. Adv. **4** (2018) eaar8332.

3.7 Supporting information

In the main text, vapor-deposited glasses have enhanced density when prepared at substrate temperatures lower than T_g. This result is also observed in glasses prepared in MD simulation. The density for glasses vapor-deposited at different substrate temperatures relative to the liquid-cooled glass is shown in Figure S1. At $T_{substrate} < T_g$, the density of vapor-deposited glasses is greater than that of the liquid-cooled glass.

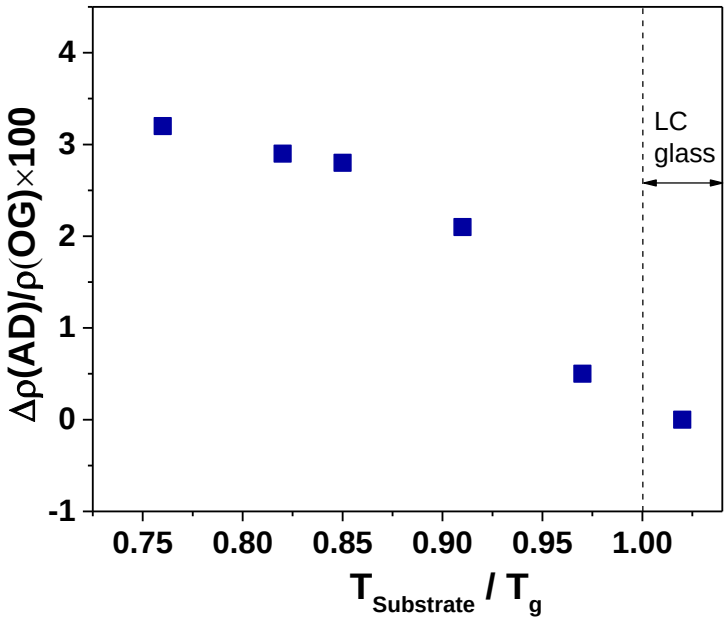

Figure S1. Glass density as a function of normalized substrate temperature for vapor-deposited and liquid-cooled (LC) glasses in computer simulations.

Chapter 4

Vapor-deposited Organic Glasses Exhibit Enhanced Stability Against Photodegradation

Yue Qiu, Shakeel S. Dalal, M. D. Ediger

Published in *Soft Matter*, 2018, **14**, 2827 - 2834

Abstract

Photochemically stable solids are in demand for applications in organic electronics. Previous work has established the importance of the molecular packing environment by demonstrating that different crystal polymorphs of the same compound react at different rates when illuminated. Here we show, for the first time, that different *amorphous* packing arrangements of the same compound photodegrade at different rates. For these experiments, we utilize the ability of physical vapor deposition to prepare glasses with an unprecedented range of densities and kinetic stabilities. Indomethacin, a pharmaceutical molecule that can undergo photodecarboxylation when irradiated by UV light, is studied as a model system. Photodegradation is assessed through light-induced changes in the mass of glassy thin films due to the loss of CO_2, as measured by a quartz crystal microbalance (QCM). Glasses prepared by physical vapor deposition degraded more slowly under UV illumination than did the liquid-cooled glass, with the difference as large as a factor of 2. Resistance to photodegradation correlated with glass density, with the vapor-deposited glasses being up to 1.3% more dense than the liquid-cooled glass. High density glasses apparently limit the local volume changes required for photodegradation.

4.1 Introduction

Organic glasses are amorphous materials widely used in modern technologies, including polymeric materials,[1, 2] pharmaceuticals,[3, 4] and organic electronics.[5] For example, active layers in organic light emitting diodes (OLEDs) are vapor-deposited organic semiconductors in the glassy state. Compared to crystals, glassy layers are smoother and, since there are no grain boundaries, more homogeneous at the

macroscopic level; both of these properties are critical for OLEDs. Organic molecules will be unavoidably degraded after prolonged illumination with light of sufficiently short wavelength,[6, 7] and photostability is a concern for both crystalline and amorphous organic solids. For example, photodegradation can cause the failure of organic electronics in both display[8, 9] and light harvesting technologies[10], and this is sometimes a more limiting factor than device efficiency.

Recently, physical vapor deposition (PVD) has been used to prepare organic glasses with exceptional properties that are not accessible by any other preparation method.[11] By properly controlling processing conditions such as substrate temperature and deposition rate, vapor deposition can form stable glasses that have higher density,[11-15] enhanced kinetic stability,[12, 14-16] and lower enthalpy[11, 12, 17-19] relative to the liquid-cooled glass. It has been estimated that thousands of years of slow cooling or physical aging would be required to achieve the same density when starting from the liquid state.[14-16, 20] The most stable glasses prepared by PVD are much deeper in the potential energy landscape than liquid-cooled glasses.[18] All of the exceptional properties of vapor-deposited glasses point to the activation barriers for molecular rearrangements in these materials being significantly higher than for liquid-cooled glasses.[11] Therefore, even though there is no precedent for modulation of photodegradation by controlling glass packing, PVD glasses are good candidates for investigation. This is particularly relevant since PVD is already used to prepare organic electronic devices such as OLEDs.

Previous work has established the importance of the solid-state molecular packing environment in controlling photodegradation by demonstrating that different crystal polymorphs of the same compound react at different rates when illuminated. We

present two examples from the pharmaceutical field where photodegradation is an important concern. For carbamazepine, it has been established that UV irradiation results in the formation of carbamazepine cyclobutane dimer and carbamazepine 10,11-epoxide. For the three crystal polymorphs of carbamazepine, the rates of photodegradation vary by as much as a factor of 5.[21] As another example, one of the three polymorphs of furosemide photodarkens at a rate six times smaller than the other polymorphs as a result of UV irradiation, indicating that some feature of the local packing provides stronger resistance to photolytic degradation.[22] Given that crystals can efficiently modulate photodegradation by as much as a factor of 5, vapor-deposited glasses might also be able to have an impact given their increased density relative to the liquid-cooled glass.

Recent work has shown that molecular packing in amorphous organic solids can also modulate the rate of some photo-induced processes. Physical vapor deposition (PVD) was used to prepare glasses of Disperse Orange 37, an azobenzene derivative, with a significant range of densities. Photoisomerization of Disperse Orange 37 was found to slow down by a factor of 50 in the most dense glass relative to the least dense glass, which was prepared by cooling the supercooled liquid.[23] In earlier work, Royal and Torkelson reported that photoisomerization of an azobenzene dispersed into a polymer glass can be slowed slightly (about 5%) as a result of physical aging for a few days.[24] References 23 and 24 provide important precedents indicating that glasses with efficient packing can inhibit at least some photo-induced processes. At present, there are not reports on whether efficient glass packing can slow photodegradation.

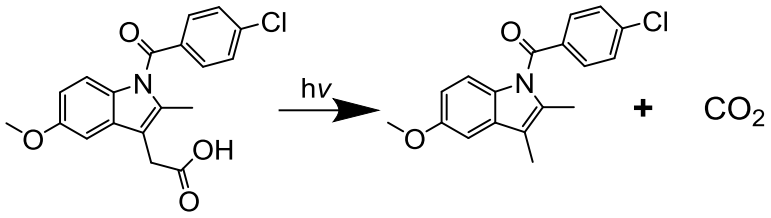

Scheme 1. Photodegradation of indomethacin under UV irradiation.

In this work, we test whether efficient molecular packing in amorphous organic solids leads to resistance against photodegradation. Here we utilized photodegradation of vapor-deposited indomethacin as a model system. It is known that indomethacin can undergo photodecarboxylation when irradiated by UV light (Scheme 1).[25] In addition, indomethacin has been found to form high-density glasses by vapor-deposition, with the density increase as much as 1.3% relative to the liquid-cooled glass.[16] In this work, we vapor-deposited indomethacin onto substrates held at different temperatures to obtain glasses with different initial densities. We used a quartz crystal microbalance (QCM) to compare the mass loss induced in the different indomethacin glasses during UV light irradiation as a result of photodecarboxylation. Experiments were also performed on liquid-cooled glasses, including aged samples.

We find that photodegradation of vapor-deposited indomethacin can be significantly modulated by substrate temperature during deposition. The optimum vapor-deposited glass, prepared at about 0.85 T_g, photodegrades as much as two times more slowly than the liquid-cooled glass, depending upon the temperature at which the sample is irradiated. This is the first demonstration that glass packing can modulate photodegradation. We observe a good correlation between decreased photodegradation and increased glass density of vapor-deposited glasses. For

indomethacin, vapor-deposited glasses can be more resistant to photodegradation than liquid-cooled glasses, and enhanced photostability might be a general phenomenon for dense glasses prepared by PVD. We discuss these new results on photodegradation together with previous results on photoisomerization. For the particular reactions studied, we propose that local volume changes required by molecular rearrangement during photodegradation are much smaller than for those required for photoisomerization. For applications such as organic electronics, where photodegradation is an important cause of device failure,[8, 9] this work suggests a pathway to improve device lifetimes.

4.2 Experimental methods

4.2.1 Preparation of vapor-deposited indomethacin glasses

Glassy films of indomethacin were prepared by physical vapor deposition (PVD). Indomethacin (99% purity) was obtained from Sigma Aldrich and used as received. PVD was performed in a vacuum chamber with a base pressure of 10^{-7} torr. Indomethacin was placed in a crucible that was resistively heated and the deposition rate was controlled by tuning the heater power. The deposition rate was monitored by a quartz crystal microbalance (QCM) and kept at a constant value of 2 Å /s for all experiments reported here. For most of our experiments, the sample substrates were gold-coated quartz crystal resonators suitable for use in a QCM device as described below. During deposition, each quartz crystal resonator was in good thermal contact with a copper finger whose temperature was controlled at a constant value. For a few experiments that did not involve mass measurements, we utilized samples deposited onto a silicon wafer with a temperature-gradient imposed upon it; thus one sample contained a library

of glasses prepared at many different substrate temperatures.[16] In all cases, the thicknesses of the as-deposited PVD glasses were about 300 nm as measured by ellipsometry. Liquid-cooled glasses were prepared by vapor-deposition at a substrate temperature above T_g, followed by cooling to room temperature at 1 K/min. For indomethacin cooled at 1 K/min, T_g = 310 K.

4.2.2 Kinetic stability and density measurements

The kinetic stabilities and densities of vapor-deposited indomethacin thin films were measured by spectroscopic ellipsometry (J.A. Woollam, M-2000). Ellipsometry is an optical technique that measures the thickness and refractive indices of thin films. Similar to our previous work,[16] we utilized measurements at three incidence angles and used an anisotropic Cauchy model to fit all the ellipsometric data between 500 and 1000 nm. To measure kinetic stability and density, ellipsometry was performed on samples placed on a custom-built hot stage, and the temperature was increased at 1 K/min from room temperature to 335 K. Immediately after heating, the supercooled liquid was cooled at 1 K/min into the liquid-cooled glass and heated/cooled two more times at 1 K/min. Please note that we use the term “kinetic stability” to refer to the ability of a glass to resist rearrangement upon increasing temperature while “photostability” is used to describe resistance to degradation induced by UV illumination.

4.2.3 Photodegradation measurement

The light irradiation experiment used to test photodegradation of indomethacin glasses was performed in a quartz reactor filled with nitrogen gas. A 312 nm UV lamp (Spectroline EBF-260C, 20 nm bandwidth) was used as the light source to induce the

photodegradation reaction. The sample was illuminated at normal incidence with irradiance of 40 μW/cm^2. For the ~300 nm thick films that we utilized, approximately 70% of the 312 nm light is absorbed in one pass through the film. During irradiation, a quartz microbalance (QCM) was placed in the quartz reactor at ambient pressure to continuously measure the mass decrease due to the loss of CO_2 that results from the reaction shown in Scheme 1. For irradiation at low temperatures, the quartz reactor was cooled by dry ice and temperature of QCM was controlled within 1 °C variation during the photodegradation, as measured by a thermal couple that was taped onto the QCM. A 5-MHz AT-cut quartz plate (Inficon Inc.) with a polished gold electrode was used as the QCM resonator. QCM is widely used as a thickness detector in many deposition techniques. For films in this thickness range, the frequency shift of the resonator can be related to the mass change of the sample by the Sauerbrey equation[26]:

$$\Delta f = -\frac{2f_0^2}{A\sqrt{\rho_q \mu_q}}\Delta m \quad (1)$$

In Equation 1, f_0 is the resonance frequency (Hz), Δf is the frequency change, Δm is the mass change, A is the piezoelectrically active crystal area, ρ_q is the density of quartz (2.648 g/cm^3), and μ_q is the shear modulus of quartz for the AT-cut crystal (2.947 x 10^{11} g·cm^{-1}·s^{-2}). Since f_0, A, ρ_q, and μ_q are all known, Δm can be calculated from Δf. In this way, we can monitor the photodegradation of the glassy thin films in real time. Below we present the fractional mass change; the initial mass is calculated using the ellipsometrically determined thickness of the film and the absolute density of amorphous indomethacin (1.32 g/cm^3).[27]

4.3 Results

4.3.1 QCM measurement of photodegradation during irradiation

To demonstrate that QCM is an effective method to characterize the photodegradation of indomethacin, we first measured the mass loss of a liquid-cooled indomethacin glass during UV irradiation. The mass loss occurs as a result of photodecarboxylation (Scheme 1) with carbon dioxide gas escaping the film. In previously published work, the modified indomethacin reaction product was identified by IR spectroscopy and liquid chromatography/mass spectrometry (LCMS).[25] As shown in Figure 1, the mass of the liquid-cooled glass begins to decrease immediately upon irradiation, indicating continuous photodegradation. After nearly two days of irradiation, the mass approximately reaches steady-state. This is consistent with the view that all indomethacin molecules have reacted at this point. By fitting the experimental data with an exponential function, the overall mass loss is estimated to be about 12.5% at steady-state, which is reasonably consistent with the theoretical maximum mass loss 12.3% calculated from stoichiometry (Scheme 1). This provides confidence that we understand the chemical transformation occurring in glassy indomethacin as a result of UV irradiation.

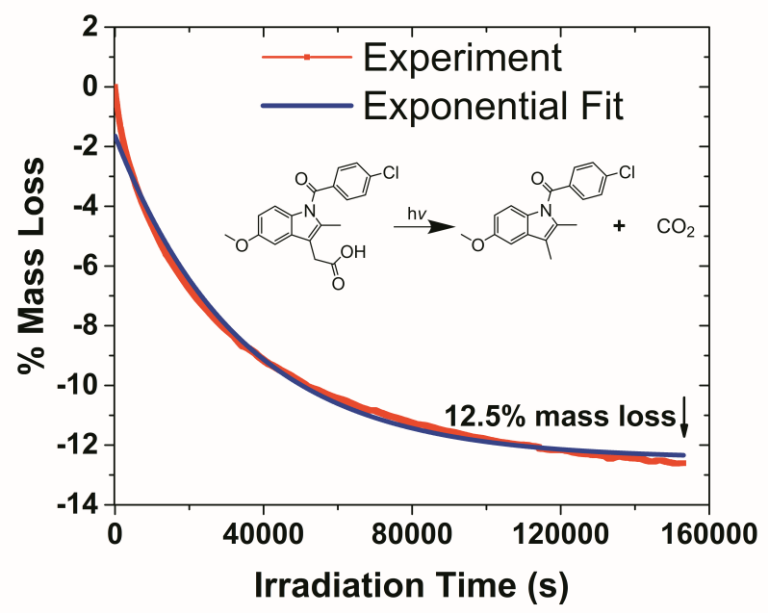

Figure 1. Mass loss for a liquid-cooled glass of indomethacin as a function of UV irradiation time. Red symbols represent experimental results obtained with the quartz crystal microbalance and the blue curve is exponential fit.

4.3.2 Determination of glass density

Spectroscopic ellipsometry was used to characterize the kinetic stability and density of PVD glasses of indomethacin. An example of this procedure is shown in Figure 2. For this experiment, the indomethacin thin film was vapor-deposited at $T_{substrate}$ = 260 K (0.84 T_g) onto a polished gold QCM resonator. The procedure used here is the same as in previous reports except for the substrate material.[15, 16, 28] Three different temperature ramping cycles were performed on each PVD glass. During the first temperature cycle, the as-deposited indomethacin was heated from 295 K to 335 K and then cooled back to 295 K. Two more heating and cooling cycles were also performed, and all heating and cooling rates were 1 K/min. During the first run of heating, the initial thickness change below 325 K is due to the thermal expansion of the glassy solid. The as-deposited sample begins to transform into the super-cooled liquid at the onset temperature of 327 K. The onset temperature, which characterizes the kinetic stability of the as-deposited glass, was determined from the beginning of the transformation into the supercooled liquid. The subsequent cooling prepares the liquid-cooled glass, with the glass transition temperature T_g = 310 K. The second and third cooling runs in Figure 2 closely reproduce the first cooling curve, as expected.

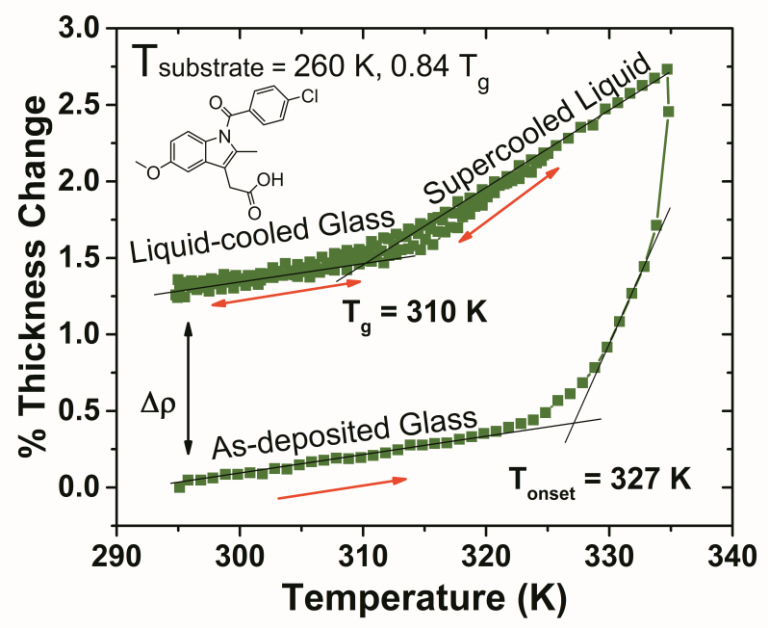

Figure 2. Thickness changes for a vapor-deposited glass of indomethacin during temperature ramping at 1 K/min. The green symbols represent experimental data for a sample prepared at $T_{substrate}$ = 260 K (0.84 T_g). The sample thickness is about 300 nm.

Figure 2 illustrates that the glass vapor-deposited at $T_{substrate}$ = 260 K exhibits a high onset temperature and high density, relative to the liquid-cooled glass. The onset temperature during the first heating is about 17 K higher than the T_g of the liquid-cooled glass, indicating increased kinetic stability. The density of as-deposited glass relative to the liquid-cooled glass was determined by the percentage thickness change as a result of the first heating/cooling cycle. In this case, the as-deposited glass is about 1.3% more dense, which is consistent with a previous report of vapor-deposited indomethacin.[16] We also prepared and characterized samples at five substrate temperatures in addition to 0.84 T_g. Photodegradation experiments were performed on all these glasses and will be discussed in the next section.

4.3.3 Influence of PVD substrate temperature on photodegradation

Figure 3 shows the comparison of the photoinduced mass loss for vapor-deposited and liquid-cooled glasses of indomethacin and reveals that the PVD glasses display slower photodegradation, i.e., enhanced photostability. These tests followed a similar protocol as described in section 3.1, with irradiation taking place at 295 K. Immediately after irradiation begins, the mass starts to decrease for all glasses. After 2000 s had elapsed, the liquid-cooled glass lost nearly 2.4% of its total mass, indicating that about 1/5 of the indomethacin had been decarboxylated. In contrast, PVD glasses photodegrade more slowly and the optimum sample ($T_{substrate}$ = 0.84 T_g) loses about 1.5% of its total mass in 2000 s. By comparing the mass loss of the most stable vapor-deposited glass and the liquid-cooled glass, a decrease in the rate of photodegradation of about 40% can be observed.

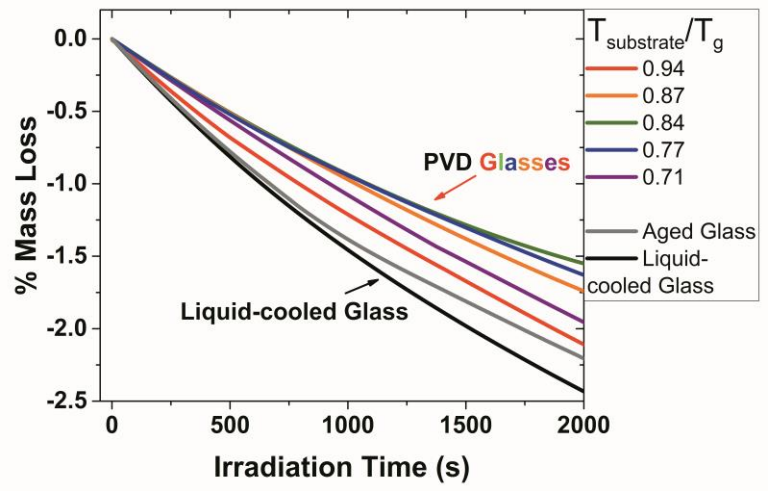

Figure 3. Mass loss for vapor-deposited and liquid-cooled glasses of indomethacin as a function of irradiation time at 295 K. The black curve is liquid-cooled glass and the colored curves represent glasses vapor-deposited at the substrate temperatures indicated.

Photodegradation of an aged liquid-cooled glass was also investigated and showed a very small change in the reaction rate relative to the freshly prepared liquid-cooled glass, as indicated by the grey curve in Figure 3. The aged glass was prepared by cooling liquid indomethacin at 1 K/min and annealing at 277 K (T_g - 33 K) for a week. The aged glass was about 0.18% more dense than the freshly prepared liquid-cooled glass, as measured by ellipsometry. As shown in Figure 3, the aged glass lost 2.2% of its mass as a result of 2000 s of irradiation.

A comparison of the rate of photodegradation for vapor-deposited and liquid-cooled glasses is summarized in Figure 4. Figure 4a shows the light-induced mass loss at the irradiation time of 2000 s. The liquid-cooled glass degrades about 1.5 times more than the optimum vapor-deposited glass, prepared at the substrate temperature of 260 K. Figure 4b shows the densities of indomethacin glasses vapor-deposited at different substrate temperatures relative to the liquid-cooled glass.[16] All glasses investigated in this study that are deposited at $T_{substrate} < T_g$ show higher density than the liquid-cooled glass.

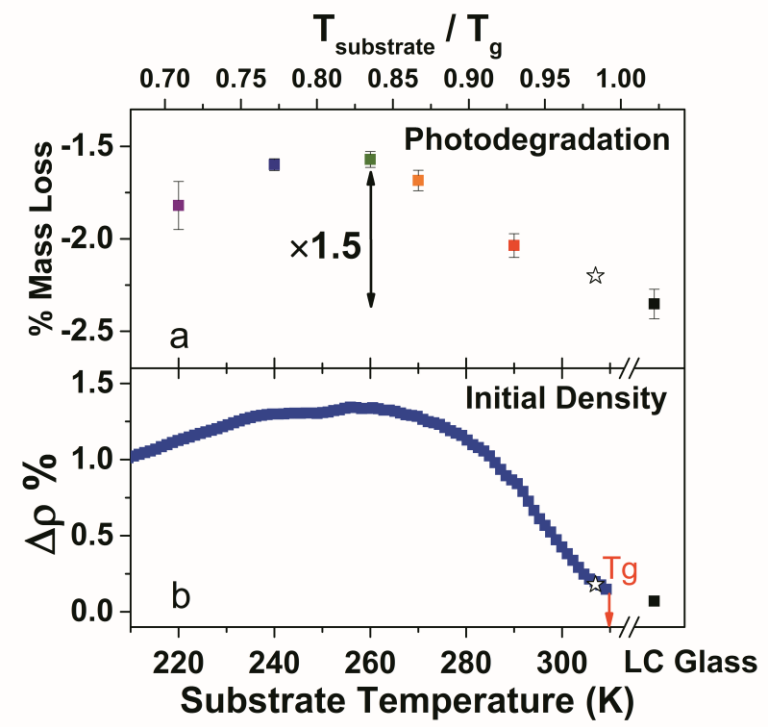

Figure 4. Mass loss as a result of photodegradation and density of vapor-deposited glasses of indomethacin as a function of substrate temperature during deposition, with comparison to the liquid-cooled (LC) glass (black solid square) and the aged glass (black open star). (a) Mass loss after 2000 s irradiation. (b) Density of as-deposited glasses relative to the liquid-cooled glass; filled symbols are data from ref. 16. A strong correlation is observed between resistance to photodegradation and density.

Comparing Figure 4a and 4b, we see a strong correlation between decreased photodegradation and increased density. For this comparison, we utilize data from the early stages of the photoreaction to best characterize the dependence of photodegradation on the state of the glass. We verified that choosing a reaction time less than 2000 s would not change our conclusions about the relative stabilities of the different glasses. The photodegradation reaction changes the density and kinetic stability of the glass, as we discuss below, and so we did not investigate longer reaction times.

The two panels of Figure 4 also include data on the aged liquid-cooled glass and this data supports the correlation between increased density and decreased photodegradation. These data points were placed in the figure as follows. The aged glass was plotted on the x-axis in Figure 4b such that the aged glass density falls on the data points measured for the PVD glasses. This same x-axis position was then used in Figure 4a to plot the mass loss observed for the aged sample.

4.3.4 Influence of irradiation temperature on photodegradation

The influence of irradiation temperature on photodegradation of indomethacin glasses was also investigated, and the stability of vapor-deposited glasses relative to the liquid-cooled glass was observed to increase at lower irradiation temperature. The solid lines in Figure 5 show the mass loss of indomethacin glasses during irradiation at 279 K. (This is 16 K lower than the irradiation temperature used for Figures 3 and 4). As a result of 2000 s of irradiation, the liquid-cooled glass lost about 1.75% of its initial mass, while the optimum vapor-deposited glass, which was prepared at 260 K, lost about 0.91% of its initial mass. The glass vapor-deposited at 290 K shows an intermediate

mass loss of 1.2%. For irradiation at 279 K, the mass loss of the liquid-cooled glass is about two times greater than that of the optimum vapor-deposited glass. For all glasses studied, photodegradation is less efficient at lower irradiation temperature, indicating that a thermal activation process is involved. Further discussion of the degradation mechanism is given below.

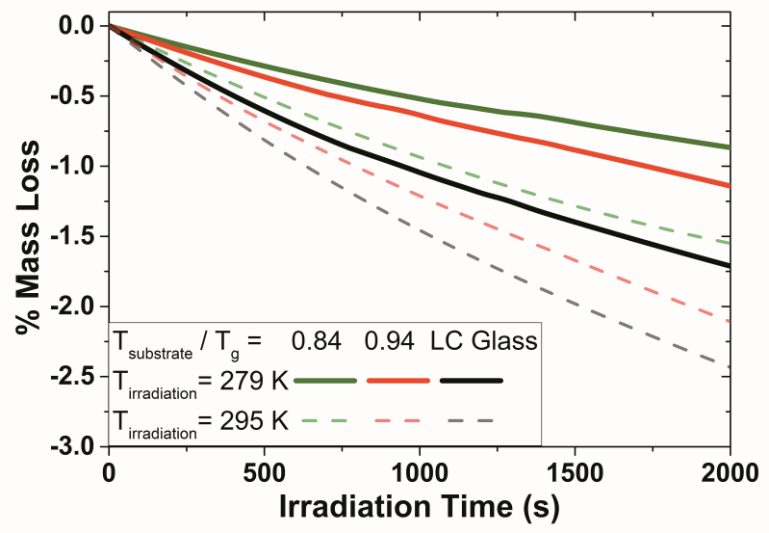

Figure 5. Mass loss for vapor-deposited and liquid-cooled glasses of indomethacin as a function of irradiation time. Solid lines are results for irradiation at 279 K; dashed lines are results obtained at 295 K.

4.3.5 Properties of vapor-deposited glasses after photodegradation

Results presented above show that the packing of indomethacin molecules in the amorphous state can have a significant influence on the rate of photodegradation. Of course, rearrangements in the glass due to photodegradation would be expected to disrupt the packing. To gain some insight into the extent to which photodegradation alters the properties of indomethacin glasses, we performed ellipsometry and x-ray scattering measurements on a few samples directly following 2000 s of irradiation.

We found that the photodegradation that occurred as a result of 2000 s of UV irradiation substantially diminished the density and kinetic stability of indomethacin glasses. For indomethacin vapor-deposited at 266 K (0.86 T_g), as shown in Figure 6, the onset temperature upon the first heating is 312 K, which is a much lower value than the 327 K value observed for similar samples that were not irradiated. Non-irradiated samples deposited at the same substrate temperature are 1.3% more dense than the liquid-cooled glass, while we only observed a 0.4% density increase after transforming the photodegraded glass. Both the onset temperature and density show that the efficient packing of the as-deposited glass was mostly destroyed after 2000 s of irradiation.

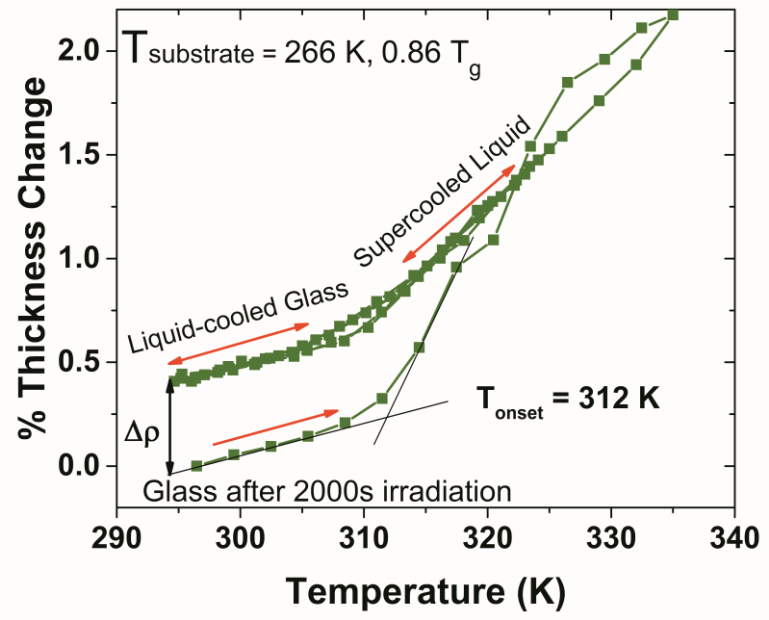

Figure 6. Thickness changes for a vapor-deposited glass of indomethacin during temperature ramping (1 K/min) immediately following UV irradiation at 295 K. The green symbols represent experimental data for a sample prepared at $T_{substrate}$ = 266 K (0.86 T_g) and irradiated for 2000 s. Irradiation partially erases the initially high density of the vapor-deposited glass and eliminates the kinetic stability.

The influence of photodegradation on the average molecular orientation of the indomethacin molecules can be inferred from birefringence measurements before and after irradiation. Figure 7 shows measurements of the birefringence of several indomethacin glasses as a function of irradiation time. As previously reported, the as-deposited glasses of indomethacin[16] and several other organic molecules[5, 29, 30] are birefringent, indicating anisotropic molecular orientation. The liquid-cooled glass has an initial birefringence of zero, which is consistent with random molecular orientation. During the irradiation, birefringence of vapor-deposited glasses is nearly constant, indicating that molecular orientation barely changed during photodecarboxylation. (In making this statement, we make the reasonable assumption that the polarizability tensors of indomethacin and its photoproduct are similar.)

We performed wide angle x-ray scattering measurements (not shown) on a few vapor-deposited glasses after photodegradation, and found that the anisotropic peak ($q = 0.57$ $Å^{-1}$) that has been interpreted[31] in terms of tendency towards molecular layering still exists after photodegradation. While Figure 6 shows that photodegradation disrupts packing enough to eliminate the kinetic stability of the PVD glass, the birefringence and x-ray scattering show that large scale molecular rearrangements do not occur as a result of photodegradation.

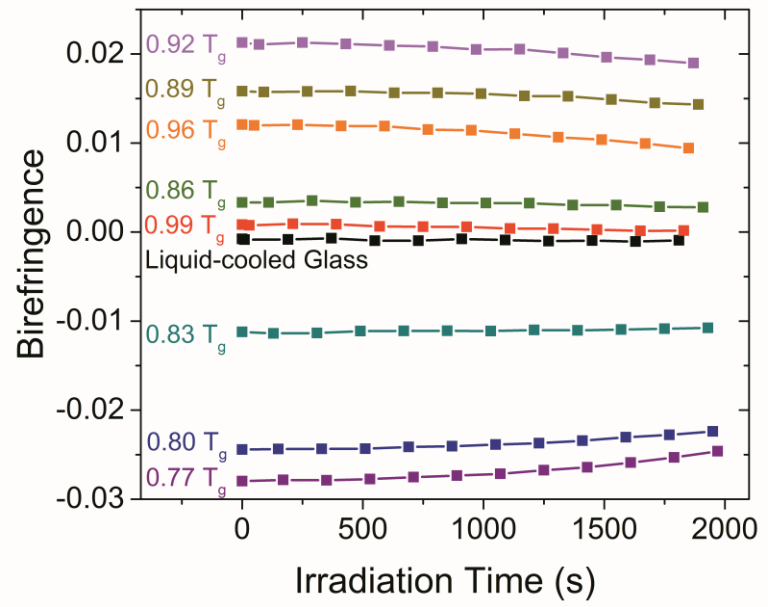

Figure 7. Birefringence measurements for vapor-deposited and liquid-cooled glasses of indomethacin during UV irradiation at 295 K. The temperature of the substrate during deposition is indicated.

4.4 Discussion

We have shown, for the first time, that photodegradation of organic molecules can be significantly modulated by packing in the amorphous state. More specifically, we have shown that PVD can prepare glasses of indomethacin that display enhanced stability against photodegradation. At the irradiation temperature of 279 K, the optimum vapor-deposited glass photodegrades more slowly than the liquid-cooled glass by a factor of 2. Previous work in organic crystals has shown that photodegradation can depend upon the crystal polymorph. For example, among the three polymorphic modifications of carbamazepine, polymorph I photodegrades 5.1 time more slowly than polymorphs II while polymorph III shows intermediate behavior.[21] For crystal polymorphs, different photochemical reactivity has been attributed to the topochemistry principle that the reaction will involve nearest-neighbor molecules or functional groups and will occur with minimum atomic and molecular movement.[32, 33] In contrast, amorphous materials have a large number of local packing motifs and this approach does not seem appropriate. So why do glasses prepared by PVD, in common with crystals, show a prominent ability to modulate photochemistry?

The current work and literature precedents suggest that glass density plays a key role in modulating the rate of photo-induced changes in organic glasses. In the present work, this connection is shown by the strong correlation between photodegradation and glass density in Figure 4a and 4b. The correlation that exists for vapor-deposited glasses also describes the behavior of liquid-cooled glasses and aged liquid-cooled glasses. Glass density also played an important role in our previous study of photoisomerization in glasses of Disperse Orange 37, an azobenzene derivative.[23] We observed that photo-

induced changes in the glass structure could be suppressed by a factor of 50 by preparing high density glasses with PVD and a strong correlation was observed between glass density and photo-induced structural changes. In that study,[23] molecular simulations demonstrated that molecular packing of higher density glasses can more effectively restrict molecules that start in the *trans* state from reaching the *cis* state after excitation. In another study of an azobenzene derivative tethered to a PMMA polymer in the glassy state, it was demonstrated that optically induced photoisomerization can be hindered by density increases caused by high pressure.[34] In a related set of experiments, the photostability of materials used in organic solar cells was tested in the presence of oxygen.[35] In this work, neat films of polymers, oligomers and small molecules, both in crystalline and amorphous states, were compared. Over the entire set of materials, a broad correlation was observed between density and photostability.

Having shown here that high-density glasses can inhibit photodegradation, we wish to speculate briefly about the mechanism of this process at the molecular level. Figure 8 shows a generic energy diagram for photodegradation in the gas phase, as proposed by Nakashima and Yoshihara,[36] and provides background for our discussion. In this scenario, after indomethacin is photoexcited to the S1 state from the ground state by a 312 nm photon, the molecule can access the repulsive potential R through a thermal excitation and dissociate such that a molecule of CO_2 is eventually formed. During this process, we imagine that the length of the C-C bond connecting the carbonyl carbon to the indole ring will be extended before it eventually breaks to release the fragment that will yield CO_2. Our results for the temperature dependence of photodegradation, as shown in Figure 5, are consistent with the presence of a thermal activation step along

the path to carbon dioxide formation. From this data, the activation energy for photodegradation of the liquid-cooled glass is estimated to be about 13 kJ/mol while 23 kJ/mol is obtained for the PVD glass that best resists photodegradation. We do not imagine that the relative energies of the molecular states are altered significantly by the packing of the glass, so we interpret the larger activation energy of the PVD glass to indicate an increased barrier for the photolytic process that is imposed by the tight packing of the surrounding molecules. Perhaps the initial lengthening of the C-C bond with the indole ring is more difficult with more tightly packed neighboring molecules. A related interpretation has been given for the photoisomerization experiments of Disperse Orange 37. For that case, molecular dynamics computer simulations indicate that neighboring molecules in the high density glass more efficiently block the twisting motion required to access the *cis* state.[23] For amorphous materials generally, we speculate that the molecular rearrangements required to reach the product state are impeded to a greater extent in a higher density glass.

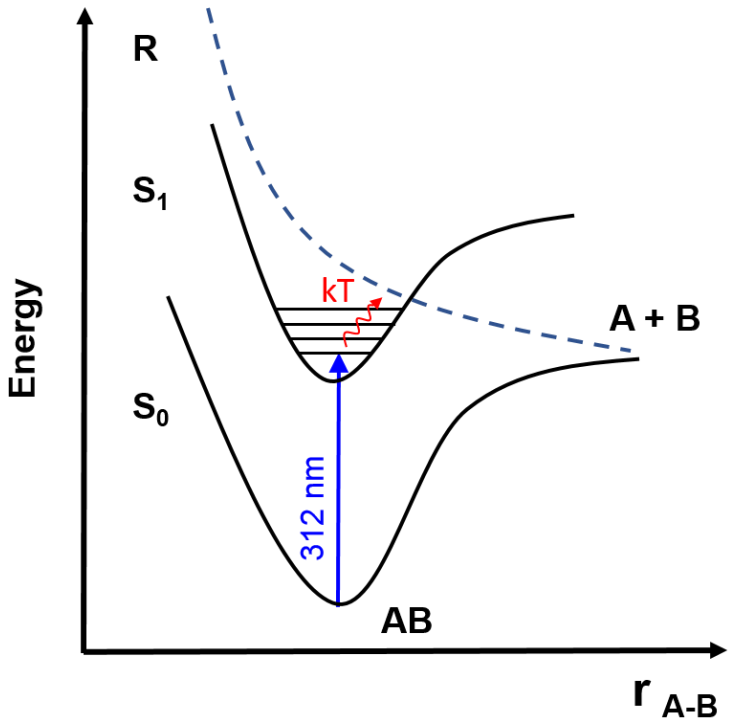

Figure 8. Schematic energy diagram for photodegradation of indomethacin.

Although efficient glass packing can inhibit both photodegradation and photoisomerization in organic glasses, the photodegradation of indomethacin depends less sensitively on glass density than does the photoisomerization of Disperse Orange 37. During illumination at 295 K, a 1.3% increase in glass density decreases photoisomerization by a factor of 50 while this same density change slows photodegradation by only a factor of 1.5. We interpret this to mean that the *trans* to *cis* reaction for Disperse Orange 37 requires a greater rearrangement of the surrounding molecules than does the photodegradation of indomethacin. It is possible that the extent of the required rearrangement would be at least approximately captured by the activation volumes for these reactions. In high-pressure experiments on an azobenzene derivative similar to Disperse Orange 37,[34] the activation volume of photoisomerization was reported to be 111 $Å^3$. We are unaware of any similar measurements for the photodegradation process of indomethacin but we expect that a considerably smaller activation volume would be obtained. It would be useful if the activation volumes for these two reactions could be obtained directly either from experiment or in a quantum calculation.

Although the experiments reported here show a strong correlation between high density and slow photodegradation in organic glasses, the reader should be cautious in inferring causality. High density glasses prepared by PVD also have low enthalpy and high moduli.[16] To a first approximation, these three properties change in a correlated manner as a function of substrate temperature during deposition. Thus, while high density might be responsible for slow photodegradation in indomethacin, the data presented here are equally consistent with the view that high moduli or low enthalpy is the cause. In order

to distinguish among these possibilities, it would be useful to test photodegradation on high density glasses prepared by an alternative method, such as pressurizing a liquid-cooled glass.[37] Glasses prepared by pressure do not have the low enthalpy that characterizes PVD glasses.

4.5 Conclusion

We have shown that the photodegradation of an organic molecule can be significantly modulated by packing in the amorphous state. The photodegradation of high-density glasses of indomethacin can be slowed down by as much as a factor of 2 relative to the liquid-cooled glass by selecting the correct substrate temperature for the vapor-deposition process. Suppression of photodegradation strongly correlates with glass density. The decreased photodegradation of high-density glasses was attributed to the constraint that the local packing exerts on the molecular rearrangement (bond extension and breaking) that happens in the PVD glasses as a result of irradiation.

We expect that the enhanced stability against photodegradation in well-packed glasses is a general effect for organic molecules and that this effect can be exploited in organic electronics. So far, PVD has been reported to prepare glasses with high density and high kinetic stability for more than thirty organic molecules, some of which are used in the active layers of OLEDs.[13] We expect that those high-density glasses will result in higher energy barriers for photodegradation, which is a common mechanism for device failure. Moreover, as PVD is already used in industry to produce OLEDs, it would be of great interest if device lifetime could be increased by optimizing the preparation conditions to produce the most dense glass. Operational lifetime is considered to be a bottleneck to the further improvement of OLED display performance, especially for blue

emitters.[9] We note that the factor of 2 increase in stability against photodegradation for indomethacin was obtained for irradiation at T_g – 31 K (279 K). An even greater relative increase in stability would be expected at T_g – 60 K, which would be typical for many OLEDs molecules if illuminated at room temperature. Although we do not know whether a factor of 2 inhibition of photodegradation will be observed in other systems, our research provides a clear proposal for how to create more photostable glasses for organic electronics. Furthermore, the deposition conditions that optimize resistance to photodegradation also produce glasses with high thermal stability[13, 29] and low uptake of atmospheric gases.[38] It is likely that all of these features work to enhance the lifetime of devices built from organic glasses. Consistent with this view, Esaki and coworkers very recently reported that the electronic properties of films of organic semiconductors were more stable over time if vapor deposition conditions were optimized to prepare the highest density glasses.[39]

Acknowledgements. We thank Robert McMahon, Christopher Ober, Fleming Crim, and Lian Yu for helpful discussions. We thank Kushal Bagchi for x-ray scattering measurements. This work was supported by the US Department of Energy, Office of Basic Energy Sciences, Division of Materials Sciences and Engineering, Award DE-SC0002161.

4.6 References

1. H. Zhou, C. Xue, P. Weis, Y. Suzuki, S. Huang, K. Koynov, G. K. Auernhammer, R. Berger, H. J. Butt and S. Wu, *Nat. Chem.*, 2017, **9**, 145-151.

2. G. B. McKenna and S. L. Simon, *Macromolecules*, 2017, **50**, 6333-6361.

3. H. Mesallati, D. Conroy, S. Hudson and L. Tajber, *Eur. J. Pharm. Biopharm.*, 2017, **121**, 73-89.

4. B. C. Hancock and G. Zografi, *J. Pharm. Sci.*, 1997, **86**, 1-12.

5. D. Yokoyama, *J. Mater. Chem.*, 2011, **21**, 19187-19202.

6. S. Schmidbauer, A. Hohenleutner and B. König, *Beilstein. J. Org. Chem.*, 2013, **9**, 2088-2096.

7. W. R. Mateker and M. D. McGehee, *Adv. Mater.*, 2017, **29**, 1603940.

8. Q. Wang, Y. Luo and H. Aziz, *Appl. Phys. Lett.*, 2010, **97**, 063309.

9. Y. Zhang, J. Lee and S. R. Forrest, *Nat. Comm.*, 2014, **5**, 5008.

10. P. Cheng and X. Zhan, *Chem. Soc. Rev.*, 2016, **45**, 2544-2582.

11. M. D. Ediger, *J. Chem. Phys.*, 2017, **147**, 210901.

12. S. F. Swallen, K. L. Kearns, M. K. Mapes, Y. S. Kim, R. J. McMahon, M. D. Ediger, T. Wu, L. Yu and S. Satija, *Science*, 2007, **315**, 353-356.

13. S. S. Dalal, D. M. Walters, I. Lyubimov, J. J. de Pablo and M. D. Ediger, *Proc. Natl. Acad. Sci. U.S.A.*, 2015, **112**, 4227-4232.

14. T. Liu, K. Cheng, E. Salami-Ranjbaran, F. Gao, C. Li, X. Tong, Y.-C. Lin, Y. Zhang, W. Zhang, L. Klinge, P. J. Walsh and Z. Fakhraai, *J. Chem. Phys.*, 2015, **143**, 084506.

15. K. L. Kearns, P. Krzyskowski and Z. Devereaux, *J. Chem. Phys.*, 2017, **146**, 203328.

16. S. S. Dalal, Z. Fakhraai and M. D. Ediger, *J. Phys. Chem. B*, 2013, **117**, 15415-15425.

17. C. Rodriguez-Tinoco, M. Gonzalez-Silveira, J. Rafols-Ribe, G. Garcia and J. Rodriguez-Viejo, *J. Non-Cryst. Solids*, 2015, **407**, 256-261.

18. S. L. L. M. Ramos, M. Oguni, K. Ishii and H. Nakayama, *J. Phys. Chem. B*, 2011, **115**, 14327-14332.

19. J. Rafols-Ribe, M. Gonzalez-Silveira, C. Rodriguez-Tinoco and J. Rodriguez-Viejo, *Phys. Chem. Chem. Phys.*, 2017, **19**, 11089-11097.

20. K. L. Kearns, S. F. Swallen, M. D. Ediger, T. Wu, Y. Sun and L. Yu, *J. Phys. Chem. B*, 2008, **112**, 4934-4942.

21. Y. Matsuda, R. Akazawa, R. Teraoka and M. Otsuka, *J. Pharm. Pharmacol.*, 1994, **46**, 162-167.

22. Y. Matsuda and E. Tatsumi, *Int. J. Pharm.*, 1990, **60**, 11-26.

23. Y. Qiu, L. W. Antony, J. J. de Pablo and M. D. Ediger, *J. Am. Chem. Soc.*, 2016, **138**, 11282-11289.

24. J. S. Royal and J. M. Torkelson, *Macromolecules*, 1992, **25**, 4792-4796.

25. K. L. Camera, J. Gómez-Zayas, D. Yokoyama, M. D. Ediger and C. K. Ober, *ACS Appl. Mater. Interfaces*, 2015, **7**, 23398-23401.

26. G. Sauerbrey, *Z. Phys.*, 1959, **155**, 206-222.

27. M. Yoshioka, B. C. Hancock and G. Zografi, *J. Pharm. Sci.*, 1994, **83**, 1700-1705.

28. Y. Zhang and Z. Fakhraai, *Phys. Rev. Lett.*, 2017, **118**, 066101.

29. D. M. Walters, L. Antony, J. J. de Pablo and M. D. Ediger, *J. Phys. Chem. Lett.*, 2017, **8**, 3380-3386.

30. J. Gómez, A. Gujral, C. Huang, C. Bishop, L. Yu and M. D. Ediger, *J. Chem. Phys.*, 2017, **146**, 054503.

31. K. J. Dawson, L. Zhu, L. Yu and M. D. Ediger, *J. Phys. Chem. B*, 2011, **115**, 455-463.

32. S. K. Kearsley, *The Prediction of Chemical Reactivity within Organic Crystals Using Geometric Criteria*, Elsevier, New York, 1987.

33. M. D. Cohen and G. M. J. Schmidt, *J. Chem. Soc.*, 1964, 1996-2000.

34. Z. Sekkat, G. Kleideiter and T. Knoll, *J. Opt. Soc. Am. B-Opt. Phys.*, 2001, **18**, 1854-1857.

35. W. R. Mateker, T. Heumueller, R. Cheacharoen, I. T. Sachs-Quintana, M. D. McGehee, J. Warnan, P. M. Beaujuge, X. Liu and G. C. Bazan, *Chem. Mater.*, 2015, **27**, 6345-6353.

36. N. Nakashima and K. Yoshihara, *J. Phys. Chem.*, 1989, **93**, 7763-7771.

37. C. Rodríguez-Tinoco, M. González-Silveira, M. Barrio, P. Lloveras, J. L. Tamarit, J. L. Garden and J. Rodríguez-Viejo, *Sci. Rep.*, 2016, **6**, 34296.

38. K. J. Dawson, K. L. Kearns, M. D. Ediger, M. J. Sacchetti and G. D. Zografi, *J. Phys. Chem. B*, 2009, **113**, 2422-2427.

39. Y. Esaki, T. Komino, T. Matsushima and C. Adachi, *J. Phys. Chem. Lett.*, 2017, **8**, 5891-5897.

Chapter 5

Dense packing produces reactivity differences of indomethacin glasses with ammonia gas

Authors: Yue Qiu, Michael E. Bieser, M. D. Ediger

Abstract

Chemically stable solids are in demand for many applications, including pharmaceuticals and organic electronics. Previous work in crystals has established the importance of the molecular packing in modulating solid-gas reactivity by investigating the response of different polymorphs. Here we show, for the first time, that chemical stability of amorphous materials can also be significantly improved by packing molecules more densely via physical vapor deposition (PVD). For these experiments, PVD is shown to create glasses with an unprecedented range of density and thermal stability. Indomethacin reaction with ammonia, a well-characterized system in crystalline polymorphs, is re-examined as a reference model system for glasses. The indomethacin-ammonia reactivity is assessed through the increase in mass induced by the addition of ammonia to glassy thin films, as characterized by a quartz crystal microbalance (QCM). Indomethacin vapor-deposited at the substrate temperature below T_g shows substantially decreased reaction rate relative to the liquid-cooled glass, and the difference is as much as one order of magnitude. We suggest that the diminished solubility of ammonia in vapor-deposited glasses contributes to the remarkable chemical stability.

5.1 Introduction

Organic glasses are important materials that are widely used in modern technologies, including pharmaceuticals[1] and organic electronics.[2, 3] Compared to their crystalline counterparts, organic glasses are frequently preferred in many applications. For example, some drugs are formulated as glasses due to higher solubility and bioavailability.[4] In the organic light emitting diode (OLED) industry, glassy thin films are used as light emission layers for smooth surfaces and large-area fabrications. One important issue for organic materials is their reactions with environmental gases. For example, several drugs are known to undergo hydrolysis reactions with the water vapor, leading to the shortened shelf life.[5, 6] For OLEDs, it has been reported that ambient

gases, containing moisture and oxygen, have a great impact on the device lifetime.[7, 8] Therefore, OLEDs require encapsulation to protect the organic parts from water and oxygen.

Work dating back 50 years has established that molecular packing in crystals can significantly modulate chemical reactivity with gases.[9, 10] The solid-gas reaction rate varies in different crystal polymorphs and, for a single polymorph, the reaction propagation rate is anisotropic on different faces. Additionally, for crystals of carboxylic acids reacting with ammonia, the reaction rates could not be correlated with acid dissociation constant, crystal density, or melting point.[11] For example, of the two polymorphs of indomethacin, α and γ, the α-form reacts readily with ammonia while the γ-form is inert to the reaction, even though α-form has a higher density.[12] Further study revealed polymorphs with certain packing can block the access of ammonia gas to the carboxylic acid group, and therefore show higher resistance to the reaction. In contrast, as glasses have no long-range order, the same principle to prevent the carboxylic acid group from ammonia may not apply to glasses. We are not aware of an investigation of molecular packing in glasses as related to the solid-gas reaction that shows a significant improvement in chemical stability.

Recently, physical vapor deposition has been reported to prepare stable glasses with exceptional properties that are not accessible by any other preparation method.[13] By properly controlling the substrate temperature during deposition, vapor-deposition can form glasses that have higher thermal stability, higher density, and lower enthalpy relative to that of traditional liquid-cooled glass.[13-16] Vapor-deposited glasses can maintain glassy states at a much higher temperature than a liquid-cooled glass.[17] Vapor-deposited glasses also have densities up to 1.4% higher than a liquid-cooled glass.[15] Moreover, the most stable vapor-deposited glass shows about 4.3 kJ/mol lower enthalpy than the liquid-cooled glass, which is approximately 25% of the enthalpy difference between the standard liquid-cooled glass and a crystal.[16]

The discovery of stable glasses prepared by vapor deposition provides a great opportunity to address questions of chemical reactions and stability in glasses. In the present work, we return to indomethacin as a model system, since the reactivity of its crystalline polymorphs have been well characterized,[12] and test whether vapor-deposited glasses with exceptional properties can also lead to exceptionally high chemical stability. It is known that indomethacin can react with ammonia to yield ammonium salt, as shown in Scheme 1. In addition, indomethacin has been found to form high-density and low-enthalpy glasses by vapor deposition, with the density increased as much as 1.4% and the enthalpy decreased by up to 4.3 kJ/mol relative to the liquid-cooled glass.[15, 16] In this work, indomethacin was vapor-deposited onto substrates held at a range of temperatures to obtain glasses with different packing. Quartz crystal microbalance (QCM) was used to continuously monitor the mass gain induced by the addition of ammonia in different indomethacin glasses. The influences of ammonia concentration, film thickness, and reaction temperature on reactivity were investigated.

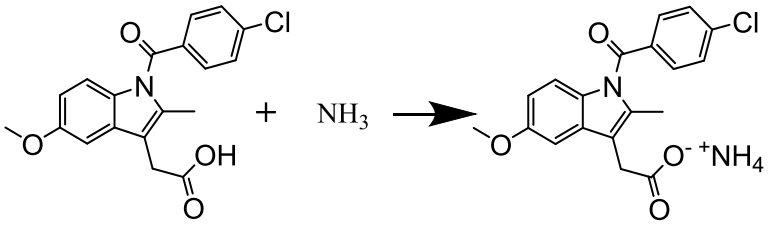

Scheme 1. Indomethacin reaction with ammonia (T_g = 310 K).

We find that vapor-deposited indomethacin can be significantly more stable against the ammonia reaction. The most stable glass is vapor-deposited at 260 K (0.84 T_g) and reacts at one-tenth the rate relative to the liquid-cooled glass at room temperature. This is the first demonstration that glass packing can significantly modulate the solid-gas reaction. We observe that chemical stability is highly correlated with the glass density. After considering the influence of glass packing on ammonia diffusivity and solubility, we suggest an important aspect of the

remarkable chemical stability of dense indomethacin glass is a diminished solubility of ammonia gas.

5.2 Experimental methods

5.2.1 Preparation of vapor-deposited indomethacin glasses

Indomethacin (99%) was purchased from Sigma Aldrich and used as received. Glassy thin films of indomethacin were prepared by physical vapor deposition (PVD), which took place in a vacuum chamber (10^{-7} Torr). Indomethacin was placed in a crucible that was resistively heated to evaporate the material into the vapor phase. The deposition rate was controlled by tuning the heating power and monitored by a quartz crystal microbalance (QCM). For all samples prepared for this paper, the deposition rate was kept at a constant value of 0.2 nm/s. Indomethacin was directly deposited onto the substrate of a gold-coated quartz crystal resonator, which is suitable for use in QCM measurement that will be introduced below. During vapor deposition, the quartz crystal resonator was in good thermal contact with the copper finger, whose temperature can be precisely controlled. The substrate temperature during deposition is an important variable for the sample preparation, as discussed later. For most of our experiments, the sample thickness was about 100 nm, as measured by ellipsometry. For a few experiments, 300 nm samples were prepared to investigate the effect of thickness. Liquid-cooled glasses were prepared by vapor-deposition at the substrate temperature at 320 K, which is 10 K above the T_g (T_g = 310 K), followed by cooling to room temperature at 1 K/min.

5.2.2 Indomethacin and ammonia chemical reaction characterization

The indomethacin-ammonia reaction was performed in a custom-built reaction chamber. Vapor-deposited indomethacin on the quartz crystal resonator was placed in a QCM device, located within the reaction chamber. Dilute ammonia gas was evolved upon bubbling nitrogen at a flow rate of 10 ml/minute through ammonium hydroxide solutions. The gas flowed through a

desiccating tube of potassium hydroxide pellets to remove water vapor before going into the reaction chamber. In this paper, ammonium hydroxide solutions of two concentrations were used to generate ammonia gases, i.e. 0.49 M (1 wt.%) and 1.5 M (3 wt.%); the ammonia gas in the ammonia-nitrogen mixture has a partial pressure of 0.0076 ± .0007 bar and 0.025 ± .004 bar for the two concentrations of solution, respectively.

Prior to each reaction, the reaction chamber was kept under a stream of nitrogen gas. To initiate the reaction, the nitrogen was turned off and dilute ammonia gas was directed into the reaction chamber. For most experiments, the reaction was allowed to proceed for fifteen minutes before turning off the ammonia gas. In some experiments, after the initial exposure of ammonia gas, the stream of nitrogen gas was turned on again to purge the sample, followed by the second run of ammonia gas. This procedure was repeated for some indomethacin samples to acquire data of multiple cycles. Most experiments were performed at room temperature (295 K). For low-temperature experiments, the reaction chamber was cooled by dry ice, with the temperature of QCM controlled at 275 ± 1 K, as measured by the thermocouple in contact with the QCM.

The mass uptake during the addition reaction of ammonia was monitored by a QCM. 5 MHz AT-cut quartz plate (Inficon Inc.) with a polished gold electrode was used as the QCM resonator. QCM is widely used as a sensitive mass detector in many gas uptake measurements.[18, 19] For films in the thickness range employed here, the frequency shift of the resonator can be related to the mass change of the sample by the Sauerbrey equation:[20]

$$\Delta f = -\frac{2f_0^2}{A\sqrt{\rho_q \mu_q}}\Delta m$$

where f_0 is the resonance frequency (Hz), Δf is the frequency change, Δm is the mass change, A is the piezoelectrically active crystal area, ρ_q is the density of quartz (2.648 g/cm^3), and μ_q is the shear modulus of quartz for the AT-cut crystal (2.947 x 10^{11} g·cm^{-1}·s^{-2}). Since f_0, A, ρ_q, and μ_q

are all known, Δm can be calculated from Δf. In this way, we can monitor the indomethacin-ammonia reaction of the glassy thin films in real time.

5.3 Results

5.3.1 Influence of PVD substrate temperature on reactivity

Figure 1 shows the comparison of the mass increase during the reaction with ammonia for vapor-deposited and liquid-cooled indomethacin, and reveals that the PVD glasses display slower reaction, i.e. enhanced chemical stability. These tests were performed on 100 nm films reacting with 0.0076 bar ammonia at 295 K. Immediately after ammonia gas is introduced, the mass starts to increase for all glasses. After 600 s had elapsed, the mass of all glasses approximately reaches a steady-state, and the overall mass increase at the steady-state is in the range of 4.6 - 4.9%. The mass gain is reasonably consistent with the theoretical value of 4.8% calculated from the stoichiometry, indicating that all indomethacin molecules have reacted. This provides confidence that QCM can precisely measure the chemical reaction occurring in glassy indomethacin.

We found that the distinctive packing of vapor-deposited glasses was destroyed as a result of the ammonia reaction after the initial exposure at the steady-state. We performed the second cycle of ammonia reaction after the sample already reacted with ammonia and purged with nitrogen. As shown in the inset of Figure 1, indomethacin vapor-deposited at 260 K shows a mass increase closely overlaps with the liquid-cooled glass (T_{sub} = 320 K) in the second cycle of reaction, indicating that glass packing of as-deposited samples has been disrupted by the first run of ammonia. Wide angle X-ray scattering measurements on vapor-deposited glasses show that the anisotropic peak (q = 0.57 $Å^{-1}$) that represents the tendency of molecular layering was also diminished after reaction (Figure S3), revealing that the initial structure of as-prepared glasses was destroyed.

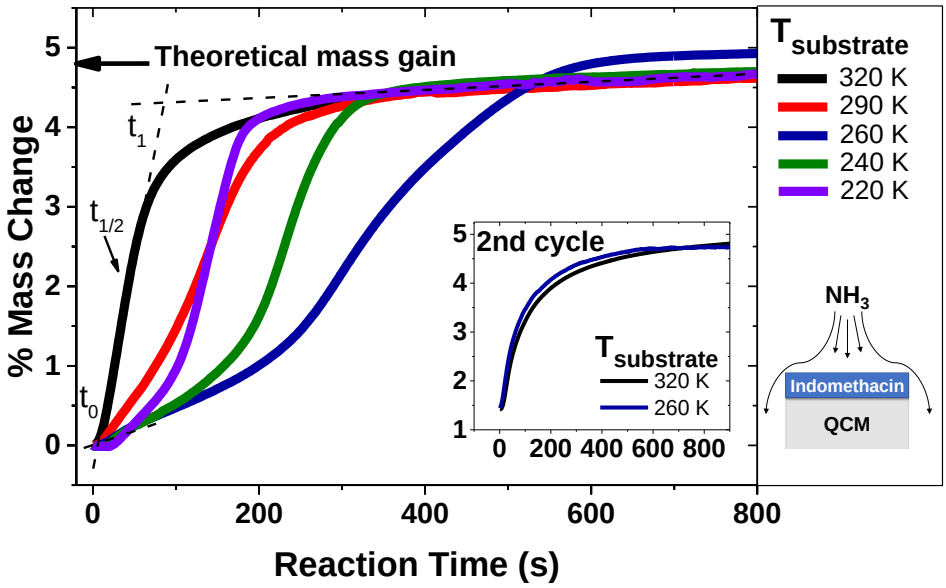

Figure 1. Mass increase for 100 nm indomethacin films reacting with 0.0076 bar ammonia as a function of time at 295 K. The black curve is liquid-cooled glass and the colored curves represent glasses vapor deposited at the indicated substrate temperatures. Here we define the glass vapor-deposited at 320 K and cooled back at 1 K/min as the liquid-cooled glass. Inset shows the 2nd cycle of reaction after as-deposited glasses have reacted with ammonia and been purged with N_2 gas. Schematic shown in the lower right represents the device geometry in measuring the indomethacin-ammonia reaction.

To better compare the chemical stability of vapor-deposited and liquid-cooled glasses, we use the reaction half-time to indicate how fast the reaction occurs in each glass. Take the liquid-cooled glass in Figure 1 for example, the mass gain proceeds in a step-wise fashion, from the initial rate to the final steady-state. Linear fits to the data in the initial and final regime are taken. A third linear curve is fit to the step (the regime where mass increases sharply), such that the intersection with the initial and final linear fits define t_0 and t_1, respectively. Reaction half-time, $t_{1/2}$, is the average of t_0 and t_1. A comparison of the reaction half-time for vapor-deposited and liquid-cooled glasses is summarized in Figure 2a. The half-time for the liquid-cooled glass is about 40 s, while all vapor-deposited glasses have $t_{1/2}$ at least 3 times longer than that, indicating enhanced chemical stability. The most stable vapor-deposited glass employed, which was prepared at the substrate temperature of 260 K, has a $t_{1/2}$ about 10 times longer than the liquid-cooled glass.

Chemical stability of vapor-deposited and liquid-cooled glasses are compared with the initial density, and a strong correlation between increased stability and increased density can be observed in Figure 2a and 2b. Figure 2b shows the density of indomethacin glasses vapor-deposited at different temperatures relative to the liquid-cooled glass. All glasses prepared at $T_{sub} < T_g$ investigated in this study show higher density. In the previous study, the correlation between density and chemical stability is not observed in crystalline indomethacin with different polymorphs. The role of density in influencing reactivity in the solid-gas reaction will be discussed below.

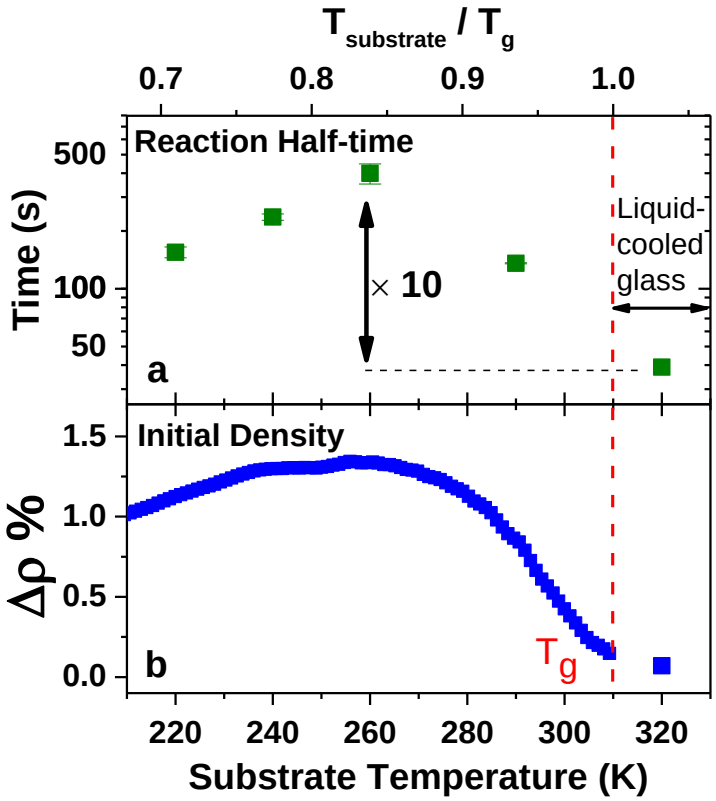

Figure 2. Indomethacin-ammonia reaction half-time and glass density as a function of substrate temperature during vapor deposition. a) Reaction half-time. (b) Density of as-deposited glasses relative to the liquid-cooled glass; data is re-plotted from Ref. #15. A strong correlation is observed between resistance to the solid-gas reaction and glass density.

5.3.2 Influence of ammonia concentrations on reactivity

To test the generality of the effect of enhanced chemical stability, we performed experiments at a higher ammonia concentration and found that and the chemical stability of vapor-deposited glasses is still higher than that of the liquid-cooled glass. As shown in Figure 3, vapor-deposited and liquid-cooled glasses were reacted with 0.025 bar ammonia at 295 K. After the reaction begins, mass starts to increase for all glasses, and the liquid-cooled glass increases faster than vapor-deposited samples. After 200 s had elapsed, the mass gain for all glasses approximately reached the same steady-state. Chemical stability was quantified by the reaction half-time, as shown in Figure S1 (supporting information). The $t_{1/2}$ is about 20 s for the liquid-cooled glass and 65 s for the most stable vapor-deposited glass. In this case, the chemical stability is increased by about a factor of 3 when indomethacin was deposited at 260 K.

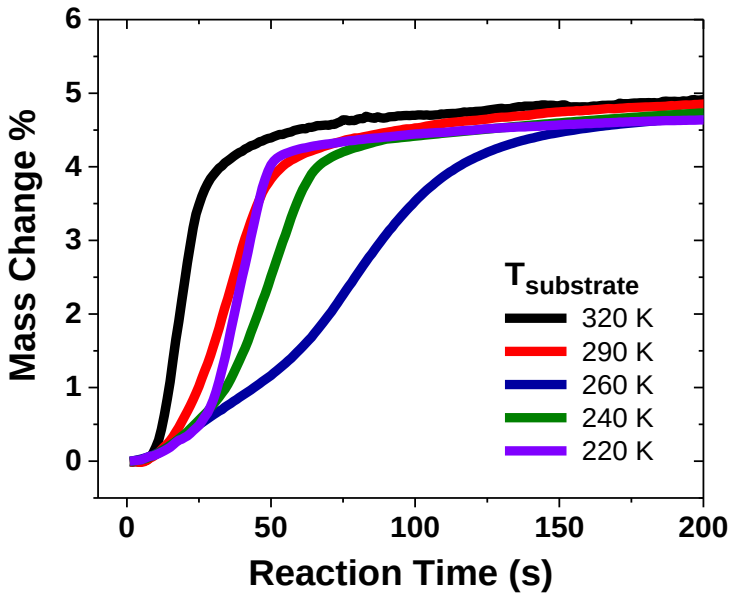

Figure 3. Mass increase for 100 nm indomethacin films reacting with 0.025 bar ammonia as a function of time at 295 K. The black curve is liquid-cooled glass and the colored curves represent glasses vapor deposited at the indicated substrate temperatures.

Figure 4 summarizes the reaction rates of vapor-deposited and liquid-cooled glasses at different ammonia concentrations, and it demonstrates the slowest reaction rates for the glass vapor-deposited at 260 K, which correspond to the densest glass shown in Figure 2. The reaction rate is calculated from the first order derivative of the mass increase and converted to molar concentrations. The solid lines show the reaction rate of indomethacin glasses at the condition of 0.0076 bar ammonia. For the liquid-cooled glass, the peak of the reaction rate occurs at about 30 s. As a comparison, the peak occurs at about 300 s for the glass vapor-deposited at 260 K, indicating a factor of 10 increase in chemical stability. Also, the maximum reaction rate for the most stable glass is about 1/3 of the liquid-cooled glass. The glass vapor-deposited at 290 K shows an intermediate stability, as shown by the peak position and height. For reaction performed at 0.025 bar ammonia, the trends of reaction rate are consistent with the results obtained at 0.0076 bar ammonia, though the peak position shifts to shorter times and the absolute value of maximum reaction rates become larger for each glass.

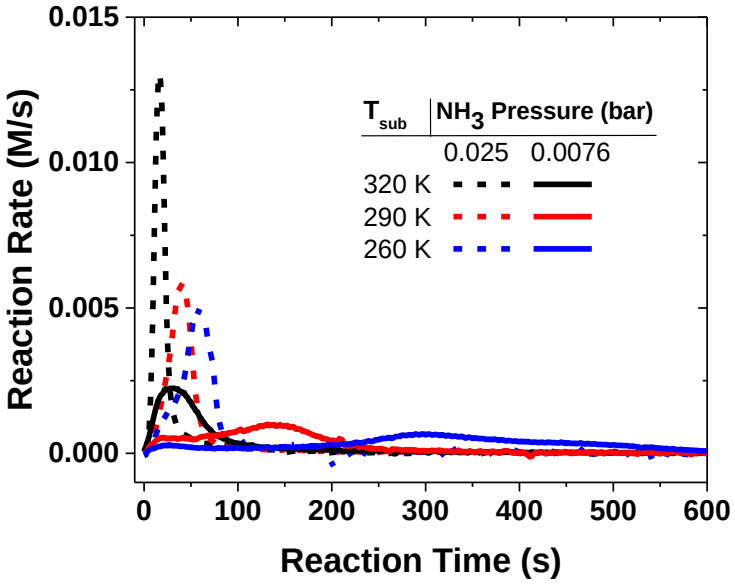

Figure 4. Reaction rate of vapor-deposited and liquid-cooled glasses as a function of reaction time. Solid lines are results for reaction with 0.0076 bar ammonia; dashed lines are results obtained at 0.025 bar ammonia.

5.3.3 Influence of sample thickness on reactivity

We did additional experiments on samples with different thickness, and found that the influence of thickness on reaction rate is quite small in vapor-deposited glasses. These tests were performed on 300 nm films reacting with 0.025 bar ammonia at 295 K. Chemical stabilities of vapor-deposited and liquid-cooled glasses, as represented by the reaction half-time, are summarized in Figure 5 and compared with the results obtained for 100 nm films under the same conditions. Vapor-deposited glasses are more stable relative to the liquid-cooled glasses. For the liquid-cooled glass, reaction half-time is about 38 s for the 300 nm film, which is about 2 times of the half-time measured for the 100 nm film. For the most stable glass, the reaction half-time only increases approximately from 65 s to 79 s (about 20% increase) even though the film thickness increased by a factor 3. This result will be discussed below to understand the reason for the remarkable chemical stability in stable glasses.

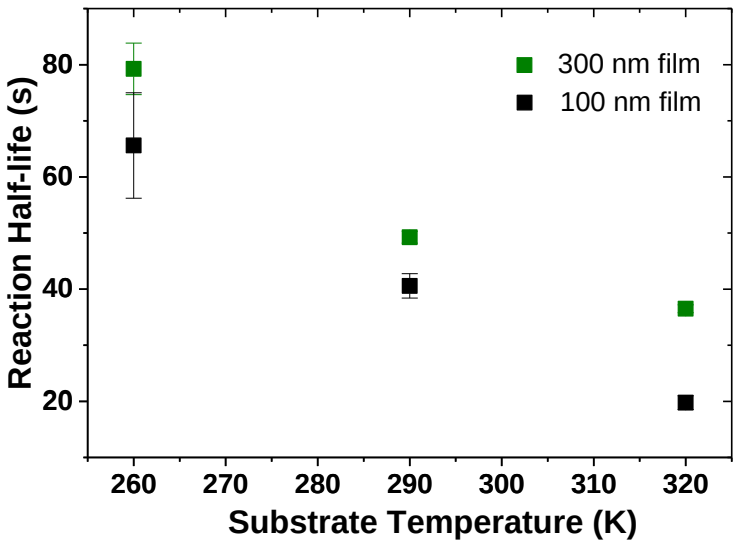

Figure 5. Reaction half-time of indomethacin films with different thickness reacting with 0.025 bar ammonia. Green and black symbols represent film thickness of 300 nm and 100 nm, respectively.

5.3.4 Influence of reaction temperature on reactivity

The influence of reaction temperature on indomethacin-ammonia reactivity was also investigated and we found that the reaction becomes faster at a lower temperature. As shown in Figure 6, the solid lines represent the mass increase of indomethacin glasses during the reaction at 275 K and the dashed lines represent the measurement taken at 295 K. For the liquid-cooled glass measured at 275 K, the reaction half-time is about 30 s (Figure S2). In contrast, for the same glass measured at 295 K, the reaction half-time increases to 40 s, indicating a slower reaction rate at the higher temperature. The increase in reactivity at a lower temperature becomes even prominent when comparing the optimum glass vapor-deposited at 260 K. By decreasing the reaction temperature from 295 to 270 K, reaction half-time of vapor-deposited glass approximately decreases from 400 s to 70 s. This behavior of faster reaction at the lower temperature is explained by the influence of temperature on the solubility of ammonia in amorphous indomethacin. At lower temperature, ammonia solubility is expected to become higher. Consistent with this view, the maximum mass gain for the measurement at 275 K is about 8% at the steady-state shown in Figure 6, indicating more ammonia has been dissolved in indomethacin at the lower temperature.

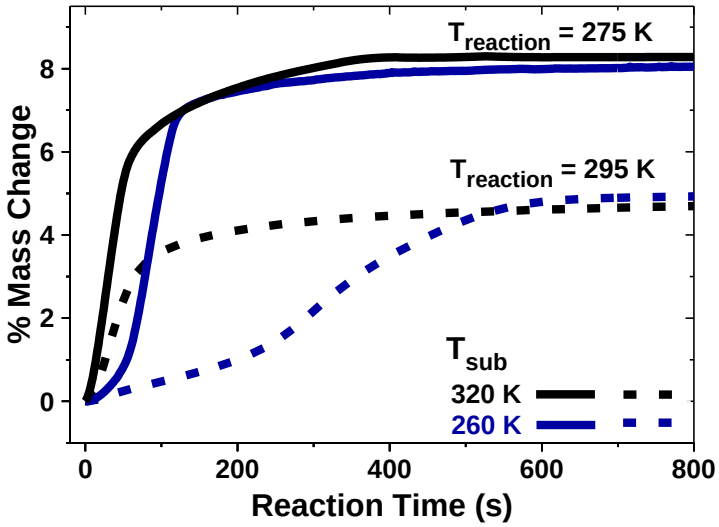

Figure 6. Mass increase for 100 nm indomethacin films reacting with 0.0076 bar ammonia as a function of time at different temperatures. Solid lines are results for the reaction at 275 K; dashed lines are results obtained at 295 K.

5.4 Discussion

In this work, we are the first to demonstrate that organic glasses prepared by PVD show substantially increased chemical stability against the reaction with gases. We show that vapor-deposited indomethacin glasses can be 10 times more stable in resisting ammonia relative to the liquid-cooled glass. Previous work shows that organic crystals can have different reactivity with ammonia. For example, of the two polymorphs of indomethacin with millimeter-sized crystals, the α-form finished the reaction with ammonia after 5 min, while the γ-form barely had any change even after 24 h. In view of the lower density of the stable γ-form as compared to the metastable α-form (1.37 and 1.42 g cm^{-3}, respectively), the significantly varied reactivity is attributed to different molecular packing in polymorphs, as the α-form exposes carboxylic acid groups at the faces that can be easily accessed by ammonia. In contrast, as amorphous materials have no long-range order and an unlimited number of local packing motifs, the principle employed to explain crystalline behavior does not seem to apply here. Next, we will focus our discussion on the reaction mechanism and the explanation for enhanced chemical stability in vapor-deposited glasses.

It was reported that the reaction of ammonia with crystalline indomethacin is through a surface mechanism, where ammonia gas begins reaction from a certain face and propagates into the bulk at a constant velocity.[12] One might ask whether vapor-deposited glasses of indomethacin also initiate the reaction from the surface. Our results indicate that the reaction of indomethacin glasses with ammonia is through the bulk mechanism. As shown in Figure 5, when the film thickness increases by a factor of 3 for the glass vapor-deposited at T_{sub} = 260 K, the reaction half-time only increases by approximately 20%. A surface mechanism would lead to a much larger increase in the reaction time. Also, in the previous study of water uptake by vapor-deposited indomethacin, it was reported that vapor-deposited glasses adsorb water through a bulk mechanism.[21] Given our results and the literature report, we infer that vapor-deposited

indomethacin adsorbs ammonia in the bulk and reactions begin to occur throughout the film soon after the sample is exposed to ammonia gas.

Our experimental results and literature study both suggest that diffusion of ammonia in indomethacin glasses is not likely to influence the reaction kinetics. If we assume the diffusion of ammonia into glassy thin films follows the Fickian model, then the time required to equilibrate the gas content within a film should scale with the film thickness squared. However, in the investigation of ammonia reaction with different film thickness, as shown in Figure 5, a factor of 3 increase in thickness only yields a reaction time difference by approximately 20% for the most stable glass, far less than the factor of 9 increase expected from a diffusion mechanism. Also, the usage of thin films helps to minimize the time required for ammonia gas to diffuse into the indomethacin film. In a previous study of water uptake, Dawson and coworkers have measured the diffusion coefficient of water in vapor-deposited indomethacin at the order of 10^{-9} cm^2/s.[21] Assuming that ammonia and water have similar diffusion coefficients, then the diffusion of ammonia in a 100 nm film is fast (less than 1 s) compared to the time scales of the indomethacin-ammonia reactions. The fast diffusion of ammonia into the film allows us to more directly characterize the solid-gas reaction and avoid the influence of the diffusion factor.

Given the correlation of glass density to chemical stability shown in Figure 2, one may speculate the role of density in influencing reactivity, and our experimental results indicate that the diminished solubility in densely packed glass is likely to contribute to the enhanced chemical stability. In the previous study of water uptake, it was demonstrated that solubility of water vapor decreased by a factor of 5 in the densest vapor-deposited glass.[21] The decrease in solubility is related to the less available space (free volume) in the high-density PVD glass. In this sense, if the solubility of ammonia decreases comparably to that of water vapor in vapor-deposited indomethacin, then we should expect a great suppression of chemical reactivity with ammonia, in accordance with what we observed in experiments. The influence of solubility on reactivity

was also observed in our low temperature measurements (Figure 6), where reaction rates become faster at a lower temperature. Faster reaction rates indicate competing processes involved in the indomethacin-ammonia reaction, such as the decreased temperature and the increased solubility. At the steady-state, ammonia adsorption at 275 K is higher than that measured at 295 K, indicating increased solubility at the lower temperature. Therefore, we suggest that the diminished solubility of ammonia is likely to be the explanation for the enhanced chemical stability in vapor-deposited glasses.

Acknowledgment

This work was supported by the U.S. Department of Energy (DOE), Office of Basic Energy Sciences (BES), Division of Materials Sciences and Engineering, Award DE-SC0002161.

5.5 References

[1] B. C. Hancock, and G. Zografi, Characteristics and significance of the amorphous state in pharmaceutical systems. J. Pharm. Sci. **86** (1997) 1.

[2] D. Yokoyama, Molecular orientation in small-molecule organic light-emitting diodes. J. Mater. Chem. **21** (2011) 19187.

[3] K. Sei-Yong *et al.*, Organic light-emitting diodes with 30% external quantum efficiency based on a horizontally oriented emitter. Adv. Funct. Mater. **23** (2013) 3896.

[4] B. C. Hancock, and M. Parks, What is the true solubility advantage for amorphous pharmaceuticals? Pharm. Res. **17** (2000) 397.

[5] L. J. Leeson, and A. M. Mattocks, Decomposition of aspirin in the solid state. J. Am. Pharm. Assoc. (Scientific ed.) **47** (1958) 329.

[6] K. C. Waterman *et al.*, Hydrolysis in pharmaceutical formulations. Pharm. Dev. Technol. **7** (2002) 113.

[7] L. S. Liao *et al.*, Ambient effect on the electronic structures of tris-(8-hydroxyquinoline) aluminum films investigated by photoelectron spectroscopy. Chem. Phys. Lett. **333** (2001) 212.

[8] J. E. Knox *et al.*, Chemical failure modes of alq3-based oleds: Alq3 hydrolysis. PCCP **8** (2006) 1371.

[9] R. S. Miller, D. Y. Curtin, and I. C. Paul, Reactions of molecular crystals with gases. I. Reactions of solid aromatic carboxylic acids and related compounds with ammonia and amines. J. Am. Chem. Soc. **96** (1974) 6329.

[10] R. S. Miller, I. C. Paul, and D. Y. Curtin, Reactions of molecular crystals with gases. Ii. X-ray structure of crystalline 4-chlorobenzoic acid and the anisotropy of its reaction with ammonia gas. J. Am. Chem. Soc. **96** (1974) 6334.

[11] S. R. Byrn, R. R. Pfeiffer, and J. G. Stowell, *Solid-state chemistry of drugs* (SSCI, Inc., 3065 Kent Avenue, West Lafayette, Indiana 47906-1076, 1999), Second edn., 256.

[12] X. Chen *et al.*, Reactivity differences of indomethacin solid forms with ammonia gas. J. Am. Chem. Soc. **124** (2002) 15012.

[13] S. F. Swallen *et al.*, Organic glasses with exceptional thermodynamic and kinetic stability. Science **315** (2007) 353.

[14] M. D. Ediger, Perspective: Highly stable vapor-deposited glasses. J. Chem. Phys. **147** (2017) 210901.

[15] S. S. Dalal, Z. Fakhraai, and M. D. Ediger, High-throughput ellipsometric characterization of vapor-deposited indomethacin glasses. J. Phys. Chem. B **117** (2013) 15415.

[16] K. L. Kearns *et al.*, Hiking down the energy landscape: Progress toward the kauzmann temperature via vapor deposition. J. Phys. Chem. B **112** (2008) 4934.

[17] D. M. Walters, R. Richert, and M. D. Ediger, Thermal stability of vapor-deposited stable glasses of an organic semiconductor. J. Chem. Phys. **142** (2015) 134504.

[18] L. Banda, M. Alcoutlabi, and G. B. McKenna, Errors induced in quartz crystal mass uptake measurements by nongravimetric effects: Considerations beyond the eernisse caution. J. Polym. Sci. B **44** (2006) 801.

[19] S. Muraoka *et al.*, A co2 sensor using a quartz crystal microbalance coated with a sensitive membrane. Electron. Commun. Jpn. **97** (2014) 60.

[20] G. Sauerbrey, Verwendung von schwingquarzen zur wägung dünner schichten und zur mikrowägung. Z. Phys. **155** (1959) 206.

[21] K. J. Dawson *et al.*, Highly stable indomethacin glasses resist uptake of water vapor. J. Phys. Chem. B **113** (2009) 2422.

5.6 Supporting information

Most experiments in this paper were paper was performed on 0.0076 bar ammonia. To test the generality of enhanced chemical stability of vapor-deposited glass, we also performed experiments at 0.025 bar ammonia. The mass increase data during reaction was shown in Figure 3, and a comparison of the reaction rate is for vapor-deposited and liquid-cooled glasses is summarized in Figure S1. The half-time for the optimum vapor-deposited glass is about 65 s, which is about 3 times longer than the liquid-cooled glass, indicating enhanced chemical stability.

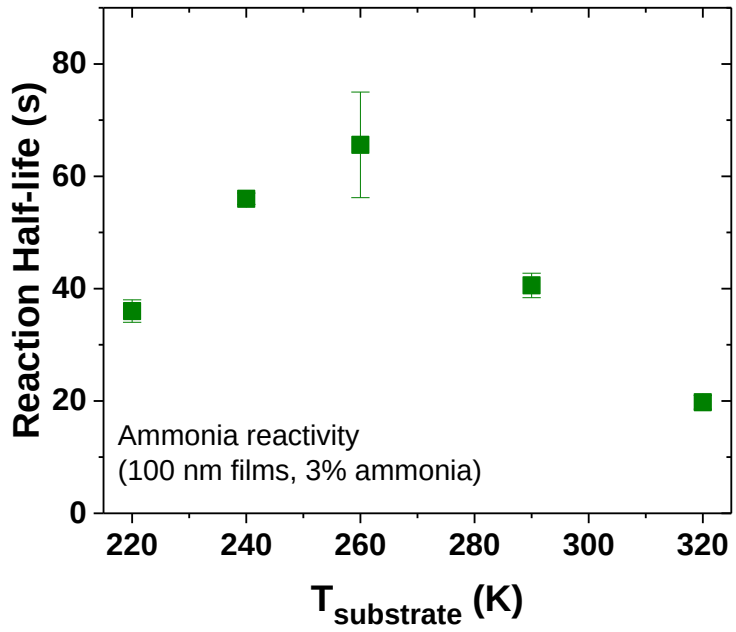

Figure S1. Indomethacin-ammonia reactivity as a function of substrate temperature during deposition. Sample thickness is 100 nm, and 0.025 bar ammonia is used.

To investigate the influence of reaction temperature on reactivity, indomethacin-ammonia reaction was also performed at 275 K, as summarized in Figure S2. The reaction becomes even faster at the lower temperature, as shown by the shorter reaction half-time.

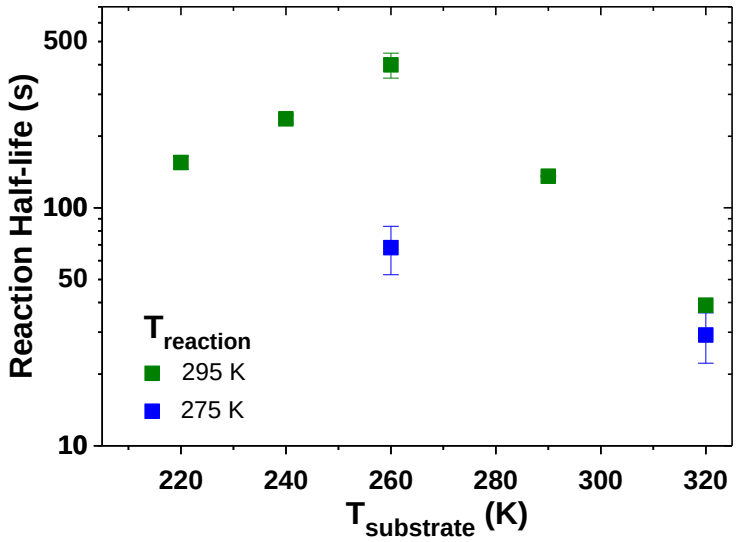

Figure S2. Indomethacin-ammonia reactivity as a function of substrate temperature during deposition. Sample thickness is 100 nm, and 0.0076 bar ammonia is used. Reactions were measured at 295 K (green) and 275 K (blue).

After the initial exposure of vapor-deposited indomethacin to ammonia gases, the glass packing was destroyed. As shown in the wide angle X-ray scattering measurements on vapor-deposited glasses (Figure S3), the anisotropic peak (2θ = 8°, q = 0.57 Å-1) that represents the tendency of molecular layering was diminished after reaction (Figure S3).

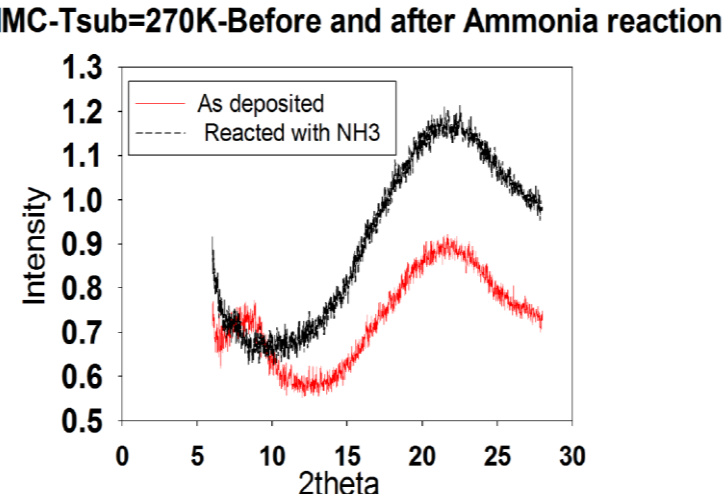

Figure S3. XRD spectrum of vapor-deposited indomethacin before (red) and after (black) reaction with ammonia.

Chapter 6

Conclusions and future directions

Yue Qiu

The main goal of this thesis is to explore the suppression of chemical reactions in amorphous materials and to deepen our understanding of vapor-deposited glasses. For that, I have investigated different types of chemical reactions in glasses, addressing the fundamental aspects of the influence of molecular packing on reactivity. To conclude, I will summarize the main contributions of this thesis and discuss how this work can provide insight into the further development of organic electronics in extending device lifetimes in section 6.1.

I will also propose future experiments that could benefit our understanding of chemical reactions and molecular packing of vapor-deposited glasses. Section 6.2 will discuss experiments of using photochemistry as a tool to probe the local structure and dynamics of vapor-deposited glasses. For example, substrates can interact with molecules and influence the packing of glasses. The length scale of the substrate effect depends on the strength of this interaction. Section 6.3 will discuss suppression of chemical degradations of some molecules that have been used in organic electronics. Section 6.4 will explore the possibility of preparing glasses by PVD that better resist crystallization.

6.1 Conclusions

The main findings in this thesis highlight the important role of molecular packing on chemical stability in glasses. Previously, modulation of chemical reactivity in organic crystals has been achieved by packing molecules differently in polymorphs. For crystals, the change in reactivity is related to the topochemistry principle that the reaction will involve nearest-neighbor molecules or functional groups and will occur with minimal atomic and molecular movement.[1] However, due to the lack of long-range order and organized structures, topochemical principles do not apply to glasses. Early efforts to increase chemical stability in glasses, such as aging, did not give a significant effect.[2] The slow dynamics in glasses make it difficult for the substantial modulation of molecular packing by the aging method. Work in this thesis has provided a route

to significantly increase chemical stability by packing molecules tightly via PVD; the optimal vapor-deposited glasses show unprecedented enhanced chemical stability. In Chapter 2 and 3, I show increased photostability of azobenzene derivatives in neat films and mixtures. In Chapter 4, I show increased photostability of indomethacin against photodecarboxylation. In Chapter 5, I investigate the effect of packing on the rate of solid-gas reaction of indomethacin with ammonia.

My work demonstrates that substrate temperature is an important variable during sample preparation for optimizing chemical stability. While PVD has been widely used in modern technology, the modulation of substrate temperature hasn't been fully employed. For example, it has been reported that vapor-deposited glasses of OLED molecules can be more resistant against chemical degradation relative to solution-processed samples.[3] There was no awareness of controlling the substrate temperature and depositions at room temperature accidentally prepared glasses with better performance. My work in this thesis supports the advantage of using PVD to prepare glasses and further shows that chemical stability can be optimized by the conscious control of substrate temperature.

My work in this thesis suggests that density plays an important role in the suppression of chemical reactions in glasses. Previously, it was reported that high-density glasses achieved by applying high external pressure[4] or tight molecular packing by incorporating azobenzene derivatives into more constrained DNA sequences[5] can significantly decrease the photoisomerization rate. My work supports this conclusion and shows that tight molecular packing acquired by PVD can also slow photoisomerization rates. Moreover, the effect from high-density glasses extends to other reaction types, including photodegradation and solid-gas reactions. Overall, in reactions that have been investigated, increased chemical stability has been found to correlate with glass density. For applications that use glasses and desire decreased reactivity and increased chemical stability, I hope that my work can provide a guide to the material synthesis.

Additionally, I demonstrate that the increase in chemical stability with increased density is general for different molecules and different reaction types. Chapter 2 shows that Disperse Orange 37, a push-pull azobenzene with fast *cis-trans* thermal isomerization, can be made 50 times more stable against photoisomerization if deposition temperatures are chosen correctly. Chapter 3 shows that the increased photostability also applies to a non-push-pull azobenzene, 4,4'-diphenyl azobenzene (DPA), in the stable glass host of celecoxib. Simulations of a coarse-grained model of azobenzene molecules performed by my collaborators also observe this behavior. By modeling the photoisomerization in vapor-deposited glasses, reaction rates are found to decrease as glass densities increase. Chapter 4 and 5 illustrate that, for vapor-deposited indomethacin, both photodegradation and solid-gas reactions can be substantially suppressed relative to liquid-cooled glasses. I hope that the suppression of chemical reactions shown in this thesis will also be observed for emitter/host glassy layers used in OLEDs, where photodegradation and solid-gas reactions will happen and harm the device lifetimes.

Furthermore, I developed experimental methods for characterizing chemical reactions in vapor-deposited glasses. Using spectroscopic ellipsometry, I measured photoisomerization of DO37 by *in situ* tracking the density and molecular orientation changes during light irradiation (Chapter 2). The successful characterization of photoisomerization relies on the highly accurate and non-destructive measurements of ellipsometry. During light irradiation, glassy thin films made of azobenzenes will photo-expand and the molecules will be reoriented by the polarized laser beam, which can be captured by the alteration of density and birefringence during ellipsometry measurements. In Chapter 3, UV-Vis spectroscopy was adopted to characterize the photoisomerization of DPA. *Trans* and *cis* DPA have different electronic spectra, which can be measured by UV-Vis spectroscopy. In this case, the measurement of *trans/cis* population provides straightforward evidence of slower photoisomerization in vapor-deposited glasses. In Chapter 4 and 5, a quartz crystal microbalance (QCM) was used to characterize

photodecarboxylation and solid-gas reactions, respectively. QCM can accurately measure the mass change of as-deposited glasses and provides real-time information about the extent of chemical reactions during light irradiation. This is especially useful for characterizing reactions that involve mass loss (gas-releasing degradations) and mass increase (addition reactions between solids and gases).

6.2 Proposed study- photochemistry as a tool to measure local structures and dynamics

6.2.1 Length scale of the substrate influence to the glass packing

Choice of the substrate in the thin film preparation can influence the structure of molecular packing from the interface towards the bulk. In the crystal growth, the substrate has been thought to play a role in the polymorph formation, where the molecular packing near the substrate can extend into the bulk.[6] However, for organic glasses, some results in the literature seem to be contradictory. For example, Yokoyama has reported that, for the linearly-shaped BSB-Cz molecules deposited onto temperature-controlled substrates, the molecular orientation of 100 nm films is different on ITO and Si substrates, as indicated by the birefringence measurements from ellipsometry.[7] He attributed this difference to the fact that the ITO surface is rougher than the surface of the Si substrate, which prevents the molecules on the surface from migrating locally and changes the molecular orientation on the ITO substrate. On the other hand, the Ediger group has deposited organic molecules of similar shapes onto many substrates, and so far, any correlation between the thin film structure and substrate has not been reported.

To investigate the substrate effect, it is important to know the length scale of the influence of a substrate to the glass structure. I propose to dope 5% Bis[2-(4,6-difluorophenyl)pyridinato-C2,N](picolinato)iridium(III) (FIrpic), as shown in Scheme 1, into the matrix of 100 nm TPD at different distances from the substrate. The doping geometry is shown in Scheme 2, where the thickness of the doping layer is 10 nm. FIrpic is a light emitter and TPD is used as the hole transport layer in OLEDs, both of which are commercially available. The 5% dilution of FIrpic in TPD is close to the concentration used in OLEDs, and previous work has shown that the dilution of 5% guest has a negligible influence on the host. The doped layer will be prepared by co-depositing of the FIrpic guest and the TPD host, and the detailed method for co-deposition has been introduced in Chapter 3. The part made of neat TPD in the 100-nm film will be deposited by regular PVD protocol.

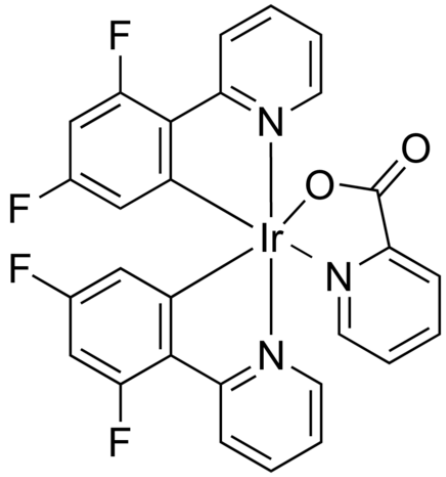

Scheme 1. Molecular structure of FIrpic.

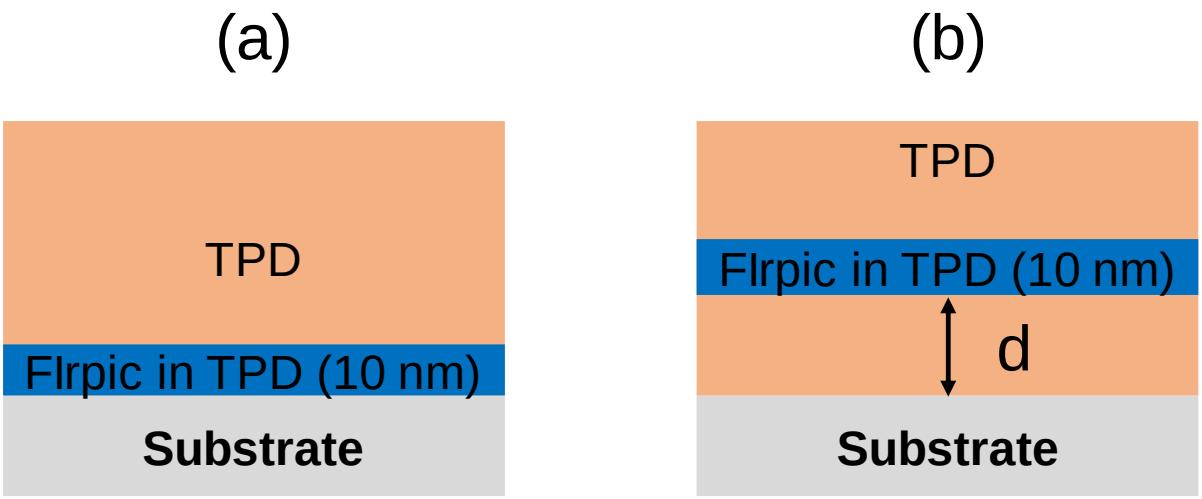

Scheme 2. A schematic illustration of the geometry of vapor-deposited glasses for investigating the substrate effect. 100 nm TPD is vapor-deposited onto a substrate. 5% FIrpic is doped in a layer of 10 nm TPD at different distances from the substrate. (a) FIrpic doped TPD is right at the interface with the substrate. (b) FIrpic doped TPD is in the middle of the TPD layer with a controlled distance d from the substrate.

I will first measure the photoluminescence lifetime of the FIrpic emitter and investigate at what distance from the substrate the bulk behavior can be recovered. The influence of substrate to glass packing will be investigated for the glass deposited on the Si substrate. The substrate temperature will be controlled at 0.85 T_g (T_g = 330 K) of TPD during deposition. Secondly, I will investigate the influence of different substrates to the glass packing. In this case, ITO will be used as the substrate for vapor-deposition, and photoluminescence lifetime of doped FIrpic will be investigated at different distances from the ITO and compare to the results obtained from the Si substrate. For measuring the time-resolved photoluminescence, the emitter molecule FIrpic will be excited with a pulsed nitrogen laser with an operational wavelength of 337.1 nm. According to our previous results, TPD is light stable at this wavelength and therefore this is a non-destructive method that detects the local molecular packing at the layer where FIrpic is doped. The photoluminescence lifetime of emitted light will be recorded with a photodetector.

Previously, it was reported that the photoluminescence lifetime depends on the local molecular packing, which lays the foundation for the proposed work. Rafols-Ribe et al. have reported that, for FIrpic emitter doped in the host matrix of TPBi, the measured photoluminescence lifetime can be 29% longer (1.38 vs 1.07 μs) for vapor-deposited samples relative to liquid-cooled glasses.[8] This enhancement was rationalized by a possible suppression of the β-relaxation—molecule vibrations within a cage formed by its neighbors—in the vapor-deposited glass of TPBi. The effect of suppressed β-relaxation has also been reported for nanoconfinement of PMMA polymers, where the hydrogen bonding between PMMA and the silica substrate decrease the magnitude of β-relaxation as opposed to the freestanding PMMA.[9] The suppression of β-relaxation near the substrate provides a precedent that substrate-glass interaction can influence the molecular packing.

I expect to see a longer photoluminescence lifetime of the molecules near substrate relative to the bulk for both Si and ITO. Literature results show that, for glassy thin films near the substrate

interface, glass transition temperature can be increased by 5 – 10 °C, possibly due to the interaction between glasses and substrates or anchoring effect.[10] The glass-substrate interaction may suppress the β-relaxation near the interface, and increase the photoluminescence lifetime. I anticipate that the influence of the substrate will decrease as we move from the substrate towards the bulk and eventually diminish after a certain distance. Torkelson et al. used fluoresce spectroscopy to measure the aging rate in polymer glasses and revealed that substrate can highly perturb the relaxation rate in the first 25 nm from the interface to the film interior, as shown in Figure 1.[11] I expect that the influence of substrate on glass packing in the proposed work has a similar length scale in terms of order of magnitudes.

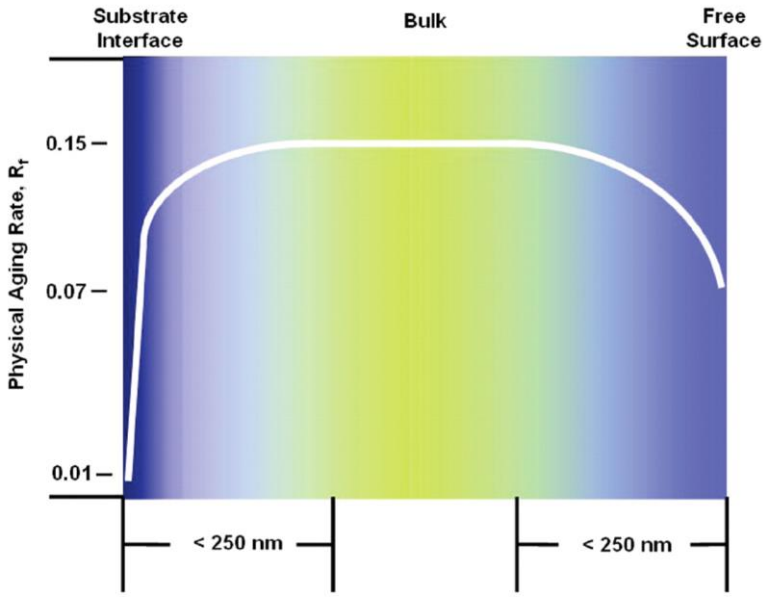

Figure 1. The effect of the substrate interface and the free surface on the distribution of structural relaxation rates in PMMA. a 25-nm-thick layer at the substrate interface exhibits a factor-of-15 reduction in relaxation rate relative to bulk. Adapted from Ref. #11 with permission.

6.2.2 Characterization of high-density glasses

During the research of vapor-deposited glasses, we occasionally work with molecules that interest us but whose density relative to the liquid-cooled glass cannot be easily accessed by the dilatometry method. This happens mainly because of crystallization during the thermal transformation of as-deposited glasses, which prevents us from measuring the thickness accurately. For samples that crystallize, results of molecular orientation and layering as characterized by ellipsometry and XRD indicate that substrate temperature plays a role for sample preparation. However, there are few clues about whether we obtain stable glasses or not. The measurement of photoluminescence lifetime provides a route to get access to the glass density in a non-destructive manner. Rafols-Ribe reported that photoluminescence lifetime is longer in vapor-deposited glasses relative to the low-density liquid-cooled glass. Therefore, I propose to use photoluminescence lifetime as an indicator of glass density for molecules including Alq3 and CBP (Figure 2). Both molecules have important applications in organic electronics, while whether or not they form stable glasses is unclear for now. This research can provide an alternative method to characterize glass density and help to answer whether bad glass formers can also form glass packing as well as those good glass formers.

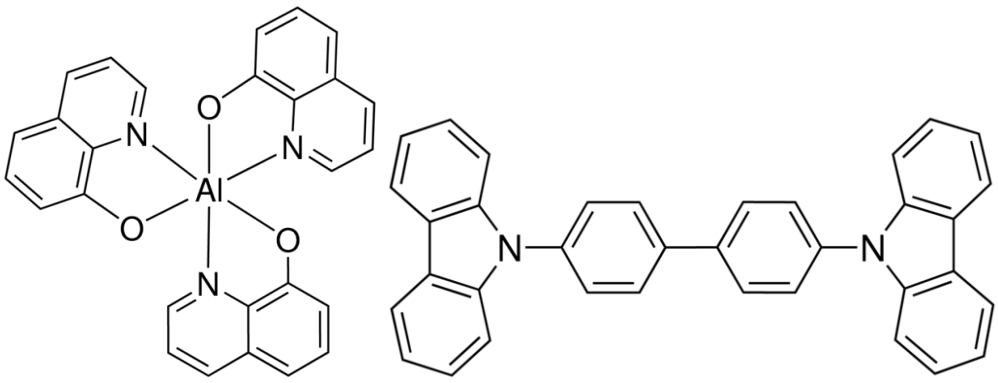

Figure 2. Molecular structure of Alq3 and CBP. Both molecules are used in OLEDs, while whether they form stable glass or not is unclear.

The experiment can be performed by vapor depositing 5% diluted FIpic emitters into the bulk of the Alq3 and CBP hosts at different substrate temperatures. Previous results have demonstrated that a 5% dilution only has an insignificant impact on the packing of glass host. CBP will be vapor-deposited at the substrate temperature of 0.75 – 1.05 T_g (T_g = 335 K). As Alq3 (T_g = 450 K) desorbs above 410 K during deposition, the ordinary glass cannot be accessed by vapor-deposition above T_g. In this case, ordinary glass of Alq3 will be prepared by spin-coating. Vapor-deposited Alq3 will be prepared at the substrate temperature from 0.75 to 0.90 T_g. Since the photoluminescence lifetime enhancement can be related directly to reduced nonradiative rates in high-density glasses, I expect to see a longer emission lifetime for glasses deposited below T_g. The densest glass is expected to be prepared at 0.85 T_g, which is reported to be the substrate temperature that generates the optimal glass for many molecules. Consistent with my anticipated results, there is a precedent for reduced nonradiative recombination rates observed in polymer-based systems that were prepared in a very rigid form that led to a higher packing density compared to a conventionally fabricated reference sample.[12]

6.3 Proposed study- Chemical stability of vapor-deposited organic electronics

Although OLEDs have been widely used in modern display technology, one challenge for the further development is the insufficient device lifetimes, which can be caused by chemical degradation. This situation becomes worse as OLEDs are made brighter. The higher the luminance of a device is, the shorter the lifetime of an OLED will be. In this section, I will discuss the possibility of increasing chemical stability of organic electronics molecules, including NPD and Alq3 by preparing glasses via PVD.

Alq3 is one of the most investigated OLED materials and was reported to undergo chemical degradation upon the interaction with oxygen, water, and light. Liao et al. exposed Alq3 layers and investigated the different responses with UPS and XPS. It shows that oxygen reacts with

Alq3, while water does not.[13] Later on, it was found that a water-induced degradation can happen to Alq3 at the elevated temperature of 180 °C.[14] Alq3 has been also been reported to photodegrade under UV exposure. Wang et al. characterized photoluminescence of Alq3 during light irradiation, and a continuous decay of emission intensity was found even without water and oxygen (Figure 3).[15]

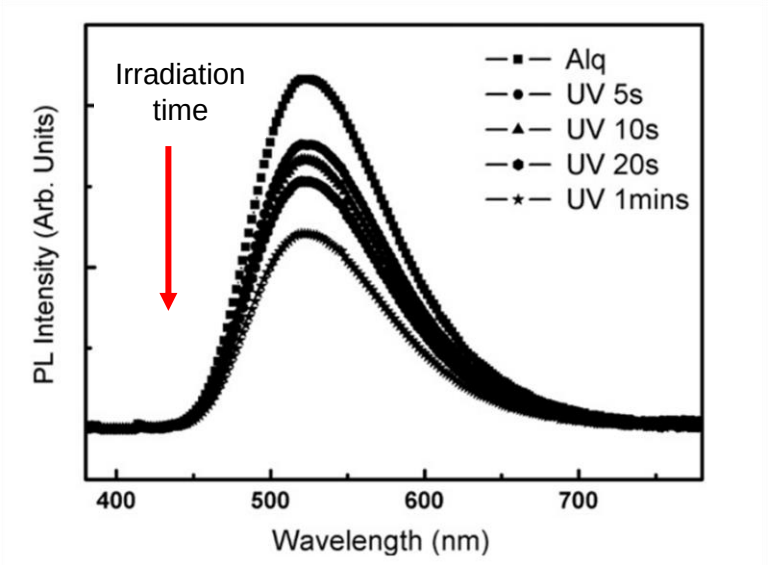

Figure 3. Photoluminescence spectra of Alq3 before and after UV irradiation. Direction of the arrow indicates the increase of irradiation time. Adapted from Ref. #15 with permission.

NPD is a common hole transport layer used in OLEDs. NPD is known to degrade (changes in their absorption and PL emission characteristics) after UV irradiation of single layers in the air.[16] The reaction products of NPD were detected with HPLC/UV and HPLC/MS methods, and fragments of the original molecule, as well as some adducts of NPD, were found, as shown in Figure 4.

To understand the influence of glass packing on photostability, I propose to prepare Alq3 and NPD glasses by PVD and spin-coating and test their resistance against photodegradation. 100 nm films will be prepared on a wide range of temperature gradient from 0.75 to 1.05 T_g for NPD

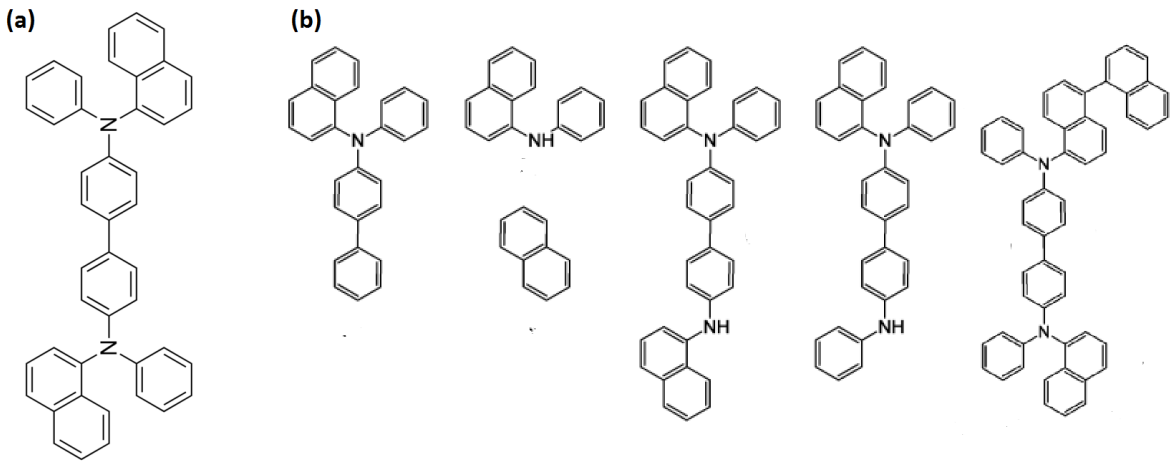

Figure 4. Molecular structure of (a) NPD and (b) photodegradation products of NPD after UV irradiation in the air. Adapted from Ref. #16 with permission.

(T_g = 380 K). Previous work has shown that NPD can form stable glasses by vapor-deposition. For Alq3, vapor-deposition will be chosen at the substrate temperature range of 0.75 to 0.90 T_g, and ordinary glass will be prepared by spin-coating. Although we are not certain that stable glass of Alq3 has been formed, we do see indications of different molecular packing in the films investigated by XRD study. UV light (365 nm) will be used to irradiate as-deposited thin films in a nitrogen atmosphere. I will use both ellipsometry and photoluminescence (PL) spectroscopy to characterize light-induced damage to Alq3 and NPD glasses. Ellipsometry measurement can provide density and refractive index information of the thin film. Previous work in DO37[17] and unpublished work of indomethacin both show that glass density will decrease as a result of degradation; refractive index also changed as the final product has a different molecular polarization relative to the initial one. However, our experience of using ellipsometry in measuring photodegradation of TPD wasn't very successful, possibly due to the small differences between the reactant and products in density and refractive index. If ellipsometry cannot measure the photodegradation of Alq3 and NPD, PL will act as an alternative method to characterize the photoreaction. As shown in Figure 3, PL was successfully used for Alq3

photodegradation measurement, and the emission decay rate indicates the kinetics of chemical degradation.

I expect that vapor-deposited glasses of Alq3 and NPD can better resist photodegradation than the ordinary glass prepared either by spin-coating (Alq3) or vapor-deposition above T_g (NPD). The photodegradation process is generally thought to involve the extension of the bond length before it breaks to releases fragments .[18] Therefore, we could imagine that vapor-deposited glasses of Alq3 and NPD with higher density can apply larger constraint to the molecular reconfiguration during the photo-dissociation of corresponded bondings. Previous work in photodecarboxylation of indomethacin shows increased photostability with increased glass density. I anticipate that the correlation between glass density and chemical stability can also be observed in vapor-deposited Alq3 and NPD.

6.4 Proposed study- Crystallization of vapor-deposition glasses

In the pharmaceutical industry, there are substantial interests in developing methods of stabilizing amorphous forms, and those efforts mainly focus on mixing drugs with polymers that have lower mobility. For example, furosemide has been reported to mix with PVP by 40% w/w to stabilize the amorphous phase.[19] IR analyses indicated that the intermolecular frusemide-PVP hydrogen bond interaction in the solid state retards or inhibits drug recrystallization by reducing molecular motion in the solid state. As stable glasses prepared by PVD have slower molecular mobility than the liquid-cooled glass, it is reasonable to check if stable glasses show a stronger resistance against crystallize.

I propose vapor-depositing 300 nm DO37 at 0.85 and 1.05 T_g (T_g of DO37 is 296 K) and cap the surface by 50 nm TPD to investigate bulk crystal growth rates for these materials. DO37 is a good crystal former, which facilitates our observation of crystallization. TPD acts as a capping

layer to prevent crystallization of DO37 at the surface, as TPD has a higher T_g and less tendency to crystallize than DO37. Optical microscopy will be used to measure the crystal growth rate. Previously, Rodriguez-Tinoco et al. reported that vapor-deposited celecoxib shows 30% slower rate of surface crystal growth at 50% relative humidity relative to the sample cooled from a melt.[20] They speculate that the crystal growth may be influenced by molecules located several molecular diameters deep into the glass, where stable glass can be more resistant against crystallization than the liquid-cooled glass. Inspired by this result, I expect that vapor-deposited glasses od DO37 show a much slower crystallization rate in the bulk than the liquid-cooled glass.

Crystallization of organic glasses will also be investigated at different relative humidity. I propose depositing 300 nm indomethacin at 0.85 and 1.05 T_g (T_g of indomethacin is 310 K) onto an optical glass and investigate the crystal growth rate at 10% and 75% relative humidity. As vapor-deposited indomethacin is transparent at the thickness been used, optical spectroscopy will be employed to measure the crystal growth rate in the bulk. Previous studies have shown that crystal growth rate can be accelerated by the adsorption of water. For example, amorphous cephalexin (Scheme 3) absorbs a large amount of water once the relative humidity is over 75%. The analysis of crystallization of cephalexin shows that crystallization became faster as the humidity increased. [21] This behavior has been known for years and explained by Zografi and co-workers who suggested that water acts as a plasticizer that lower the glass transition temperature.[22]

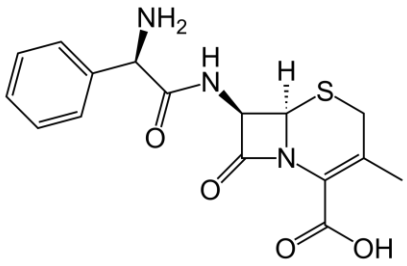

Scheme 3. Molecular structure of cephalexin. This antibiotic molecule is more supcecible to crystallization as humidity increases.

I expect that the crystal growth rate of indomethacin will be faster at 75% relative humidity than the case of 10% and stable glasses of indomethacin can resist crystallization better than the liquid-cooled glass. For vapor-deposited indomethacin, it has been shown that the relative water uptake increases by a factor of 10 when the relative humidity increases from 10% to 50%. The increase in water vapor uptake can accelerate the crystallization rate. Also, the relative water uptake was reported to decrease by a factor of 5 when indomethacin was deposited at 0.85 T_g ,as compared with the liquid-cooled glass.[23] The decrease in water uptake in vapor-deposited indomethacin is likely to contribute to a slower crystallization rate.

6.5 References

[1] M. D. Cohen, and G. M. J. Schmidt, 383. Topochemistry. Part i. A survey. J. Chem. Soc. (1964) 1996.

[2] J. S. Royal, and J. M. Torkelson, Photochromic and fluorescent probe studies in glassy polymer matrices. 5. Effects of physical aging on bisphenol a polycarbonate and poly(vinyl acetate) as sensed by a size distribution of photochromic probes. Macromolecules **25** (1992) 4792.

[3] Y. J. Cho, and H. Aziz, Root causes of the limited electroluminescence stability of organic light-emitting devices made by solution-coating. ACS Appl. Mater. Interfaces **10** (2018) 18113.

[4] Z. Sekkat, G. Kleideiter, and T. Knoll, Optical orientation of azo dye in polymer films at high pressure. J. Opt. Soc. Am. B-Opt. Phys. **18** (2001) 1854.

[5] Y. Yan *et al.*, Photoisomerization quantum yield of azobenzene-modified DNA depends on local sequence. J. Am. Chem. Soc. **135** (2013) 8382.

[6] J. H. Harding, C. L. Freeman, and D. M. Duffy, Oriented crystal growth on organic monolayers. Cryst. Eng. Comm. **16** (2014) 1430.

[7] D. Yokoyama, Molecular orientation in small-molecule organic light-emitting diodes. J. Mater. Chem. **21** (2011) 19187.

[8] J. Ràfols-Ribé, in *Departament de Física* Organic vapour-deposited stable glasses: From fundamental thermal properties to high-performance organic light-emitting diodes (Universitat Autònoma de Barcelona, 2017), p. 210.

[9] D. P. Rodney *et al.*, Evidence for the molecular-scale origin of the suppression of physical ageing in confined polymer: Fluorescence and dielectric spectroscopy studies of polymer–silica nanocomposites. J. Phys. Condens. Matter **19** (2007) 205120.

[10] K. Soyoung, R. C. B., and T. J. M., Effect of nanoscale confinement on the glass transition temperature of free-standing polymer films: Novel, self-referencing fluorescence method. J. Polym. Sci. B **46** (2008) 2754.

[11] R. D. Priestley *et al.*, Structural relaxation of polymer glasses at surfaces, interfaces, and in between. Science **309** (2005) 456.

[12] D. Lee *et al.*, Room temperature phosphorescence of metal-free organic materials in amorphous polymer matrices. J. Am. Chem. Soc. **135** (2013) 6325.

[13] L. S. Liao *et al.*, Ambient effect on the electronic structures of tris-(8-hydroxyquinoline) aluminum films investigated by photoelectron spectroscopy. Chem. Phys. Lett. **333** (2001) 212.

[14] J. E. Knox *et al.*, Chemical failure modes of alq3-based oleds: Alq3 hydrolysis. PCCP **8** (2006) 1371.

[15] X. Z. Wang *et al.*, Photodegradation of organic light-emitting devices observed in nitrogen-filled environment. Thin Solid Films **516** (2008) 2171.

[16] D. Y. L. Kondakov, W. C.; Nichols, W. F., Role of chemical reactions of arylamine hole transport materials in operational degradation of organic light-emitting diodes. J. Appl. Phys. **104** (2008) 084520.

[17] Y. Qiu *et al.*, Photostability can be significantly modulated by molecular packing in glasses. J. Am. Chem. Soc. **138** (2016) 11282.

[18] N. Nakashima, and K. Yoshihara, Role of hot molecules formed by internal conversion in uv single-photon and multiphoton chemistry. J. Phys. Chem. **93** (1989) 7763.

[19] C. Doherty, and P. York, Accelerated stability of an x-ray amorphous frusemide-polyvinylpyrrolidone solid dispersion. Drug Dev. Ind. Pharm. **15** (1989) 1969.

[20] C. Rodriguez-Tinoco *et al.*, Highly stable glasses of celecoxib: Influence on thermo-kinetic properties, microstructure and response towards crystal growth. J. Non-Cryst. Solids **407** (2015) 256.

[21] M. Otsuka, and N. Kaneniwa, Hygroscopicity and solubility of noncrystalline cephalexin. Chem. Pharm. Bull. **31** (1983) 230.

[22] C. Ahlneck, and G. Zografi, The molecular basis of moisture effects on the physical and chemical stability of drugs in the solid state. Int. J. Pharm. **62** (1990) 87.

[23] K. J. Dawson *et al.*, Highly stable indomethacin glasses resist uptake of water vapor. J. Phys. Chem. B **113** (2009) 2422.